A STUDY OF DISTURBED BOUNDARY LAYERS USING A HOT-WIRE ANEMOMETER.

Thesis
submitted by

LEONARD KERSLEY, B.Sc. (Edinburgh).

for the degree of
DOCTOR OF PHILOSOPHY.

University of Edinburgh,
May, 1965.

TABLE OF CONTENTS.

Page.

Preface i

Symbols ii

Note iv

CHAPTER I

INTRODUCTION AND HISTORICAL SURVEY OF BOUNDARY - LAYER RESEARCH

I.1. Introduction 1

I.2. Historical Survey 2

a) Reviews

b) The boundary layer

c) Hydrodynamic stability

d) Instability of the laminar boundary layer

e) Non-linear theories

f) Experimental work

I.3. Conclusion 22

CHAPTER II

DESCRIPTION AND CALIBRATION OF THE WIND TUNNEL

II.1. Description of the Wind Tunnel . . . 24

II.2. The Flat Plate and False Walls . . . 26

II.3. The Traversing Mechanism 27

II.4. Control of Wind Speed 28

II.5. Calibration of Wind Speed 30

II.6. Adjustment of the Pressure Gradient along the Flat Plate 31

II.7. The Boundary Layer on the Flat Plate . . 33

CHAPTER III

THE VIBRATING RIBBON TECHNIQUE

III.1. Introduction 34

III.2. Preliminary Experiments with Ribbon Systems 36

a) Experimental arrangement

b) Experiments and results

III.3. Measurement of Ribbon Amplitude . . . 43

III.4. Ribbon Arrangement for Boundary-Layer Studies 47

CHAPTER IV

THE HOT-WIRE ANEMOMETER

IV.1. The Hot-Wire Method 50

IV.2. Requirements for the Hot-Wire System . . 51

IV.3. Components of the Hot-Wire Anemometer . 52

IV.4. Hot-Wire Probes 53

a) The hot-wire head

b) Preparation of the wire

c) Mounting of wires

d) Etching

e) Mounting in the tunnel

IV.5. Control of the Mean Operating Conditions . 59

a) Basic Circuit

b) Bridge and potentiometer

c) The two-channel system

IV.6. Amplifiers and Compensating Units . . 64

a) Amplifiers

b) Compensating circuits

c) Practical compensating amplifier

IV.7. Signal Manipulating Equipment . . . 68

IV.8. Output Meters 70

IV.9. Calibration of the Hot-Wire . . . 71

IV.10. Determination of the y-position of the Hot-wire 74

CHAPTER V

PRELIMINARY STUDIES OF
BOUNDARY-LAYER PHENOMENA

V.1. Mean Flow Measurements 76

V.2. Distribution of the Intensity of the Disturbance through the Boundary Layer . 77

V.3. Reduction of Boundary-Layer Traverse Data . 81

V.4. The Growth of Disturbances in the Boundary Layer 81

V.5. Observations in the Spanwise Direction . 86

a) Mean flow variations

b) Variations in disturbance intensity

V.6. Downstream Growth of Disturbances at Several Spanwise Positions 90

V.7. Comparison of Experimental and Linear-Theory Growth Rates 91

V.8. Distortion of the Mean Flow . . . 96

V.9. Conclusions 100

CHAPTER VI

HARMONIC CONTENT OF WAVE DISTURBANCES IN THE BOUNDARY LAYER

VI.1. Introduction 101

VI.2. Analysis of Linear Recordings . . . 102

VI.3. Downstream Development of the Second Harmonic 104

VI.4. Preliminary Observations of Second Harmonic Intensity Distributions 107

VI.5. Distribution of the Second Harmonic Intensity through the Boundary Layer . . 110

VI.6. Note on Errors 116

VI.7. Further Experiments on the Nature of the Harmonic 117

VI.8. Non-linearity of the Hot-Wire . . . 119

VI.9. Harmonic Content of the Ribbon Vibration . 121

CHAPTER VII

CONCLUSIONS ON THE NATURE OF THE SECOND HARMONIC CONTENT

VII.1. Conclusions 122

VII.2. Suggestions for Further Work . . . 129

APPENDIX I

AN OUTLINE OF THE THEORY OF LAMINAR OSCILLATIONS . 130

APPENDIX II

OUTLINE OF THE THEORY OF HOT-WIRE MEASUREMENTS . 135

APPENDIX III

SIRIUS AUTOCODE PROGRAM FOR THE REDUCTION OF BOUNDARY-LAYER TRAVERSE DATA 139

APPENDIX IV

PROCEDURE FOR CALCULATION OF HARMONIC AMPLITUDES . 140

APPENDIX V

SIRIUS AUTOCODE PROGRAM FOR NUMERICAL HARMONIC ANALYSIS 141

APPENDIX VI

ATLAS AUTOCODE PROGRAM FOR CALCULATION OF SECOND HARMONIC CONTENT RESULTING FROM NON-LINEARITY OF HOT-WIRE 142

REFERENCES 143

ACKNOWLEDGEMENTS 149

PREFACE.

The research in this thesis was carried out in the Heriot Watt College, Edinburgh, under the joint supervision of Dr. M. A. S. Ross and Dr. J. G. Burns of the Department of Natural Philosophy, University of Edinburgh. The early boundary-layer studies were carried out in conjunction with Mr. J. Morgan and the later work on harmonic content with Mr. F. H. Barnes.

SYMBOLS.

The following symbols are used to describe the quantities indicated in this list unless otherwise stated in the text.

x	distance from leading edge of the flat plate.
y	distance from the surface of the flat plate.
z	distance from the centre line of the plate perpendicular to x and y.
U_∞	free stream velocity.
U	mean velocity at a point in the boundary layer.
u	x component of fluctuation velocity.
v	y component of fluctuation velocity.
w	z component of fluctuation velocity.
u', v', w'	intensities or root mean square values of u, v, w.
c_r	wave velocity.
$\beta_r = 2\pi f$	where f = oscillation frequency.
$\alpha = 2\pi/\lambda$	wave number.
ρ	density of air
ν	kinematic viscosity
δ	boundary layer thickness.
δ^*	boundary layer displacement thickness.

$\delta^* = 1.72\sqrt{\frac{\nu x}{U_o}}$ for Blasius distribution.

$\delta^* = 0.341\,\delta$ relation used by Tollmein and Schlichting.

$R = \frac{U_o \delta^*}{\nu}$ boundary-layer Reynold's number.

H rate of heat loss from a heated wire.

T_w temperature of wire when heated.

T_a air temperature and temperature of wire when cold.

T instantaneous temperature of wire.

T_o reference temperature.

R_w resistance of hot-wire at temperature T_w

R_a 'cold' resistance of wire at temperature T_a

R_o resistance of wire at temperature T_o

i current through hot-wire.

R.A. ribbon vibration amplitude.

NOTE.

The graphs in this thesis have been plotted on millimeter ruled paper, but the rulings have not been reproduced in the photographic copying process. Transparent sheets of graph paper are provided in the pocket inside the back cover.

CHAPTER I

INTRODUCTION AND HISTORICAL SURVEY OF BOUNDARY - LAYER RESEARCH

I.1. Introduction

One of the most important problems in fluid mechanics which has attracted the interest of investigators for many years is the transition from laminar to turbulent flow. This problem is of greatest importance in practice for flows over aerofoils and in closed channels, where the effects of transition are marked. Little is known, however, about the fundamental physical processes which cause a laminar flow to break down to turbulence.

The particular case of boundary-layer flow has received considerable attention and has been treated with some measure of success. Linearized theories have been useful in predicting the nature of the mechanism of instability of a laminar flow; but the non-linear problem, namely, the transition from an unstable laminar to a fully developed turbulent flow, presents formidable mathematical difficulties, so that few theoretical results have been obtained. The development of air and water tunnels together with improved measuring techniques in fluid flow has led to attempts by engineers and experimental physicists to relate the unstable laminar to the turbulent flow regime.

The aim of the work reported in this thesis was to gain further insight into the mechanism of transition in the boundary layer. The present experimental work was confined to the simplest example, the flow of an incompressible fluid along a smooth flat plate at zero angle of incidence with zero pressure gradient in the flow direction. The intention was to develop a hot-wire anemometer system to study the downstream development of disturbances introduced under controlled conditions into the boundary layer. As the work progressed emphasis was placed on one particular aspect of the non-linear development of the disturbances, the generation of higher harmonics of the fundamental wave.

I.2. Historical Survey

a) Reviews

The following survey of the published literature deals in detail only with the stability and transition of the boundary-layer flow over a flat plate and other closely allied flows. More complete reviews of the wider field of boundary-layer problems have been made by several authors. These include Prandtl (1935), Dryden (1955a), (1955b), (1956) and (1959), Kuethe (1956), Morkovin (1958), Schlichting (1959), (1960a) and (1960b) and Stuart (1960a). Books by the following authors or editors contain material of relevance: Lin (1955), Schlichting (1955) and Rosenhead (1963).

b) The boundary layer

Before the concept of the boundary layer was introduced in 1904 a large body of fluid flow theory was already in existence. It was based, for the most part, on Euler's equation of motion for an inviscid fluid, which had been formulated in the mid-eighteenth century. The Navier-Stokes equations of motion for a viscous fluid had been developed in 1820, but the mathematical problems encountered in the solution of these equations had proved to be so formidable that interest had centred on the inviscid fluid theory. This theory, which had been constructed by some of the best mathematical physicists of the nineteenth century using very reliable physical principles, had yielded much information. Even the simplest observation of the experimental facts, however, led to large areas of disagreement with the theoretical predictions. The failure of the theory was particularly disturbing for the motion of bodies through the atmosphere because the only known mechanical properties of air which had been neglected, namely viscosity and compressibility, could reasonably be supposed to produce small effects. The divergence between theory and experiment is illustrated by the prediction of perfect fluid theory that the drag on a body should be zero in steady flow. This so-called d'Alembert's paradox was the focal point of much interest towards the end of the nineteenth century.

As early as 1851 Stokes, considering the effect of viscous fluids on the motion of pendula, had shown that agreement between theory and experiment could be obtained by taking the condition of zero relative velocity of the fluid at the solid surface as the boundary condition in the solution of the equations of motion for a viscous fluid. It was, however, not until 1904 with the advent of the boundary-layer theory of Prandtl (1904) that theory and experiment were reconciled. Prandtl first introduced his theory to resolve the difficulty that, for fluids of small viscosity, the flow solutions derived by neglecting viscosity required slip over a solid surface. His theory retained the inviscid flow solution, but postulated the existence, between this flow and the solid surface, of a thin layer of fluid in which the velocity increased steeply from zero at the wall to the inviscid theory surface value at the edge of the layer. The influence of the viscosity of the fluid was restricted to this 'boundary layer', which was responsible for drag, separation and heat transfer, while outside the layer the flow was nearly that of an inviscid fluid.

The assumption of such a layer allows approximations to be made which lead to a simplification of the Navier-Stokes equations. The solution of the resulting boundary-layer equations (see Appendix I) is mathematically easier than that of the full Navier-Stokes equation.

The boundary layer equations for two-dimensional flow over a semi-infinite flat plate at zero incidence with zero pressure gradient in the flow direction were solved by Blasius (1908) in terms of an infinite power series. Improvements to the solution were made by Goldstein (1930) and Howarth (1938), the latter tabulating the results for the distribution of velocity across the boundary layer.

Experimental verification of the boundary layer theory was first supplied by Burgers (1925) and van der Hegge Zijnen in Delft. Further confirmation of the velocity distribution through the boundary layer has been made by Nikuradse (1942).

c) Hydrodynamic stability

The above description of the boundary layer has been confined to laminar flows. Prandtl and others, however, soon realised that turbulent flow and the transition from laminar to turbulent flow were subjects of great practical importance.

The recognition of the two flow regimes, laminar and turbulent, stems from the work of Reynolds (1883). His experiments on the flow of water through pipes running full showed that transition from laminar to turbulent flow was roughly characterised by a certain value of a dimensionless parameter (the product of velocity and length divided by kinematic viscosity), now known as Reynold's number.

The theory of instability of a perfect fluid was developed by Lord Rayleigh in a series of papers, beginning with those of 1880 and 1887. The method used was to study the effect on the flow of a small perturbation, instability being indicated by amplification of the perturbation. An important result obtained by Rayleigh (1887) was that a necessary condition for instability of an inviscid fluid is that the mean flow profile should contain a point of inflexion.

Lorentz (1896) and Orr (1907) discussed hydrodynamic stability from the viewpoint of energy exchange. They argued that, when a disturbance in a fluid grows, the energy available for growth must come from the mean motion. Studies of energy transfer between mean flow and disturbance enabled them to estimate the Reynold's number for transition, the critical Reynold's number. The disturbance velocities chosen by them were, however, not solutions of the equations of motion, so that the critical Reynold's numbers obtained were much lower than those observed experimentally.

About this time experiments had shown that the laminar boundary layer develops instabilities and becomes turbulent. In particular, Prandtl (1914) studied the effects of transition on the boundary layer by observing the variation with Reynold's number of the flow patterns round bodies of various shapes. He was

to show also, that flow separation of the boundary layer and transition were connected phenomena, an idea which was later developed by Taylor (1936). Taylor's theory was that transition resulted from separation, either momentary or permanent, of the laminar layer. From the Karman-Pohlhausen parameter for laminar separation he was able to find a relation to determine the Reynold's number for transition in the boundary layer. Experiments with flat plates, spheres and elliptic cylinders confirmed that this relation did control transition, but only when the free stream turbulence level was high.

The main objection to Taylor's theory is that separation has not been shown to be necessary for transition. From experimental studies on the effect of free stream turbulence on transition in the boundary layer on a flat plate, Bennett (1953) has suggested that, above a certain level of free stream turbulence, transition may be controlled by the laminar-separation theory of Taylor. Bennett concludes, however, that this level of turbulence is much higher than had previously been anticipated.

d) Instability of the laminar boundary layer

The theory of instability of boundary-layer flows was first studied by Tietjens (1925) for velocity profiles consisting of a combination of straight lines. It was,

however, Tollmein (1929) who achieved the first major breakthrough in stability theory by considering the effect of an infinitesimal disturbance on the flow. Important contributions to this linearized theory were made by Schlichting (1933a), (1933b) and (1935), who carried out detailed calculations of the characteristics of the oscillations arising from the instability. His work predicted the conditions for the boundary layer to be unstable, when small disturbances would be amplified in time. Disturbances of this type, moving down the boundary layer, are known as Tollmein-Schlichting waves. The theory showed that small disturbances with frequencies in a certain range would be amplified by the boundary layer, whilst those of lower or higher frequency would be damped. The main result of this work can be summarised by a curve in the $(\beta\nu/U_0^2, R)$ plane, known as the neutral stability curve, which separates the 'amplifying' and 'damping' regions of the boundary layer.

Developments of the Tollmein-Schlichting theory have been made by Lin (1945) and Shen (1954), the former recalculating the neutral curve, while the latter has used the curve to obtain curves of constant amplification in the amplifying zone. Growth curves for disturbances in this amplifying region can thus be found.

The distribution of amplitude across the boundary layer was first calculated by Schlichting (1935) for neutral oscillations. Zaat (1958) has made similar calculations, as well as obtaining a slightly modified neutral curve.

Figure A.I.1. shows the neutral stability curve of Schlichting together with that of Lin and Zaat.

An outline to the theoretical approach to the problem of boundary-layer instability, by the method of small disturbances, is given in Appendix I.

It should be noted here that the theoretical work so far described was concerned only with two-dimensional disturbances. The justification for this restriction stems from the conclusion of Squire (1933), extended by Watson (1960), that the problem of the instability of an infinitesimal three-dimensional disturbance at a given Reynold's number is equivalent to a two-dimensional problem at a lower Reynold's number. It should be noted, however, that recent work by Meksyn (1964) has shown that, for disturbances of finite amplitude, three-dimensional oscillations are less stable than two-dimensional ones.

Experimentally, Dryden (1936) was the first to observe velocity fluctuations in the boundary layer, but he was unable to relate their behaviour to the small disturbance theory. Nikuradse (1933) attempted to

introduce disturbances into the boundary layer on a flat plate in water, but obtained inconclusive results, mainly due to high natural disturbance level present in the flow.

For the next decade the theory of small disturbances went untested, and it was generally believed (c.f. Taylor (1938)) that selective amplification of small disturbances had little to do with the phenomenon of transition.

It was with the advent of the very low turbulence level wind tunnel that Tollmein-Schlichting waves were observed experimentally in the boundary layer on a flat plate, This important series of experiments was carried out by Schubaucr and Skramstad (1947) using a wind tunnel at the National Bureau of Standards, Washington. With hot-wire anemometers, they were able to show that transition was preceded by instability waves of the kind predicted by Tollmein and Schlichting, provided that the free stream turbulence level was of low enough intensity. It should be noted here that, while Schubauer and Skramstad took this maximum permissible level of turbulence to be about 0.08 per cent. of the free stream speed, Bennett (1953) has shown that Tollmein-Schlichting waves play a role in the boundary layer even when the turbulence level is as high as 0.42 per cent.; a fact which is of importance in the present work.

The observations of Schubauer and Skramstad allowed them to compare the frequencies of the natural sinusoidal oscillations present in the boundary layer with the frequencies of the waves predicted by instability theory. They found that when the non-dimensional frequency parameter $\beta_r \nu / U_o^2$ was plotted against R, the experimental points lay close to the upper branch (Branch II) of the neutral stability curve. From this observation they inferred that a disturbance of a given frequency was amplified as it passed downstream, and reached its maximum amplitude at a point on the upper branch of the neutral curve, unless it had by then caused transition.

Once it had been established that instability waves of the kind predicted by theory did occur, Schubauer and Skramstad performed controlled experiments with artificially produced disturbances of suitable frequency. These disturbances were injected into the boundary layer using a vibrating ribbon. In this way, they were able to show good qualitative agreement between experimental points of neutral stability and the theoratical curve, even better agreement being obtained when Lin's more recent curve was used (Figure A.I.1.). Further confirmation of the theory was provided by their observations of the distribution of the amplitude and phase of the disturbance across the boundary layer.

e) Non-linear theories

While the linearized theory of Tollmein and Schlichting, together with its experimental confirmation, described the early stages of instability of the laminar boundary layer, no clue was provided by it as to the subsequent nature of the breakdown process when the perturbation had grown to such an extent that the linear approximations of the theory could no longer be applied.

Although Noether (1921) and Heisenberg (1924) had derived and discussed equations including non-linear terms, the first paper to give any definite predictions about the effects of non-linearity on instability was that of Landau (1944) who put forward a theory of successive instabilities as a precursor to turbulence.

For the past two decades, work on the theory of hydrodynamic stability has tended to emphasise, more and more, its non-linear aspects. The work described below has been concerned for the most part with Poiseuille flow between parallel planes where local Reynold's number is independent of the co-ordinate in the stream-wise direction, a fact which makes this flow easier to treat mathematically than boundary-layer flow. It was hoped, however, that the general features of non-linear instability in this flow could be applied to boundary-layer flow over a flat plate, where the boundary-layer growth is relatively slow. Most of this work, again

for reasons of mathematical simplicity has been concerned with the amplification of disturbances with time, although Bradshaw, Stuart and Watson (1960) have shown how amplification with streamwise distance may be considered.

The differential equation important in non-linear instability theory first derived by Landau has been obtained by an independent method by Stuart (1960b) and Watson (1960), considering disturbances of finite amplitude. Stuart (1960a) has pointed out the physical significance of the three non-linear terms in its solution. These non-linear features which control the amplification of a disturbance are the distortion of the mean motion, the generation of a second harmonic of the fundamental Tollmein-Schlichting wave, and the distortion of the fundamental wave. Meksyn and Stuart (1951) had considered terms associated with the first and third of these and had shown that the effect of a disturbance of finite amplitude was to cause distortion of the mean flow profile by the Reynold's stresses of the fundamental wave, this in turn altering the amplitude distribution of the disturbance across the boundary layer. An analysis by Stuart (1958), using an energy balance method, dealt only with the distortion of the mean flow, the change in the distribution of the disturbance being shown to be small enough to be neglected. From this analysis

he concluded that a disturbance amplitude of approximately 10 per cent. of the maximum velocity was required before distortion of the mean flow was observed.

An interesting point arising from the work of Stuart (1960a), (1960b) and (1960c) is the possibility of amplification of a disturbance which is in a region stable according to linear theory provided the disturbance amplitude is above a threshold value, an observation which has some relevance to the present work.

The second of the non-linear features mentioned above, the generation of higher harmonics, has been considered by Lin (1958) in an order of magnitude analysis. His conclusion was that 'for disturbances in a parallel flow, all the harmonic components of the oscillation simultaneously become important around the critical layer (the region in the boundary layer where the wave velocity equals the local flow velocity) before the amplitude of the fundamental component is large enough to cause any significant distortion of the mean flow'. This statement has been taken up briefly by Bradshaw, Stuart and Watson (1960) and Stuart (1960b) who show it to be at variance with their work, where the mean motion distortion and second harmonic component are found to be of the same order of magnitude, while higher harmonic components are of much smaller order of magnitude, even in the critical layer. In an analysis of

Lin's work they conclude that it can be applied only to disturbances much larger than those considered by themselves.

The non-linear theory so far described has been for two-dimensional flow. However, since 1960, following experimental observations which showed the inadequacy of the two-dimensional approach, three-dimensional flows have been considered theoretically with some measure of success.

In the work formulated by Lin and Benney (1960) and taken up by Stuart (1960c) the interaction of a two-dimensional Tollmein-Schlichting wave with a three-dimensional wave disturbance of the same wave number in the streamwise direction was treated to the second order of amplitude. The interaction produced non-linear effects of several kinds including the generation of harmonics of the fundamental wave, the modification of the original mean motion, and the generation of new harmonic components which are non-periodic in time. Benney (1961) has considered these latter components, two in number, and has shown that they possess streamwise vorticity which gives rise to a spanwise transfer of energy in the boundary layer. Energy transfers of this kind had been observed experimentally by Klebanoff and Tidstrom (1959), a fact which had influenced the theoretical model formulated by Lin and Benney.

Benney (1964) has extended this work to a boundary layer with a profile consisting of two straight lines, again examining the terms, non-perodic in time, associated with longitudinal vortices.

A further theoretical approach leading to components with streamwise vorticity has been made by Görtler and Witting (1958). They suggest that the Tollmein-Schlichting wave motion possesses regions where the total flow (mean flow plus oscillation) is unstable due to the action of centrifugal forces, an idea in accord with Landau's theory of successive instabilities. According to their work, streamwise vorticity will develop at positions where the streamlines are concave relative to an observer moving with the wave speed. However, for boundary-layer flow it has been observed experimentally to develop at positions where the streamlines are convex, qualitative agreement being obtained in this point with the Lin-Benney theory.

An entirely new theoretical approach to instability has been made by Raetz in an unpublished paper reported by Stuart (1960a). His suggestion was that two three-dimensional oscillations, themselves in a neutral or damping region of the boundary layer may interact and 'resonate' to produce an amplifying oscillation. This theory allows the possibility of much larger rates of growth of boundary layer oscillations than the usual instability theory.

Finally in this account of the theoretical work

on boundary layer instability mention must be made of the work of de Santo and Keller (1962). They attempted a numerical integration of the flow equations using an electronic digital computer. While of limited success itself, this paper may pave the way for future theoretical work, as it offers prospects for a unified view of the transition process in the boundary layer, most of the work up to the present having been concerned only with local aspects of flow instability.

f) Experimental work

While theoretical work has been unable to provide a clear picture of the mechanism of transition in the boundary layer, experimental work, using both air and water tunnels, has proceeded without this help.

The later stages of transition, as turbulence was neared, were studied experimentally by Emmons (1951) using a water table and flow visualization techniques. He noted that, when disturbances in the boundary layer reached a certain size, a turbulent burst, or 'spot', appeared, which was observed to move with the fluid gradually fanning out to make turbulent all before it. A theory was proposed by Emmons to predict the percentage of time that each position on the plate will be turbulent, taking into account the effect of the turbulent spots formed upstream as well as those formed at the point in question.

A hot-wire anemometer was used by Schubauer and Klebanoff (1955) to study both naturally occurring and artificially produced turbulent spots, the two being found to be similar in character.

Measurements of the intermittency factor (γ), the fraction of time during which a point in the transition region is turbulent, have been made by Schubauer and Klebanoff, Narasimha (1957) and Dhawan and Narasimha (1958). These latter workers have deduced an empirical formula relating the intermittency factor with the downstream position in the transition region.

Experimental visual studies, using dyes, of the processes leading up to, and resulting in, breakdown on a water table, were perfected by Fales (1955). He observed that an initially uniform bed of dye was gathered into lines after passing over a trip wire, evidently being concentrated by the vortices shed by the trip. The subsequent warping of these lines was studied by Hama, Long and Hegarty (1957), loops being formed which stretched out in the flow direction as they advanced downstream. From near the forward part of each loop bursts of turbulence occurred, the succession of turbulent spots being concentrated, in the first instance, in streets in the flow direction. Hama (1960) has replied

to objections of Schubauer (1958) by showing that the breakdown process induced by a vibrating ribbon is essentially similar in character to that behind the trip wire.

Weske (1957), in dye studies in water flow over a stationary plate, has observed spanwise variations in boundary-layer thickness associated with disturbance growth, followed by the development of vortex loops of the type proposed theoretically by Theodorsen (1955) with turbulence originating within the loop. Weske reports also that local separation occurred under these loops when the disturbance level was sufficiently high.

Tani (1960) and Tani and Komoda (1962) have studied instability by introducing two-dimensional disturbances into a three-dimensional boundary layer. In experiments where the degree of three-dimensionallity of the boundary layer could be controlled observations were made of amplitude and phase distributions of the disturbance across the boundary layer under various conditions.

However, the most productive work towards an understanding of the mechanism of transition has been carried out at the National Bureau of Standards, Washington, where emphasis has been placed on the three-dimensional nature of the process.

Spanwise variations in boundary-layer thickness, shown to be a feature of the Washington wind tunnel, were

first reported by Schubauer (1958) and Klebanoff and Tidstrom (1959). These variations were shown to have a part in shaping the phenomena leading to transition since associated with them were variations in the streamwise growth of disturbances in the boundary layer. Observations, using a hot-wire anemometer, were interpreted by these workers as indicating a spanwise transfer of energy in the boundary layer.

An important extention to this work has been carried out by Klebanoff, Tidstrom and Sargent (1962). By making modifications to the damping screens in the tunnel they were able to reduce the spanwise variations in boundary layer thickness to within the limits of experimental observation. An adaptation of the vibrating ribbon technique of Schubauer and Skramstad was then used to introduce controlled three-dimensional disturbances into an effectively two-dimensional boundary layer. Surveys, using a hot-wire anemometer, of the longitudinal and spanwise components of the mean velocity as well as of the intensity and instantaneous values of the longitudinal and spanwise fluctuations were made across the boundary layer at different spanwise positions in the region from ribbon to wave breakdown. It was established that associated with the three-dimensional wave motions

there were longitudinal vortices . This eddy system consisted of a pair of counter-rotating eddies, one on each side of the peak in the spanwise distribution of wave amplitude. Studies were made also of the downstream changes in the eddy system and their relation to wave growth. Sufficient data were obtained by these workers for an evaluation of the various existing theoretical approaches. Those considered were the generation of higher harmonics, the interaction of the mean flow and the Reynold's stresses, the concave streamline curvature associated with the wave motion, and the vortex loop concept. Each of these was shown to be inadequate in describing the observed phenomena. However, some qualilative agreement was obtained with the theoretical work of Lin and Benney.

As well as considering the growth of the wave motion, some attention was given in this work to the breakdown of the wave motion into turbulence. It was shown that the onset of turbulence was preceded by intense high frequency fluctuations; the results suggested that the actual breakdown was a consequence of a new instability which arose from the three-dimensional disturbance. This mechanism was shown to be analogous to that observed by Kovasznay (1960) in breakdown behind a roughness element.

Further important observations were made by Klebanoff, Tidstrom and Sargent on natural transition. They concluded from these that the same basic mechanism was present in this as in artifically-induced transition.

I.3. Conclusion

A conclusion to be drawn from this outline survey is that the existing theoretical approaches to boundary layer instability do not appear to be realistic when viewed from the light of experimental knowledge of the subject. This does not imply that they are necessarily incorrect; they may indeed play a role in some aspect of local behaviour of the flow. However, a unified theoretical approach is required and the advent of the digital computer would seem to offer hope that progress will be made in this direction.

The low-turbulence wind tunnel and the hot-wire anemometer are the main tools available to the experimenter. Using these Klebanoff et. al. have been able to reveal some of the main features of the transition process in the boundary layer on a flat plate, but much remains to be done. Considerable scope is afforded to workers, even those with limited resources, by observing local flow behaviour in selected regions of the transition process and attempting to relate such observations to the existing theories. A further experimental approach would be the use of a hot-wire anemometer

system with the required data processing facilities to map the flow behaviour in the boundary layer in the transition region. Results from such a study would be an invaluable check on a computed solution of the boundary layer equations.

The present work falls into the first category. The intention was to build a hot-wire anemometer system and to use this to study local aspects of the transition mechanism. This hot-wire anemometer system was made, however, sufficiently versatile to enable it to become an integral part of much larger instrumentation which could be used in a very low-turbulence wind tunnel, when this became available, to make a complete survey of the transition process.

CHAPTER II

DESCRIPTION AND CALIBRATION OF THE WIND TUNNEL

II.1. Description of the Wind Tunnel

The wind tunnel used in this work was a modification of the N.P.L. Design No. A155. This tunnel is of open-circuit type with 18 inch octagonal working section and a 3.16:1 contraction ratio. The modification to the original design took the form of additional settling lengths, both before and after the contraction, to ensure a smooth flow and as low a turbulence level as possible in the working section.

A diagram of the tunnel is shown in Figure II.1.

The tunnel was situated in a basement room, 50' x 26' x 10.1/2', the walls, floor and ceiling of which were of reinforced concrete. To ensure that spurious vibrations were kept to a minimum, the 2 inch angle iron legs of the tunnel were bedded in heavy slabs of concrete. These blocks were insulated from the floor of the room by felt pads, and located by rubber covered steel pegs set into the floor.

The tunnel itself was of sectional construction, adjoining sections being firmly bolted together. The frames were of white wood, while the tunnel walls were of hardwood. The working section was constructed from

1/4 inch perspex sheet, cemented together to be of regular octagonal section.

A honeycomb straightener, constructed from 4 inch hexagonal brass tubes measuring 3/8 inches from face to face, was fitted in the inlet section. Downstream of the honeycomb were two mesh screens constructed from 32 S.W.G. wire with 30 wires to the inch. The optimum locations for these screens were found by Burns (1958) and Nicol (1958) to be 15 inches and 27 inches downstream of the honeycomb. These screens were found to collect dust, and had to be removed and cleaned at regular intervals.

With this arrangement the free stream turbulence level in the working section at 25 ft./sec. was found, using the hot-wire anemometer (see Chapter IV), to be approximately 0.25 per cent. of the mean flow velocity.

The air was drawn through the tunnel by a four-bladed fan mounted directly on the shaft of a 7.5 H.P. D.C. motor, coupled to a Ward-Leonard speed control system. This consisted of a three-phase 7.5 H.P. motor directly coupled to a D.C. generator, whose output was fed to the fan motor armature. An external 240 volt D.C. source supplied the field coils of the generator through a potential divider, which was used to provide speed control of the fan motor.

A diagram of the speed control circuit is shown in Figure II.2.

Windspeeds up to approximately100 feet/sec. could be attained in the working section, but during the course of the present work speeds in excess of 30 feet/sec. were rarely used.

A full description of the design and construction of this tunnel has been given by Burns (1958).

II.2. The Flat Plate and False Walls

The flat plate used in the boundary-layer measurements was mounted vertically along the centre of the working section of the tunnel. The plate was made from a single sheet of perspex, 6 feet long by 1/4 inch thick, which spanned the tunnel from floor to ceiling. Its leading edge, situated 1 foot upstream from the start of the perspex working section, was smoothly tapered over a distance of 4 inches to a symmetrical knife edge. The top and bottom of the plate were bolted to 1 inch brass angle bars, which were in turn bolted to the tunnel ceiling and floor, the plate being held under slight transverse tension.

Marks scratched at one inch intervals, along the centre line on the reverse side of the plate, were used to position instruments in the streamwise direction.

An aluminium fin was attached to the trailing edge of the plate, so that there was greater blockage to the flow on the working side of the plate than on the reverse side. The stagnation point at the leading edge of the plate was thus kept on the working side which ensured that the early growth of the boundary layer was laminar on this side.

To counteract the negative pressure gradient in the parallel-walled working section, false walls of 1/16 inch thick perspex sheet were fitted vertically, close to the vertical walls of the tunnel. These commenced in the contraction, were parallel in the settling length, and diverged to meet the tunnel walls near the end of the working section. The profile of false wall on the working side of the tunnel could be varied, within small limits, by means of adjusting screws at various positions along its length. This allowed fine adjustments to be made in the pressure gradient along the working section.

II.3. The Traversing Mechanism

The traversing mechanism, to carry instruments in the tunnel, could be moved along the working section on ball races located in U-section brass rails which were mounted, parallel to the flat plate, on the floor and ceiling of the working section. The main carriage

was a brass plate spanning the tunnel vertically. On this the boom with its pivot mount could be located at various heights, allowing for change in the spanwise position of the instruments to be made. The upstream end of this boom was made to bear on the flat plate by means of a spring, a further arm being pivoted at this point. The instrument situated at the upstream end of this second arm could be moved perpendicular to the surface of the plate by a flexible clutch cable pulling against a spring, the micrometer drive for this being mounted on the outer tunnel wall. A clock-gauge, with its probe bearing on the flat plate, was attached to this arm, and gave the distance of the instrument from the plate.

The side elevation of the carriage is shown in Figure II.3., while Figure II.4. shows a plan view of the boom system for movement in the y-direction.

II.4. Control of Wind Speed

The fan speed could be controlled coarsely by a stepped potentiometer in the field-coil circuit of the generator of the Ward-Leonard system. A feed-back system was employed to provide continuous control over wind speed, and also to reduce the wind speed variations resulting from fluctuations in the external D.C. supply.

The sensing element for this system was a pitot-static tube mounted permanently in the flow on the reverse side of the working section, the differential pressure from it being applied to an inverted-cup type of pressure balance. Electrical contacts closed when the balance was displaced from equilibrium. This operated a relay system, which in turn allowed a small, reversible, variable speed motor to drive a contact along a rheostat. This rheostat provided fine control of the current in the field coils of the generator, and hence fine control of the fan speed. Limit switches ensured that the contact could not be driven beyond the ends of the rheostat.

A diagram of this feed-back system for automatic control of windspeed is shown in Figure II.5.

In action the system worked as follows: Weights corresponding to the chosen windspeed (see II.5.) were set on the seale pan of the pressure balance. A small increase in windspeed above this chosen value resulted in an increased pressure difference between total head and static pressures in the tunnel. This destroyed the equilibrium in the pressure balance thus the relays were activated, causing the servomotor to drive the contact along the rheostat to reduce the field-coil current of the generator. This resulted in a decreased fan speed, with a corresponding reduction in windspeed.

In the same way a drop in windspeed resulted in compensatory increase in the speed of the fan motor.

The speed of the servomotor was an important factor in this system. If the contact on the rheostat were driven too quickly, then the system tended to 'hunt', never reaching a stable position. In practice, for maximum sensitivity, the speed of the servomotor was decreased until the system just ceased to 'hunt'. The 'hunting' was caused by the contact moving faster than the increase in speed of the fan motor, the inertia of the fan being the limiting factor in the response of the feedback system. The time taken for the speed control to increase the windspeed of the tunnel by 1 per cent. of its original value was approximately ten seconds. The system thus reduced only the very low frequency fluctuations but had little effect on high frequency fluctuations.

It was found that this feedback system controlled fluctuations in mean windspeed to within 2 percent. in a test run over a period of several hours.

II.5. Calibration of Wind Speed

To set the tunnel at a particular windspeed, a weight was placed on the scale pan of the pressure balance, the coarse-control stepped-potentiometer adjusted to the appropriate position and the fine control mechanism run

until equilibrium was reached. The weight required for a given wind-speed was determined by calibration of the pressure balance.

For this, a pitot-static tube, of N.P.L. design, was placed in the working section of the tunnel at a position 2 feet from the leading edge of the flat plate. The difference between total head and static pressures was measured on a paraffin filled inclined-tube manometer, which had been calibrated previously by making a direct measurement of its slope using a travelling microscope.

By making a comparison of the weights placed on the pressure balance with the manometer readings once the windspeed in the tunnel had reached equilibrium, a calibration for the pressure balance was obtained, allowing the weight required to give a desired windspeed to be ascertained.

II.6. Adjustment of the Pressure Gradient along the Flat Plate

Schlichting (1955) has shown that the rate of amplification of a disturbance in the boundary layer is dependent on changes in the local pressure gradient. For the present work, it was thus necessary to ensure that variations in the static pressure along the flat

plate were reduced to a minimum.

For this purpose, a static pressure tube, 0.2 inches in diameter, was mounted in the free stream on the working side of the plate. This could be traversed along the vertical centre line of the tunnel, at a constant distance from the flat plate and parallel to it. Comparison of the static pressure at the centre line with that at a fixed tapping in the tunnel wall was made using the sloping-tube manometer. Readings were taken at two inch intervals in the streamwise direction. The false wall profile was adjusted after each traverse until further improvement towards constant static pressure was impossible due to the inflexible nature of the perspex sheet.

A graph showing the pressure distribution obtained is plotted in Figure II.6. The static pressure is given as a non-dimensional quantity allowing comparison to be made with the pressure distributions obtained by other workers using nominally zero pressure gradients in the stream direction.

In the consideration of the stability of boundary-layer flows with pressure gradients the Pohlhausen shape factor (Λ) is of importance. This parameter is defined by the equation

$$\Lambda = \delta^2/\nu \cdot dU_o/dx .$$

Values of this parameter have been calculated for the pressure gradient obtained by considering the curve in Figure II.6. to consist of a series of straight lines joining adjacent experimental points. Extreme positive and negative values up to x = 3 feet obtained in this way are + 0.2 and - 0.4. The calculations of Schlichting (1955) show that for values of Pohlhausen shape factor as small as these, the pressure gradient can be taken to have a negligible effect on the position of Branch I of the neutral stability curve, the rate of disturbance amplification, and the shape of the boundary-layer profile.

II.7. The Boundary Layer on the Flat Plate

A study of the undisturbed boundary layer on the flat plate in the Heriot-Watt tunnel, under conditions essentially similar to those of the present work, was carried out by Whitelegg (1961) and Morgan (1964).

Using total-head and static pressure tubes made from hypodermic tubing they determined the extent of the laminar region of the layer, boundary layer profiles in good agreement with the theoretical Blasius profile being obtained. The extent of the laminar area of the boundary layer was shown to be limited by the wedges of turbulence shed from the top and bottom of the leading edge of the flat plate. The two turbulent regions were shown to meet on the centre line of the flat plate at a distance approximately 3.75 feet from the leading edge.

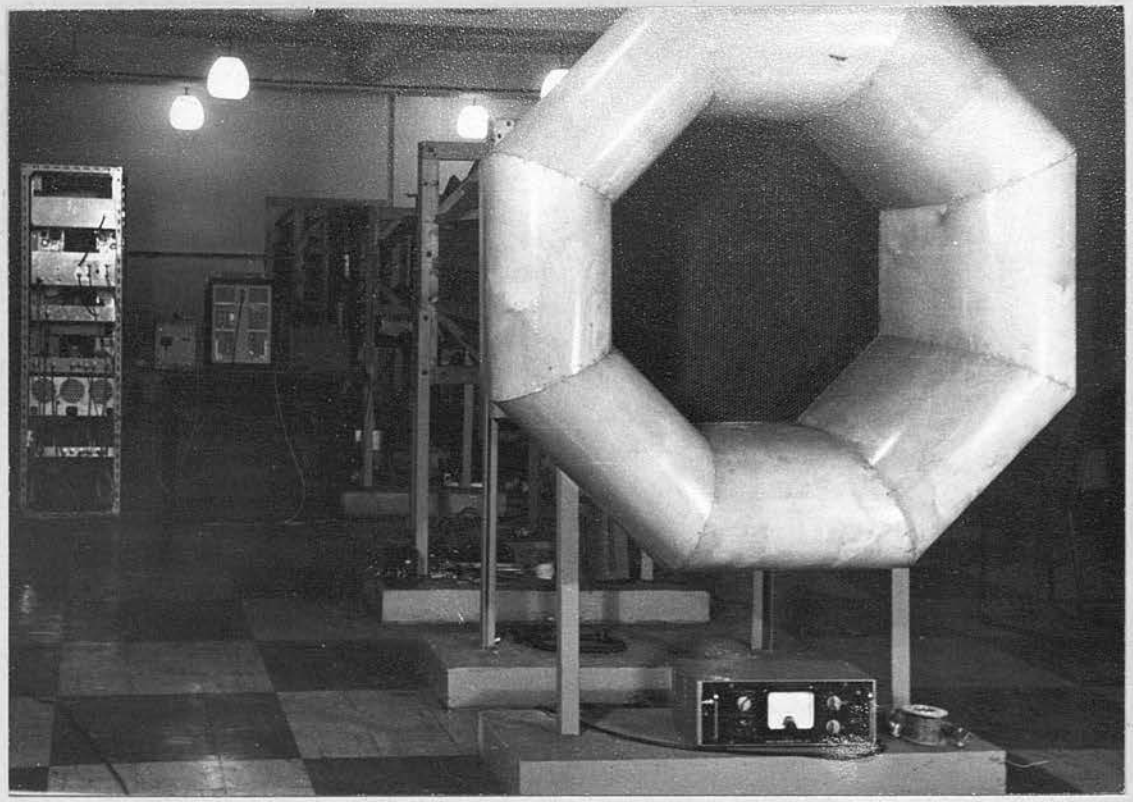

Figure II.1b. Photograph of Wind Tunnel.

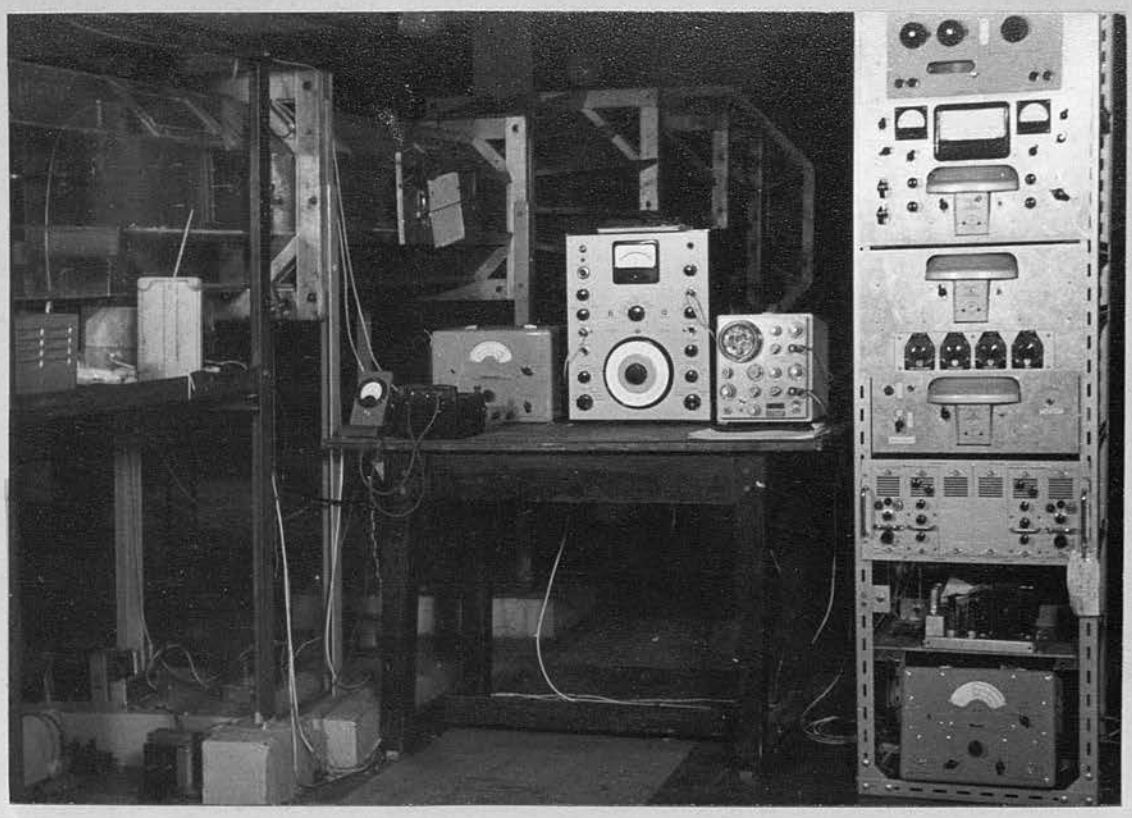

Figure II.1c. Photograph of Wind Tunnel and Instrumentation.

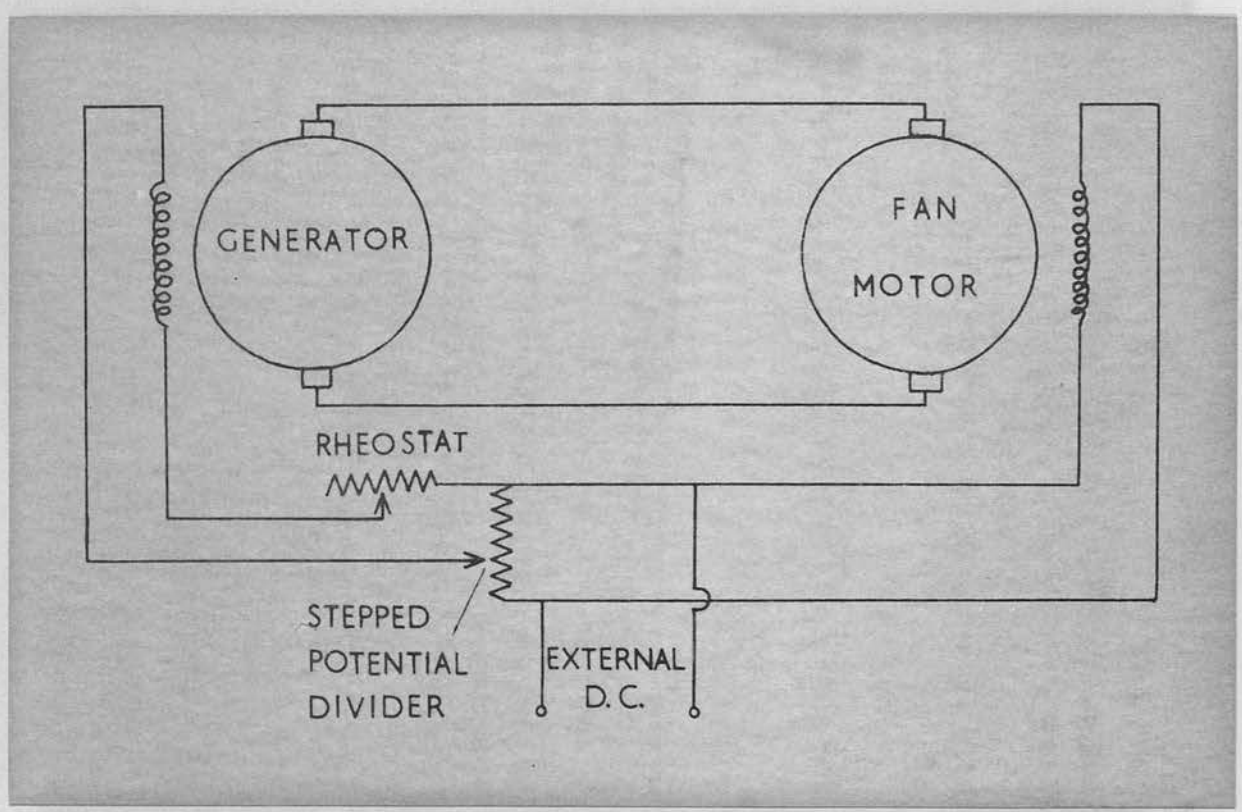

Figure II.2. Speed Control Circuit.

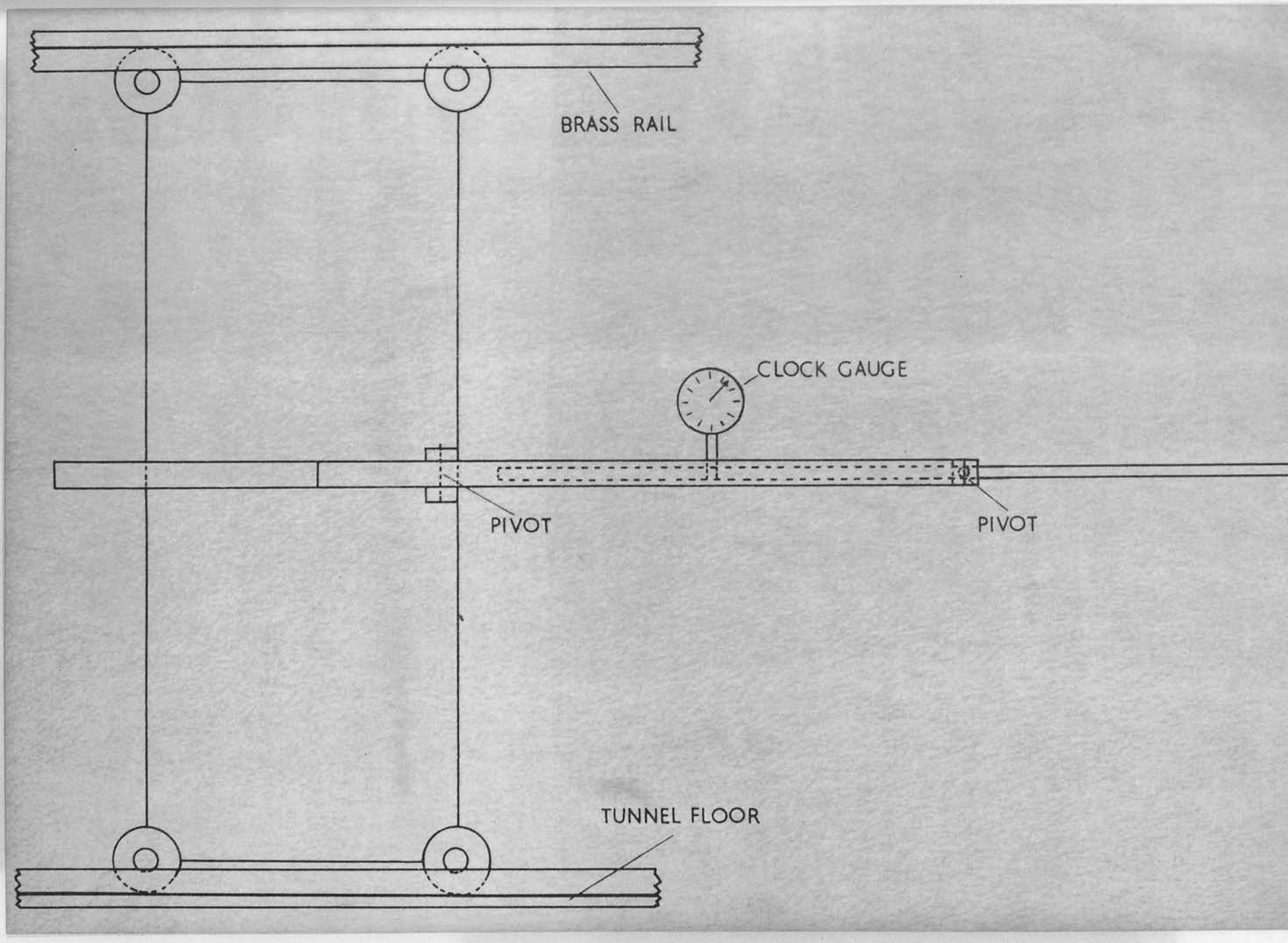

Figure II.3. Side Elevation of the Carriage.

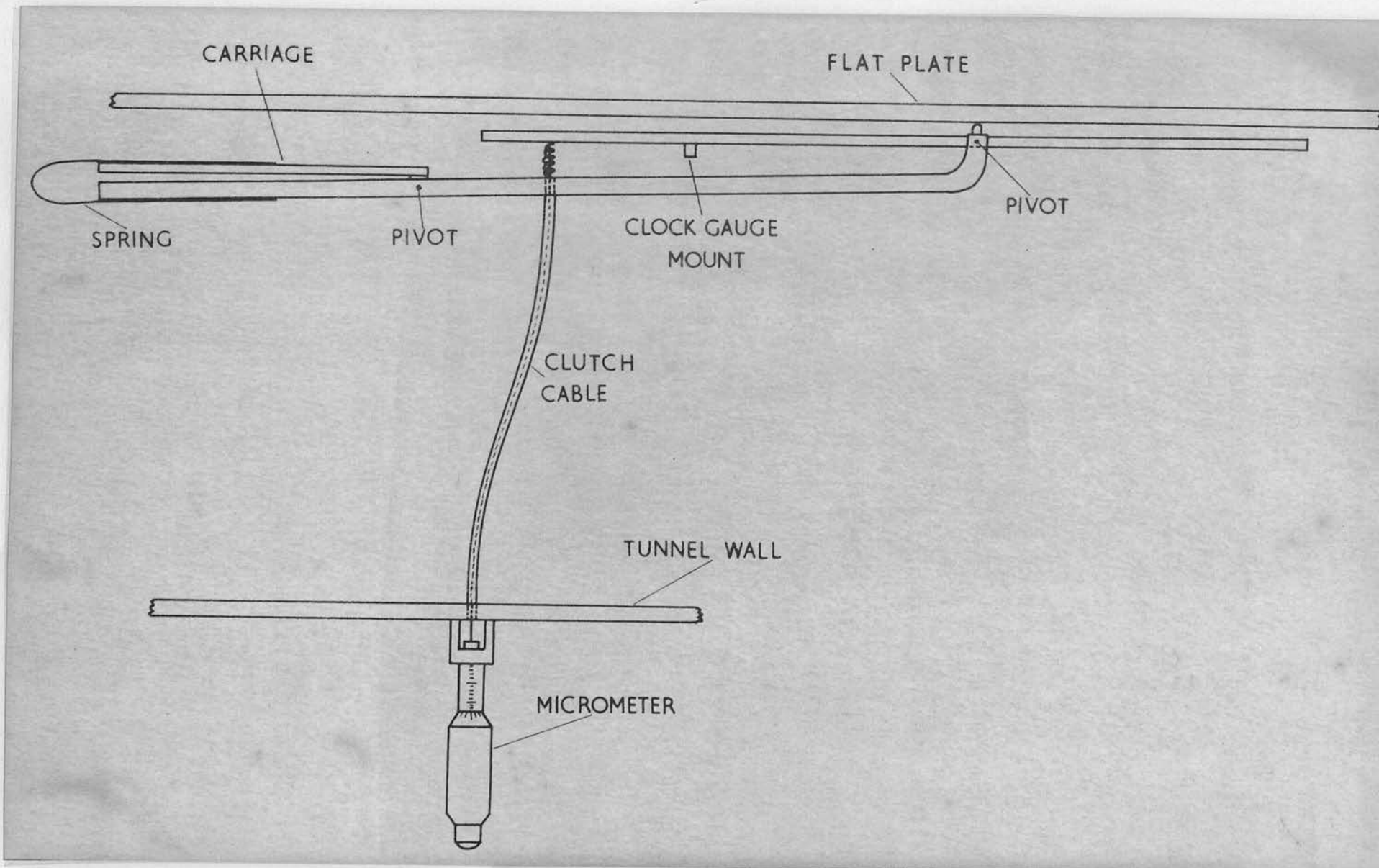

Figure II.4. Plan View of the Boom System.

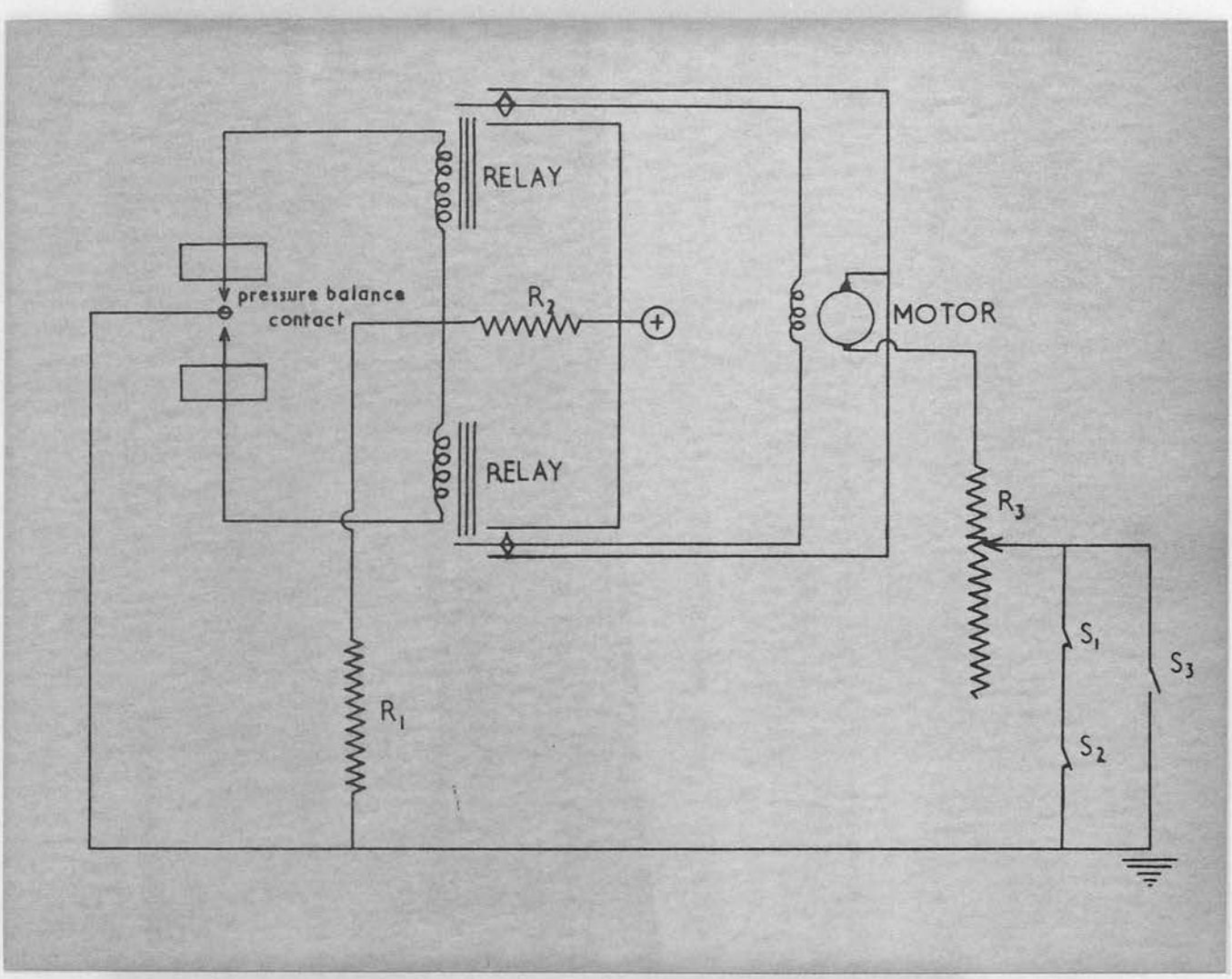

Figure II.5. Automatic Speed Control Circuit.

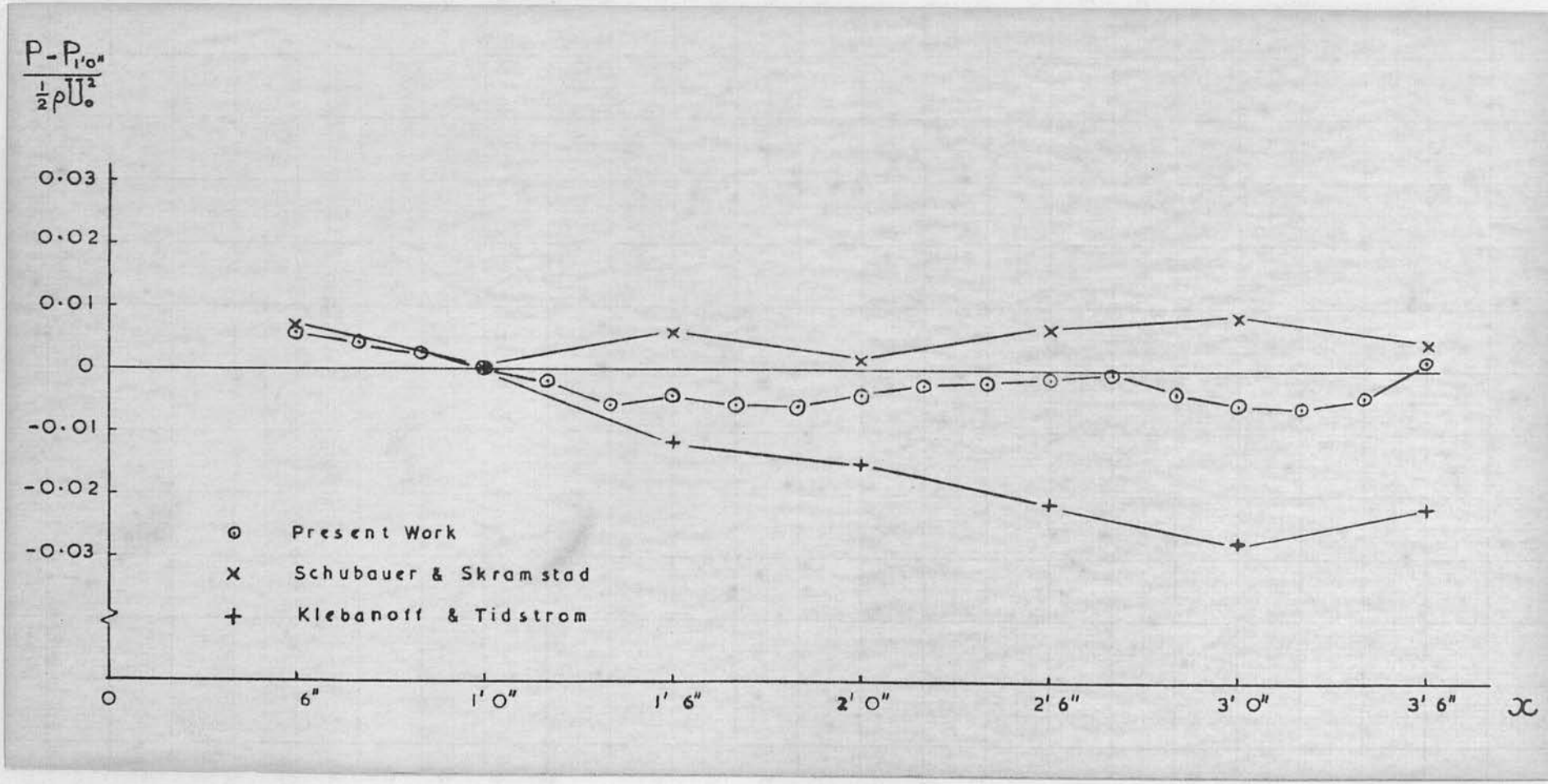

Figure II.6. Pressure Gradient in the Working Section.

CHAPTER III

THE VIBRATING RIBBON TECHNIQUE

III.1. Introduction

The vibrating ribbon technique for the introduction of controlled disturbances into the boundary layer was first used by Schubauer and Skramstad (1947). In their experiment a thin flat ribbon of phosphor-bronze was placed, edgewise to the flow in the boundary layer, a few thousandths of an inch from the surface of the flat plate. Sellotape spacers were used to mount the ribbon to the plate; a further layer of sellotape along the length of the ribbon, with the exception of the vibrating span, held it in position. Rubber bands attached to ends of the ribbon kept it under tension. The ribbon was made to move in a direction perpendicular to the plate surface by passing through it a small current alternating at the desired frequency in the presence of a strong magnetic field from an electromagnet on the opposite side of the plate. In this way approximately two-dimensional disturbances of a chosen frequency could be fed into the boundary layer. When the ribbon was not vibrating, its effect on the boundary layer could not be detected. The width of the ribbon, its distance

from the plate surface and the length of the vibrating segment were features which appeared to have little effect on ribbon performance.

No attempt was made by these workers to estimate the amplitude of the ribbon vibration and no mention was made by them of the relative values of forcing frequency and ribbon resonant frequency. They did state, however, that forcing frequencies of from 10 cycles/sec. to 260 cycles/sec. were used.

Subsequent workers at the National Bureau of Standards have continued to use the vibrating ribbon technique, but in their reports have given few practical details about methods of usage. Klebanoff and Tidstrom (1959) mention that the ribbon resonant frequency was kept near the working frequency by means of the rubber bands attached to the ends. By placing pieces of sellotape on the plate beneath the vibrating span of the ribbon, Klebanoff, Tidstrom and Sargent (1962) were able to use this technique to inject controlled three-dimensional disturbances into the boundary layer.

The vibrating ribbon technique has been used by other workers in studies of aspects of transition on a flat plate (c.f. Kovasznay (1960), Tani (1960)). In general, the systems used appear to have been similar to that of Schubauer and Skramstad with only minor modifications. However, once again few details were reported.

The technique has been applied in the study of flow over a water-table by Hama (1960). To meet the very low frequency requirements for work in water (about one hundredth those for air), the roles of the ribbon and the electomagnet were reversed in this experiment; a direct current was supplied to the ribbon while the electromagnet was excited by a sine-wave signal of the desired frequency fed from a power oscillator.

In view of the limited amount of information available on ribbon systems, and, in particular, on the best method of mounting, the best mode of operation, and the extent to which the ribbon could be considered to produce two-dimensional vibrations, it was felt that the technique warranted further study. Consequently, before a ribbon was used in boundary-layer studies, a series of preliminary experiments were carried out with a view to finding out more about the ribbon system itself.

III.2. Preliminary Experiments with Ribbon Systems

a) Experimental arrangement

For the first part of this subsidiary investigation of ribbon behaviour a small wind tunnel with 9 x 2.3/4 inch working section and 9:1 contraction ratio was used. The ribbon was mounted, transverse to the flow, in the boundary layer on the roof of the tunnel working section. This position allowed the permanent magnet, and the probe used to study the ribbon motion, to be placed on the

outer surface of the 1/4 inch perspex roof, which was suitably stiffened to prevent sagging due to the reduced pressure inside when the tunnel was running.

The method of mounting the ribbon is shown in Figure III.1a. The ribbon, a phosphor-bronze strip, 0.001 inches thick, by 0.1 inches wide, by approximately 15 inches long, was held a fixed distance from the roof of the tunnel at two bridges of drawn glass tubing, the spanwise separation of which was 6 inches. The distance of the free segment of the ribbon from the surface was set by the diameter chosen for the glass bridges. A diameter of 0.007 inches was used throughout these experiments. The regions of the ribbon between bridge and tunnel wall were held firmly against the tunnel roof with sellotape. At one side no freedom of movement was allowed, but at the other side the ribbon could be moved in its longitudinal direction enabling tension to be maintained throughout its length. This end of the ribbon was passed through a slit in the tunnel wall, and a hook soldered to it. A rubber band, stretched between this hook and a clamp fixed to a firm support, was used to tension the ribbon. Adjustments could be made to the clamp to alter the tension and consequently the resonant frequency of the ribbon.

This method of maintaining the tension was used after another method had proved unsuccessful. In this,

the free end of the ribbon, after emerging from the tunnel, was passed over a horizontal rod to hang vertically. Tension was applied by hanging weights from the hook. Various types of bearing and methods of lubrication between ribbon and rod were tried, but in all cases the friction between these surfaces prevented a constant tension being maintained.

A small permanent horseshoe magnet, 1.1/8 inches long, was mounted on the tunnel roof over the centre of the free segment of the ribbon. The alternating current used to excite the ribbon was supplied from a power oscillator.

The ribbon motion was studied using an electronic system sensitive to small changes in capacitance which had been developed at Edinburgh University by Burns (1958) and Nicol (1958). In this system fluctuations in capacitance of order $\pm 10^{-3}\mu\mu$F. produced frequency modulation of a 1Mc./sec. wave. The frequency modulation was converted to amplitude modulation in a high Q filter when the mean operating frequency of the oscillator coincided with the frequency of maximum slope on the response curve of the filter circuit. The output of the filter circuit was passed through a detector stage to a low frequency amplifier and thence to a cathode ray oscilloscope or valve voltmeter.

A special probe to be used as a transducer for ribbon motion in conjunction with these electronics was constructed. This is illustrated in Figure III.1b..

The sensing element, a thin piece of copper, 1/8 inch square, was mounted near the centre and embedded flush with the surface of a 6 x 1/2 inch strip of 3/8 inch thick perspex. An area of the perspex surface, 2 x 1/2 inch, surrounding the copper square was covered with metal foil screening (Figure III.1b.). Screenedcable was used to connect the copper plate to the electronics.

The perspex strip was placed on the outer surface of the tunnel roof immediately above the ribbon, as shown in Figure III.1a. It could be moved across the roof to allow the copper plate to be placed above any part of the segment of the ribbon which was free to vibrate.

The ribbon was maintained at earth potential as was the metal foil screening; the copper plate acted as the static plate of a capacitor; an area of ribbon immediately beneath it, small in size due to the screening, acted as the other plate. Changes in capacitance as the ribbon vibrated were detected by the electronic system, allowing the amplitude and waveform of the vibration of each element of ribbon along the free segment to be studied as a linear relation existed between ribbon amplitude and output voltage.

b) Experiments and results

In the first experiment using this system, the probe was placed above the centre of the free segment of the ribbon. The output voltage of the electronics,

a measure of the ribbon amplitude, was determined for a number of frequencies of sine-wave input signal in the range from 40 cycles/sec. to 250 cycles/sec., with the current in the ribbon circuit adjusted to be the same at each frequency. A graph of output voltage against frequency gave a resonant curve for the ribbon system. A typical graph for frequencies close to the resonant frequency of 180 cycles/sec. is shown in Figure III.2. This graph illustrates the change in the resonant frequency and the change inribbon amplitude observed when the tunnel was running. From curves of this kind it was found that the resonant frequency of the ribbon system decreased as the windspeed increased.

The resonant frequency of the ribbon was found also to be very sensitive to changes in temperature. A 1°C. rise in temperature was on occasion observed to result in a 50 per cent. drop in ribbon amplitude due to a slight fall in resonant frequency.

These results indicated the inadvisability of operating the ribbon with a forcing frequency at or near to the resonant frequency of the system, since a small drift in resonant frequency resulted in a large change in ribbon amplitude even though the current through the ribbon was kept constant.

For forcing frequencies close to one third of the resonant frequency, observation of the output from the electronics, as displayed on a cathode ray oscilloscope, showed that the ribbon motion contained a component at the resonant frequency. This component was dominant when the forcing frequency was exactly one third of the resonant frequency. This fact limited the lower end of the useful operating range of frequencies of the ribbon in relation to the resonant frequency.

The range of forcing frequency for which satisfactory stable operation of the ribbon could be expected is shown in Figure III.3. for a resonant frequency of 180 cycles/sec. In this range it was shown that the ribbon would vibrate at the forcing frequency with only small changes in amplitude resulting from drift in the resonant frequency.

The criteria used throughout the present work have been that the forcing frequency should be not more than five-sixths of the resonant frequency and at least ten cycles/sec. above one third of the resonant frequency.

Under certain conditions the frequency response curve of the ribbon system showed twin resonant peaks, separated, on occasions by as much as 20 cycles/sec. as in Figure III.4. Observations of the ribbon motion using a stroboscope showed that a torsional vibration of

low frequency was present under these conditions. The cause was traced to a graduation in tension across the width of the ribbon. This graduation occurred only when the hook, used to connect the rubber band to the ribbon, was soldered at a slight angle to the ribbon axis. Other methods of attaching the rubber band to the ribbon were tried, but a wire hook, soldered parallel to the edge of the ribbon, was found to be the most satisfactory; if care were taken a frequency response curve with only one resonant peak could be obtained.

The probe was moved to spanwise positions above the ribbon other than the centre of the vibrating segment, and the output voltage, a measure of the amplitude of the ribbon beneath the probe, was determined. In this way it was possible to obtain a profile of the ribbon amplitude along its length. Profiles were determined for a wide range of forcing frequencies and currents in the ribbon circuit. For frequencies in the range described above, the ribbon was shown to vibrate in a single loop, although over only a small region about the centre of the vibrating span could the amplitude be considered to be effectively constant, as can be seen in Figure III.5a.

An investigation of the magnetic field distribution along the axis of the magnet with a search coil and flux-

meter showed that this fell off rapidly with distance from the centre of the magnet, (Figure III.5b). To provide a more uniform field over the central region of the ribbon three magnets were fixed adjacent to each other on the tunnel roof. The magnetic field distribution of this arrangement is shown in Figure III.5d. With three magnets in position the profile of ribbon amplitude obtained was more uniform over the central region, (Figure III.5c.), and thus the disturbance injected into the boundary layer could be considered to be effectively two-dimensional over a two inch region about the centre of the vibrating span. For this reason it was decided to use three permanent magnets in the ribbon system for the boundary-layer investigations.

From this preliminary experiment on vibrating ribbon systems information was gained about experimental arrangements and methods of usage which was to prove invaluable in the operation of the ribbon system in the boundary-layer studies.

III.3. Measurement of Ribbon Amplitude

As the proposed boundary-layer work was not to be confined to the study of one particular frequency of disturbance, it was felt that a quick and reliable method of measuring the amplitude of the ribbon vibration, which could be used over the range of frequencies of interest, would be of advantage. The electronic system used in

the preliminary experiments described in III.2. was unsuitable for measurement of the ribbon amplitude in the boundary-layer studies, because constant monitoring was required in its successful operation.

Other workers using the vibrating ribbon technique had used for the most part a single frequency of vibration. In their reports no indication was given of the method of estimating the ribbon amplitude and it seems possible that in most cases no quantitative estimate of the amplitude was made. It appeared that the ribbon amplitude was set according to its effect on the boundary layer at a downstream position as determined by a hot-wire anemometer.

To investigate the problem of measurement of the ribbon amplitude, a ribbon system, essentially similar in design to that described in Section III.2., was set up on a small flat plate outside the tunnel. As the plate was vertical, tension was maintained in the ribbon by hanging weights from it. An estimate of the ribbon amplitude was made by observing the ribbon motion from an edgewise position with a microscope, fitted with a graduated eyepiece. With suitable illumination the ribbon appeared as a light coloured line against a dark background, broadening into a band as the amplitude of the motion was increased. From these observations it was shown that a linear relationship existed between

ribbon amplitude and the current in the ribbon circuit (Figure III.6.).

It was realised that this relationship could provide the basis for a method of estimating the ribbon amplitude. However, to determine the absolute ribbon amplitude at a given frequency it was necessary to know the current through the ribbon at some reference amplitude for this frequency. The amplitude of the ribbon when it just touched the surface of the plate was found to provide a convenient reference, as this was known, from the diameter of the glass bridges, to be 0.007 inches.

Several methods of determining the point when the ribbon just touched the plate surface as the current was increased were tried. The ribbon system mounted on the perspex plate outside the tunnel was used for these tests. In all of these methods indication that the ribbon was touching the plate was given when an electrical contact was made between the ribbon and a conductor on the plate surface. The first conductor used was a layer of very thin aluminium foil glued to the plate surface beneath the ribbon. An improvement on this was a film of 'aquadag', a suspension of graphite in water, which was deposited on the plate surface beneath the ribbon. However, difficulties in attaching leads to the silver foil and the 'aquadag' film without interfering with the boundary layer flow made these methods impractical, but a further modification of this technique was tried successfully.

For testing of this, a brass plug, 1/8 inch in

diameter, was fitted into a hole in the perspex plate, at a position corresponding to the centre of the vibrating segment of the ribbon. The surface of the plug was milled to be accurately flush with the surface of the perspex beneath the ribbon. A lead was taken from this plug on the reverse side of the plate to a cathode ray oscilloscope. With the ribbon earthed, the display of the shorting of the oscilloscope input as the ribbon touched the brass plug during each cycle of vibration proved to be an accurate method of judging when the ribbon amplitude was 0.007 inches.

The following procedure was finally adopted for setting of the ribbon amplitude. The desired frequency was chosen on the oscillator and the current in the ribbon circuit increased until contact between the centre of the ribbon and the brass plug was just detected on the cathode ray oscilloscope. The weights hanging from the ribbon were altered, changing the tension and ribbon resonant frequency until the current required to cause the ribbon to make contact with the brass plug was 0.7 amperes. The amplitude of the ribbon could then be set as desired using the relation of 0.001 inches per 0.1 amperes current. Care was taken to ensure that the criteria for forcing and resonant frequencies laid down in Section III.2b. were not violated.

This method of setting the ribbon amplitude could be applied to any frequency and was used throughout most of the present work. Experience of this technique in use during the boundary layer studies showed that its accuracy was certainly no better than ± 10 per cent.

III.4. Ribbon Arrangement for Boundary-Layer Studies

The information gained from these preliminary experiments was employed in the design and operation of the ribbon system used to introduce disturbances into the boundary layer.

The phosphor-bronze ribbon, 0.001 inches thick by 0.1 inches wide, was mounted transverse to the flow at a distance of 12 inches from the leading edge of the flat plate in the 18 inch tunnel. Glass bridges, 0.007 inches in diameter, held in place with sellotape, were again used as spacers. The distance between the bridges was 9 inches; they were situated symmetrically about the centre line of the flat plate for most of the present work. The centre of the vibrating segment of the ribbon was displaced, however, to $Z = 0.75$ inches for the later studies. The upper end of the ribbon was held firmly against the plate with sellotape; the lower end was also held against the plate, but was free to move in the vertical direction. Slots were cut in the brass angle mountings for the flat plate and in the roof and floor

of the tunnel, through which the ends of the ribbon were passed. The upper end was clamped to the outside of the tunnel roof, while the lower end hung freely below the tunnel. A hook, which carried a scale pan, was carefully attached to this end; the tension in the ribbon was maintained by placing weights in the scale pan.

Electrical contact was made to the top and bottom of the ribbon. At the lower end this was done by bringing up a rod to just touch the flat surface of the ribbon above the hook. This rod helped to reduce the transmission of small torsional vibrations of the scale pan to the vibrating segment of the ribbon. The current was supplied to the ribbon through an ammeter and switch, by a power amplifier fed from a signal generator.

Three permanent magnets were bound tightly together and mounted, symmetrically about the centre of the vibrating span, on a shelf on the reverse side of the plate.

A brass plug, similar to that used in Section III.3., was fitted flush with the plate surface at the centre of the ribbon. This was used in conjunction with a cathode ray oscilloscope in the estimation of the amplitude of the ribbon vibration.

A small probe, 1/10 inch by 1/4 inch, was fixed to the surface of the reverse side of the plate 1/2 inch be-

low the brass plug. This probe was used to provide an input signal for the capacitance electronic system described in Section III.2a. This electronic system was ideally suited for use in qualitative monitoring of the waveform of the ribbon vibration, the output wave form being displayed on a cathode ray oscilloscope.

Diagrams of the ribbon system used in the 18 inch tunnel are given in Figure III.7.,

With the ribbon arrangement described in this section it was possible to introduce effectively two-dimensional sinusoidal disturbances of controlled amplitude and frequency into the boundary layer on the flat plate.

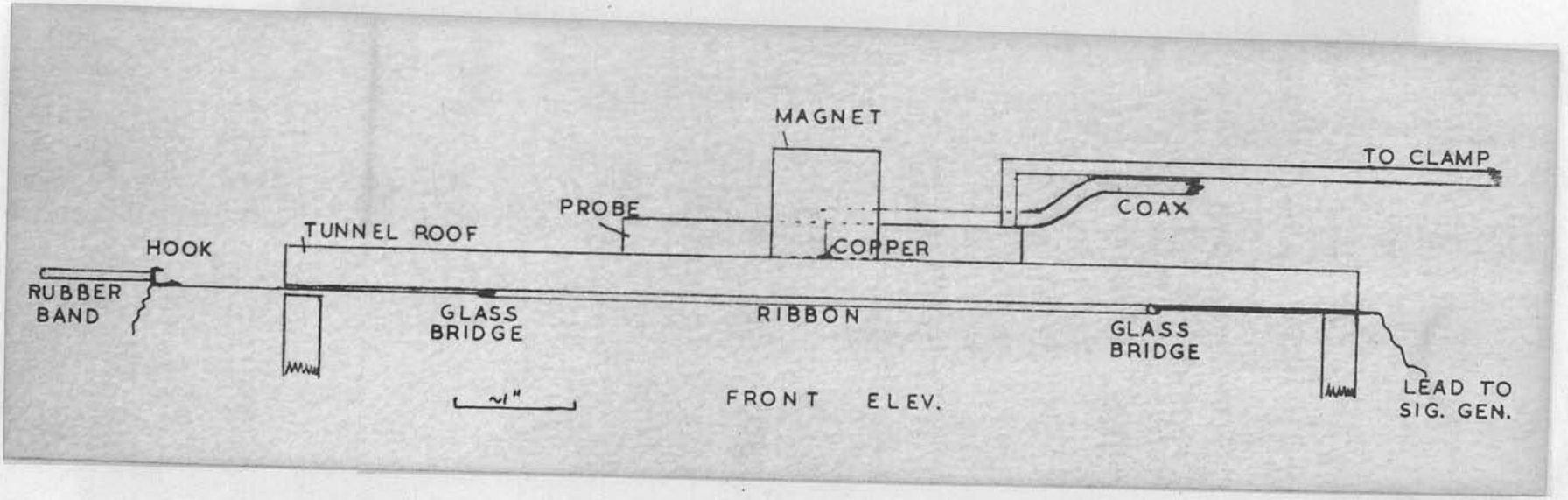

Figure III.1a. Experimental Arrangement for Ribbon Performance Study.

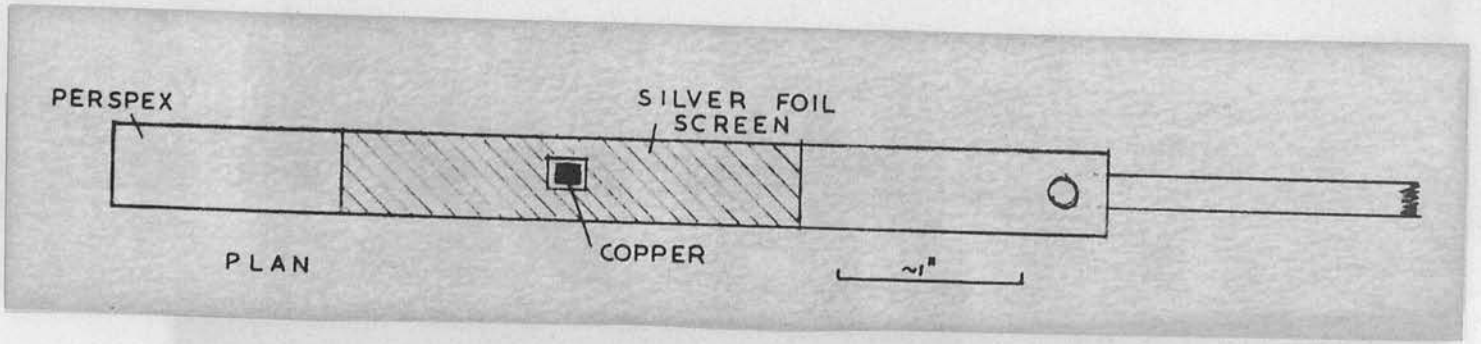

Figure III.1b. Plan View of Probe.

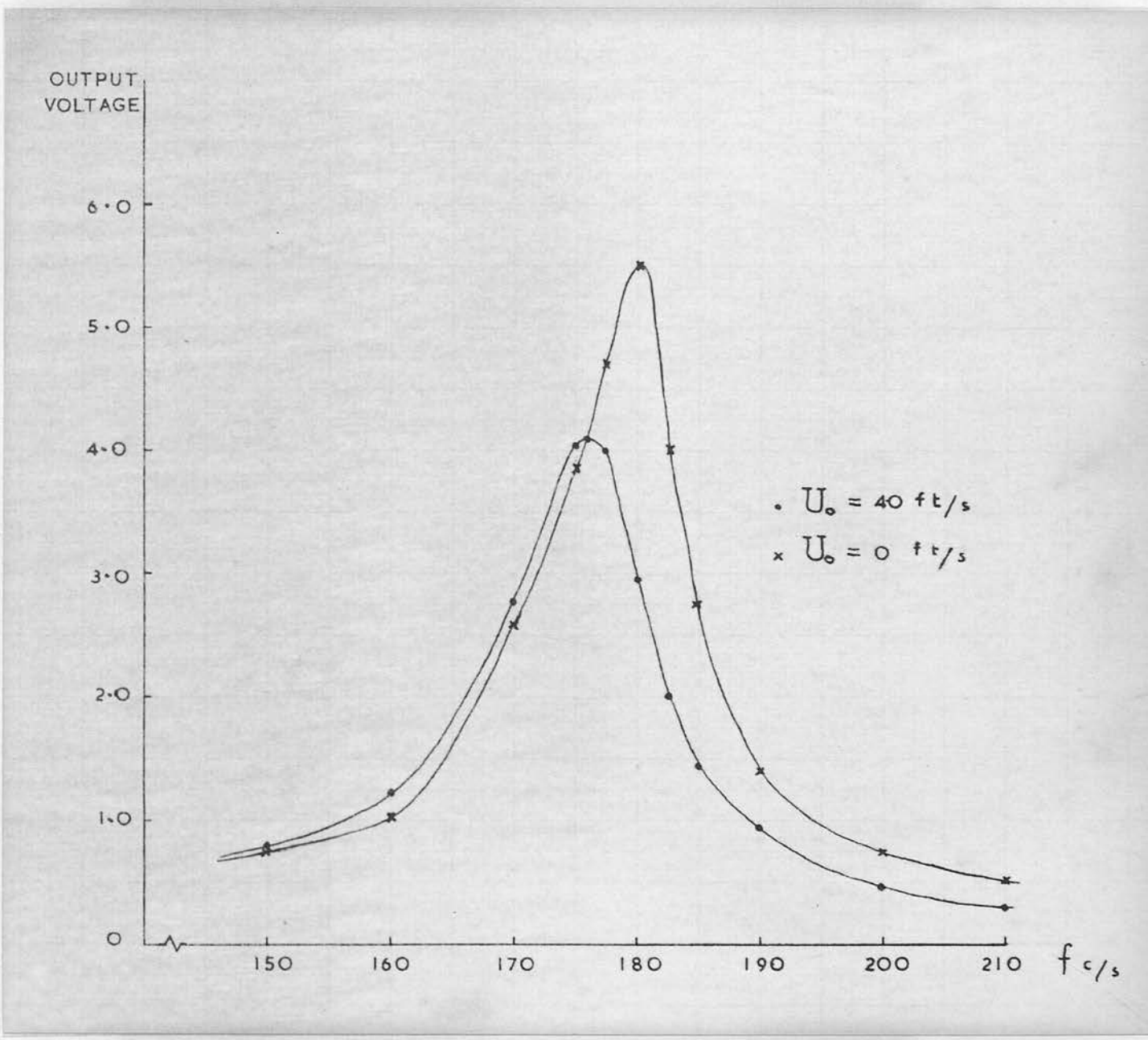

Figure III.2. Frequency Response of Ribbon.

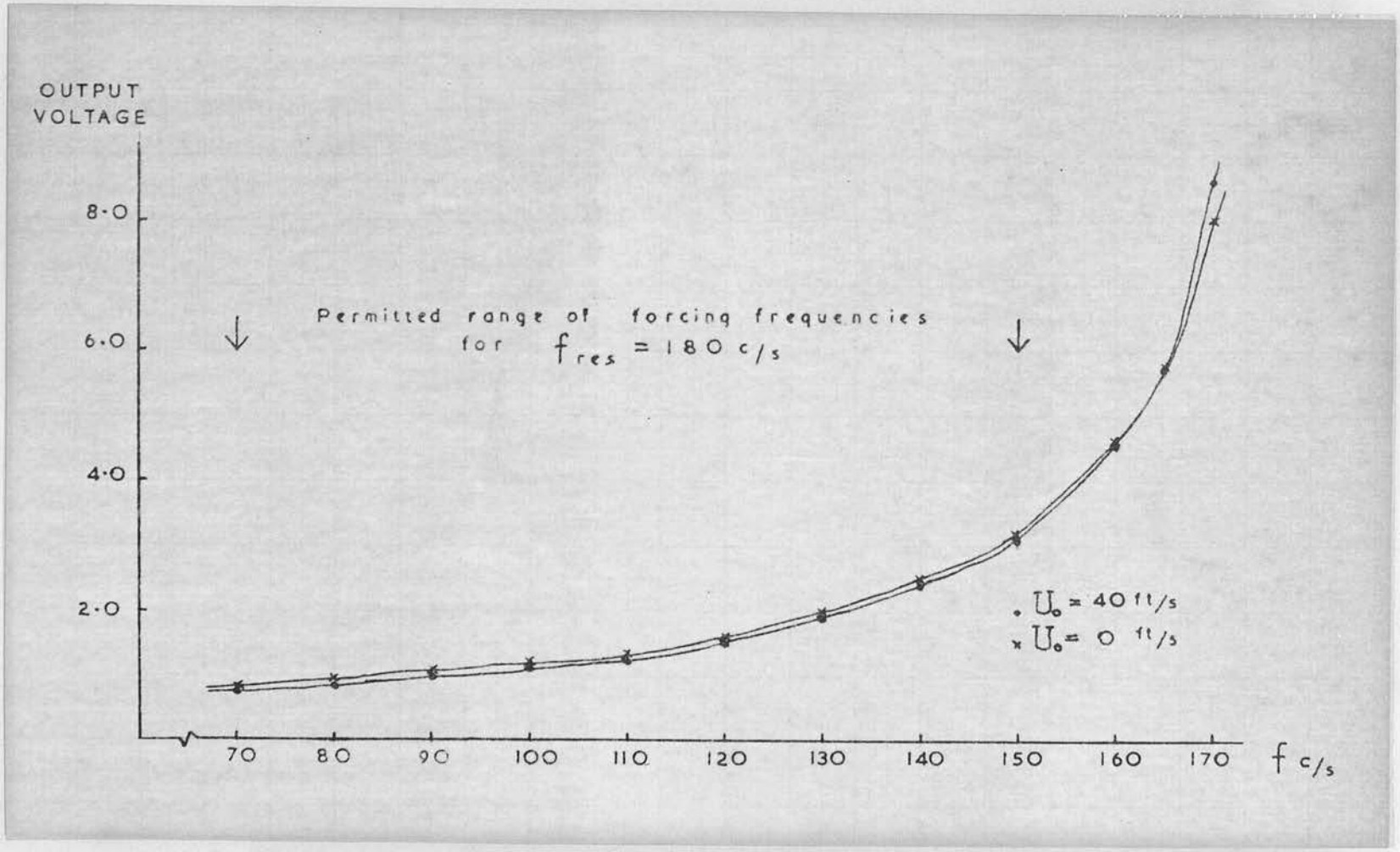

Figure III.3. Frequency Response of Ribbon below Resonance.

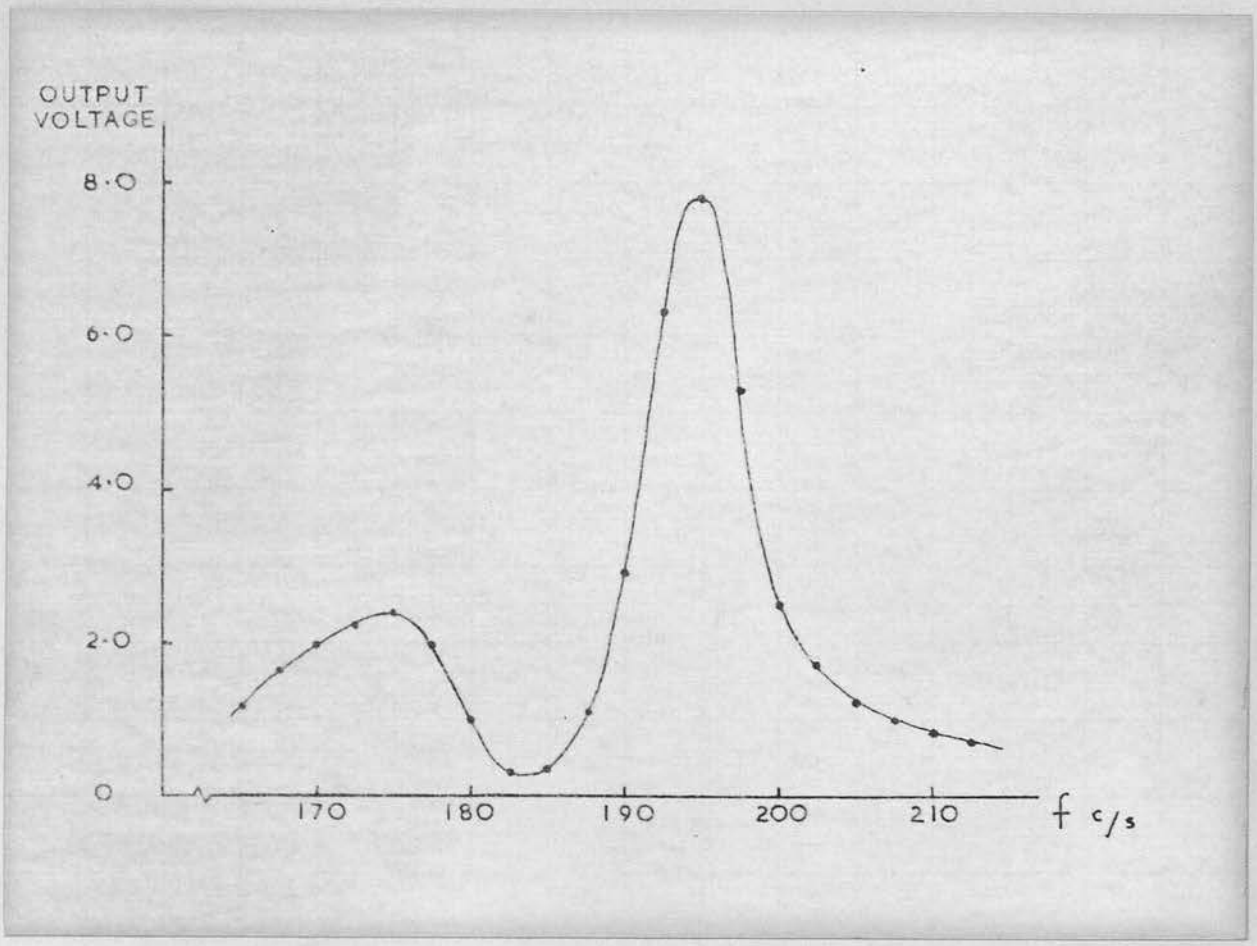

Figure III.4. Frequency Response of Ribbon with Twin Resonant Peaks.

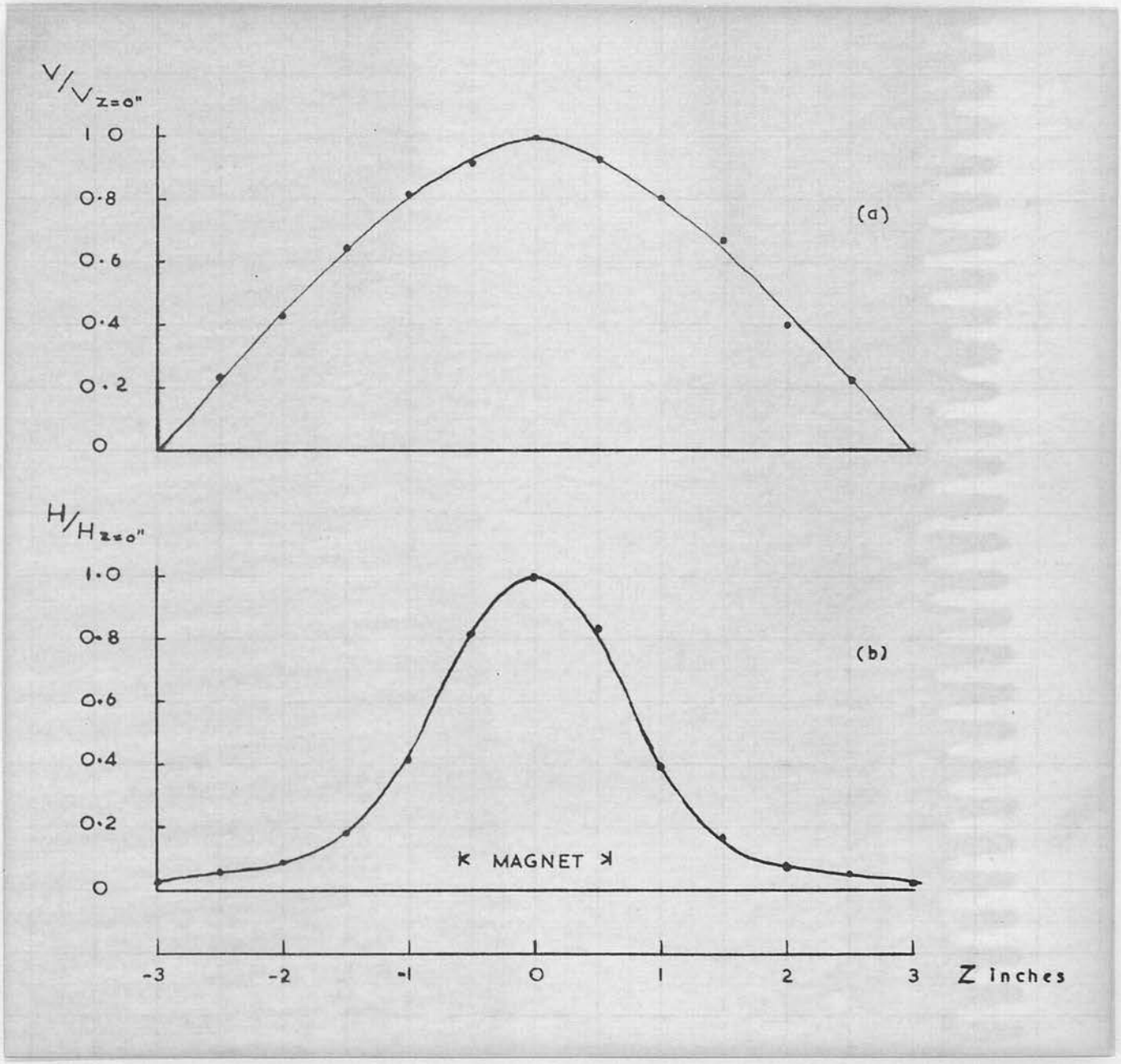

Figure III.5a. Ribbon Profile using One Magnet.

Figure III.5b. Field along Axis of One Magnet.

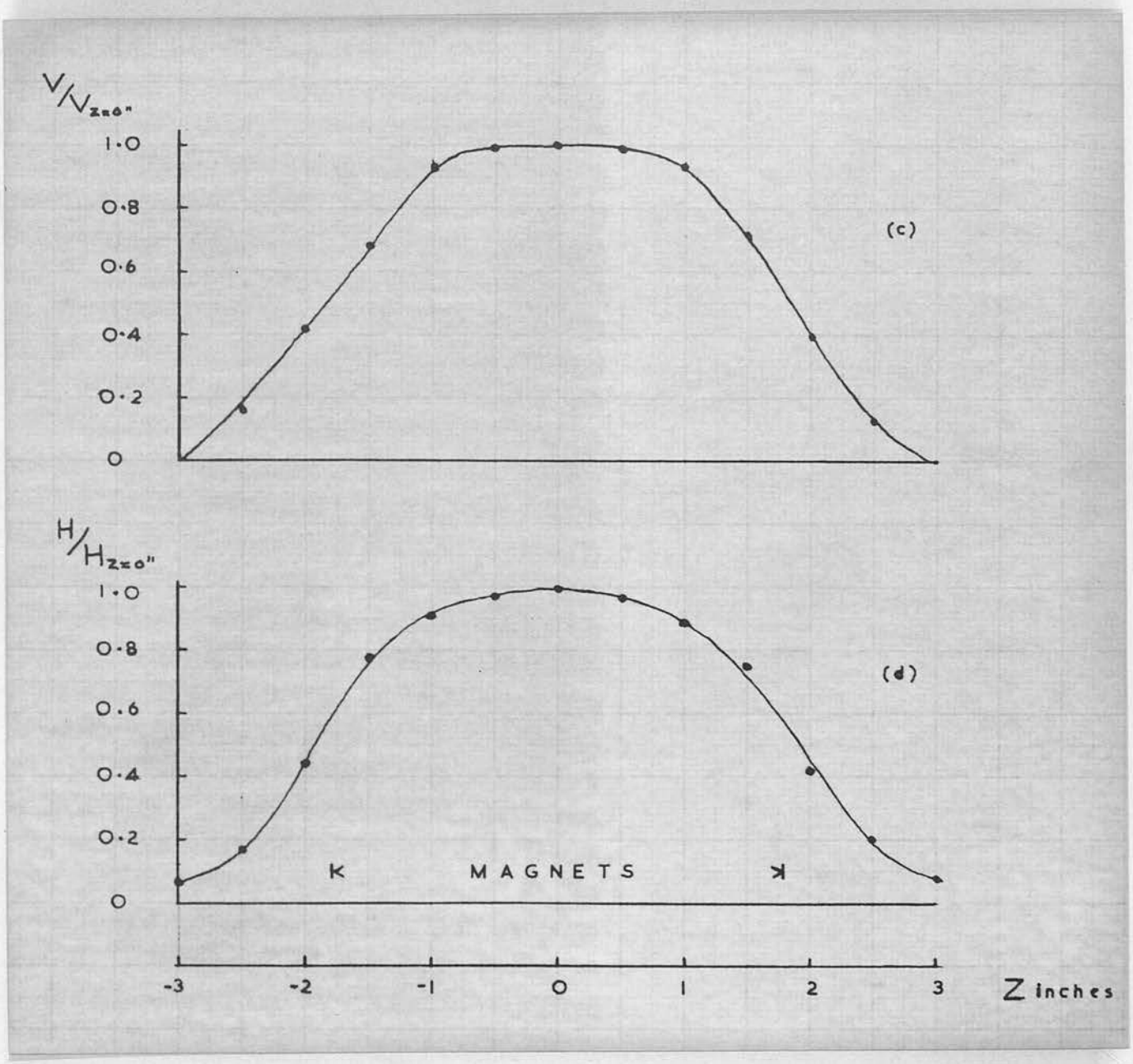

Figure III.5c. Ribbon Profile using Three Magnets.

Figure III.5d. Field along Axis of Three Magnets.

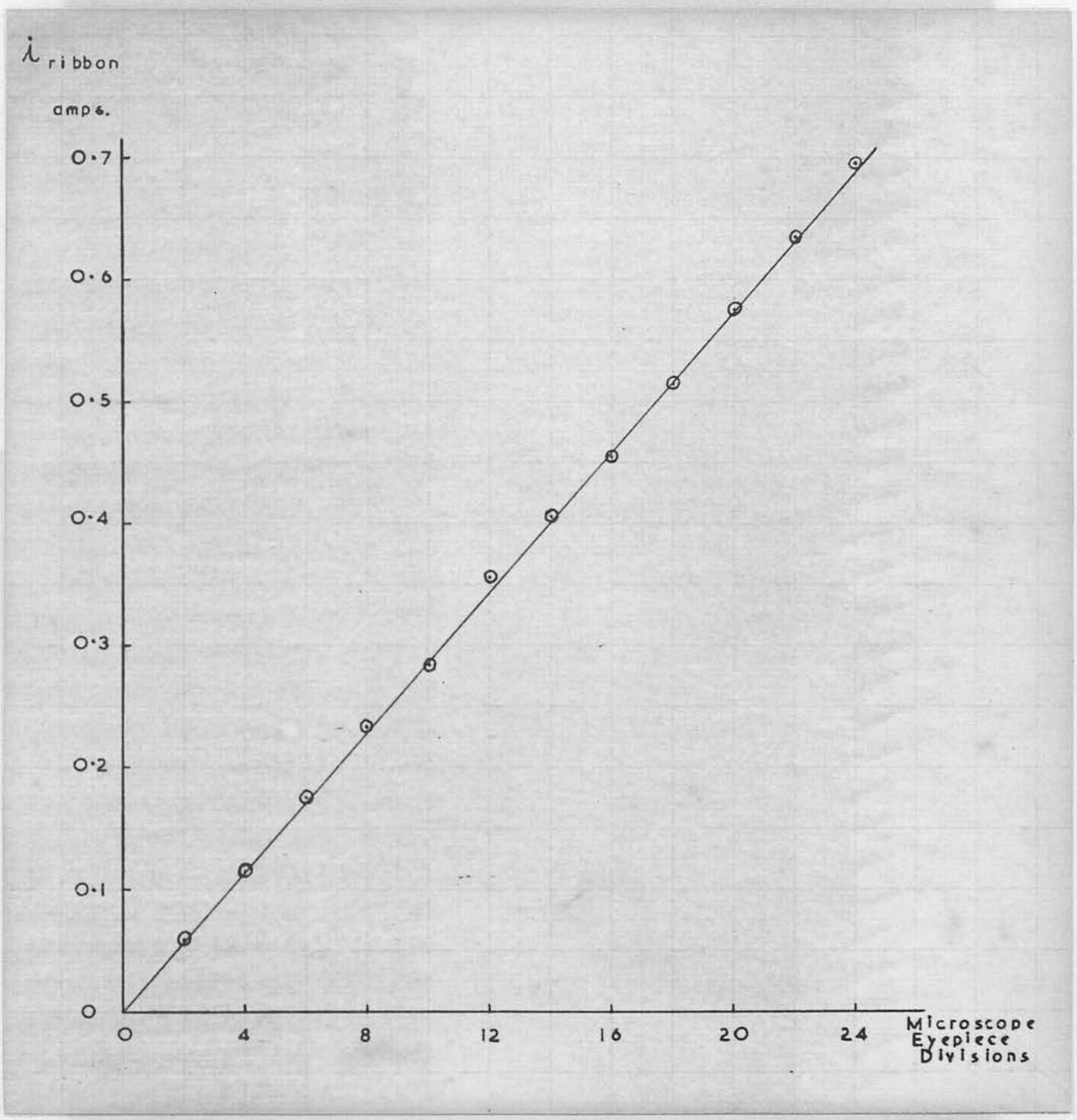

Figure III.6. Optical Calibration of Ribbon Amplitude.

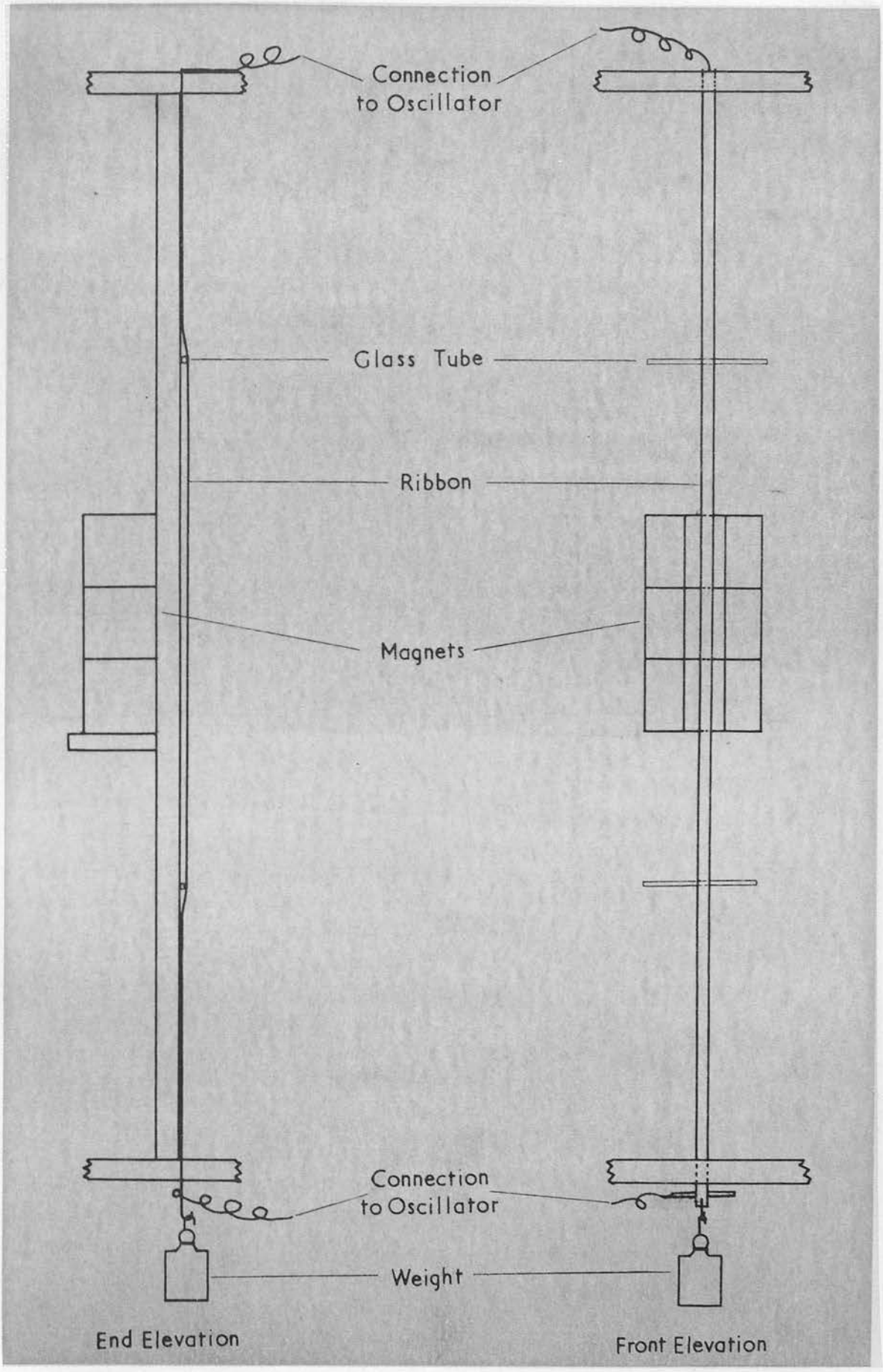

Figure III.7. Ribbon System used in Boundary-layer Studies.

CHAPTER IV

THE HOT-WIRE ANEMOMETER

IV.1. The Hot-Wire Method

The hot-wire anemometer consists essentially of a fine electrically heated wire which is convectively cooled when placed in an airstream.

The relation between the rate of loss of heat from a heated wire and the speed of the airflow over it was the subject of a considerable amount of research in the early years of the present century. King (1914) showed that the equation relating the rate of heat loss from a fine wire (H) and the speed of the fluid in which it was immersed (U) was of the form

$$H = B\sqrt{U} + C \quad ;$$

an equation which has become known as King's law. From experiments with electrically heated platinum wires he was able to verify that the 'constants' B and C were functions of temperature and of the physical properties of the wire and the fluid; moderately good agreement between theory and experiment was obtained.

Experimentally, hot-wire anemometry was confined to the measurement of mean flow speeds (hence the name 'anemometer') for many years. Hot wires several inches long were used for this. Simmons and Bailey (1927)

developed the hot-wire technique and were able to measure flow direction with a three wire array. An account and bibliography of mean flow measurements with early hot-wire anemometers was given by Ower (1933).

A hot-wire anemometer held transverse to the stream was used first to record the variation of longitudinal speed in the flow by Dryden and Kuethe (1929). Since then the hot-wire method has been developed by many workers, some of whom will be referred to later in this chapter. The extent of this development is illustrated by the recent report by Kovasznay, Komoda and Vasudeva (1962) of a ten-channel, transistorised, linearized and compensated hot-wire anemometer system.

Papers dealing comprehensively with hot-wire anemometery include those by Cooper and Tulin (1955), Kovasznay (1959), Bradshaw (1961) and Bradshaw and Johnson (1961).

A brief account of some of the theory of hot-wire anemometry relevant to the present work is given in Appendix II.

IV.2. Requirements for the Hot-Wire System

In the design of the hot-wire anemometer certain requirements had to be met. These were influenced by the proposed aquisition by the research group of a very low turbulence wind tunnel, the specification of the hot-wire system allowing it to be used as a major tool in such a tunnel.

It was decided to build a two-channel hot-wire unit with provision for addition and subtraction of the signals from the separate wires. A low electronic noise level was essential; a typical voltage fluctuation across a wire is 1mV. for 1 per cent turbulence. An upper frequency response of at least 10 Kc./sec. was made necessary by the 100 feet/sec. capability of the proposed tunnel. A further requirement was the ability to supply steady currents of between 1mA. and 100mA. to hot-wires with resistances between 2 ohms and 100 ohms.

Two methods of hot-wire operation present themselves to the designer and potential user of the method: constant current operation and constant temperature operation. Although the constant temperature method is the simpler to use, the design of stable feedback amplifiers poses problems. Non-linearity restricts constant current operation to the measurement of low intensity turbulence, but this was no limitation in the present work. The decisive factor in favour of constant current apparatus was, however, the lower electronic noise level possible with this system.

IV.3. Components of the Hot-Wire Anemometer

The equipment required to make measurements on fluctuating air flows by the constant current hot-wire anemometer method can be conveniently divided into the following five categories:

1) The hot-wire probe, which is installed in the desired position in the airstream and serves as a transducer.

2) The control circuit, bridge and potentiometer whose functions are to control and monitor the mean operating conditions of the hot-wire.

3) The amplifier and compensating unit, which are used to raise to a convenient working level a signal whose time lag distortion has been restored by electrical means.

4) Signal manipulating equipment, used to perform operations on the primary signal. In the present work this equipment was limited to frequency analysis units.

5) The metering circuits used to make quantitative measurements on both the primary and the manipulated signals.

In the following sections these various components are discussed in greater detail with reference to the two-channel hot-wire anemometer constructed for the present work. A block diagram of this system is shown in Figure IV.1. and a photograph in Figure IV.2.

IV.4. Hot-Wire Probes

In the present work, where studies have been confined to the measurement of the longitudinal fluctuating component of velocity and the longitudinal mean velocity only single hot-wires, mounted normal to the flow, have been used.

a) The hot-wire head

The support members of the hot-wire head to which

the sensing element is attached must have a high mechanical strength and must be vibration free. Large amplitude vibrations may cause rupture of the wire, but small amplitude vibration can introduce strain-gauge type resistance fluctuations in the wire which are difficult to distinguish from those due to velocity fluctions. This effect is less likely to be encountered at the lower wind speeds. Other desirable properties of support members are low thermal conductivity and an affinity for soft solder. Consistent with strength requirements, the complete hot-wire head should be as small as is practical to minimise the effects of disturbance of the air flow.

The body of the hot-wire heads was machined from a piece of 1/4 inch outside diameter brass tube. The support members in each head utilised two nickel-plated steel sewing needles, 0.04 inches in diameter and 2 inches in length. These were embedded in 'araldite' in the brass tube approximately 0.1 inches apart, the points of the needles protruding 5/8 inches beyond the streamlined end of the body. Near the rear of the body, one needle was soldered to the tube; the other, insulated from the tube, extended 1/8 inch beyond the end.

A photographic enlargement of a hot-wire head is shown in Figure IV.3.

b) Preparation of the wire

Tungsten and platinum are the most commonly used hot-wire materials. Apart from preliminary studies with 0.001 inch diameter platinum wire, tungsten wire of diameter 0.0002 inches was used throughout the present work. Tungsten, which has a tensile strength some seven times that of platinum, was considered to be more suited to use in the dust contaminated open-circuit wind tunnel. This material, however, oxidises rapidly at temperatures above 300°C., and, unlike the platinum-cored Wollaston wire, is not wet by soft solder. To overcome this latter restriction, special techniques have been developed to attach the tungsten sensing elements to the supports. These include:

1) Soft-soldering of a length of copper-plated tungsten wire to the supports and subsequently exposing the tungsten by etching the copper with dilute nitric acid (Bradshaw (1961)).

2) Controlling the copper-plating process so that the required length of tungsten is left unplated (Schubauer and Klebanoff (1946), Wise and Schultz (1955) and Miller (1963)).

3) Spot-welding of the bare tungsten wire to the supports. (van der Hegge Zijnen (1951)).

4) Attaching wire to the supports with silver conducting paint (van Meel and Vermij (1963)).

The first of these techniques has been used throughout the course of the present work.

To ensure good adhesion and even plating it was essential that the wire was clean. A cleaning bath, of the type suggested by Bradshaw (1961), using a strong sodium carbonate solution, was set up. It was found that the wire fused for a current comparable with that listed by Bradshaw. As it proved impossible to clean the wire satisfactorily by this method, it was abandoned.

The wire could be cleaned by suspending it in a bath of carbon tetrachloride for about 20 minutes. A small blob of solder in which the end of the wire was embedded was used as a weight.

The cleaned length of wire, hanging from the reel, was washed in distilled water and then transferred to a copper plating bath. This bath contained a saturated solution of copper sulphate with 10 per cent. by volume of concentrated sulphuric acid and had a copper anode. Electrical contact with the wire was made by gently placing a metal rod on the reel of wire as shown in Figure IV.4.

Plating was carried out slowly to ensure good adhesion between tugsten and copper; with excessive currents uneven plating and a brittle wire results. A current of 0.3 mA. was used over a period of several hours. Optimum diameter of the plated wire was found

to be about 0.001 inches. Wires thinner than this were difficult to handle, while thick wires were often brittle and were found to be difficult to fix to the supports.

c) Mounting of wires

The mounting of the plated wire on the supports was a delicate operation which required considerable practice.

The hot wire head was firmly clamped with its prongs parallel to and about 1/2 inch above the surface of a glass plate. A sheet of white paper below the plate and a light improved the illumination.

A length of copper plated tungsten wire was gripped about 1/2 inch from the end with a pair of tweezers. It was then held vertically with its end touching the tip of one of the needle supports, the ends of which had been 'tinned' with solder. A touch from a fine soldering iron was sufficient to fix the contact between wire and prong. The wire was then bent round this prong until it touched the other prong round which it was also bent and soldered. Figure IV.5 illustrates this sequence of operations in the mounting of wires. The wire was placed under a small tension, to prevent deformation under the aerodynamic forces, by lightly compressing the prongs together while the second contact was being soldered. Fine adjustments in the positioning of wires on the prongs could be made by stroking the prong at the wire position with the solder coated tip of a solder-

ing iron. The surface tension of the solder was sufficient to move the wire by a small amount on the prongs.

The joints between wire and prongs were viewed under a microscope to ensure that good contact existed between them, poor wires being rejected at this stage.

d) Etching

The method employed for etching the copper from part of the wire was that described by Betchov and Welling (1949) and Bradshaw (1961). A fine jet of 10 per cent. nitric acid was directed onto the wire which was connected to the anode of a 6 volt battery. The cathode of the battery was joined to a platinum electrode in the nitric acid reservoir held above the wire. The hot-wire probe was mounted in a jig so that the acid jet impinged on the wire. The jig allowed movement of the wire beneath the jet in a longitudinal direction. In this way a controlled length of wire could be etched in a few seconds. A diagram of the etching apparatus is shown in Figure IV.6.

Hot-wire lengths of 1mm to 2mm have been used in this work. Schubauer and Klebanoff (1946) have shown that the minimum length of wire which can be satisfactorily used is restricted by the effect of heat conducted from its ends. The length to diameter ratios of wires in the present work are above the minimum value quoted by Schubauer and Klebanoff. ($\ell \sim 200:1$)

e) Mounting in the tunnel

The hot-wire probe was mounted in the tunnel on the boom of the traversing mechanism described in Section II.3. The hot-wire head was machined to plug into a brass tube at the end of the boom. The end of the needle extending from the rear of the head made contact with centre lead of a coaxial cable in the tube but insulated from it. The brass tube itself formed the earth lead. The coaxial cable was led to the input on the control unit. In this way the hot-wire circuit was screened all the way to the needle supports.

IV.5. Control of the Mean Operating Conditions

a) Basic circuit

In most applications of hot-wire anemometry, the transducer constitutes one arm of a Wheatstone bridge circuit. Constant current operation is effected by supplying the bridge from storage batteries or regulated D.C. power supplies through large dropper resistances which are used to control the current.

As no suitable D.C. supply was available in the wind-tunnel laboratory a new approach to constant current operation of a hot-wire anemometer had to be made. This approach was to use a transistor, supplied from a low voltage D.C. source, in the stabilization and control of the hot-wire current.

After a series of tests on various types of circuit, the circuit whose basic form is shown in Figure IV.7. was

chosen.

The Wheatstone bridge, one arm of which contained the hot-wire, was incorporated in the collector circuit of the transistor. Control over the current through the hot-wire was effected by a variable resistance in the base circuit of the transistor. Dry cells and later accumulators were used as the 12 volt D.C. source after tests had shown that the ripple factor across the hot-wire from a transistor power pack was larger than the noise level requirements permitted. A 1.1/2 volt dry cell provided base bias, and the fixed resistance in the base circuit prevented a 'runaway' condition being reached when the variable resistance was zero.

A resistance in series with the hot-wire could be varied in 10 ohm steps from 0 ohms to 100 ohms. In this way the resistance in the collector circuit could be kept at an approximately constant value for all hot-wire resistances.

A voltmeter monitored the voltage across the transistor. To maintain the stability of the collector current this voltage was not allowed to drop below 3.5 volts. A further requirement of the transistor used was that its power dissipation did not exceed 500 m.watts. The decade resistance in the collector circuit permitted these requirements to be met over a wide range of operating conditions. Greatest stability

was achieved when the voltage drop across the transistor was at its largest value consistent with the maximum permissible power dissipation in the transistor.

Another important design feature of this circuit was that one side of the hot-wire and the negative terminal of the battery were both at earth potential.

With this circuit, hot-wires of resistances in the range 2 ohms to 100 ohms could be supplied with appropriate currents in the range 5 m.amps to 100 m.amps. With a hot-wire of resistance 5 ohms and a current of 20 m.amps., a 1 per cent. change in hot-wire resistance resulted in a 1/300 per cent. change in the hot-wire current. This stability was better than that claimed for any hot-wire control units available commercially at a reasonable cost at that time.

b) Bridge and potentiometer

The mean resistance of the hot-wire was measured with the Wheatstone bridge circuit. The fixed resistances were Muirhead precision resistances with an accuracy of $\pm$ 0.02 per cent. The decade box, also by Muirhead, gave values from 0 ohms to 10 k.ohms. in 10 ohm steps and had a similar accuracy. The galvanometer was a moving coil Cambridge 'Scalamp' type.

The bridge ratio was chosen to be 5000:1. This ensured that changes of resistance in the variable arm

of the bridge had negligible effect on the current through the hot-wire.

Under the most unfavourable conditions, namely in the measurement of the hot-wire resistance at ambient temperature, the bridge accuracy was better than ± 0.5 per cent.

Resistances in the range 0 ohms to 20 ohms could be measured with the bridge as shown. An interchange of terminals allowed the range to be altered to 5 ohms to infinity.

An accurate value of the hot-wire current was obtained by estimating the voltage across the 10 ohm standard resistance in series with the hot wire. The potentiometer used in this estimation was a Tinsley Type 3184D which had an accuracy under typical operating conditions of ± 0.04 per cent. This instrument was modified to allow it to operate in a vertical position in a standard 19 inch rack.

c) <u>The two-channel system</u>

The circuit of the two-channel current control system finally adopted is shown in Figure IV.8. It consists essentially of two of the circuits described above supplied from one battery source. The switch circuitry allows the bridge and potentiometer to be used

in conjunction with either channel. The main switch was a Pye low-resistance switch. The combination of two signals before amplification required the use of wires whose resistance was more closely matched than was possible by the control of the etching processes. However, the matching circuit enabled the sum and difference of matched outputs from two hot-wires whose resistances differed by up to 20 per cent. to be obtained. The two variable resistances in each base circuit gave coarse and fine control over the current in that channel. Frequent monitoring and fine adjustment of the hot-wire current was made during operation. Provision to supply each wire with a small current (approximately 1 m.amp.) was incorporated in the switching. With this current the ambient or 'cold' resistance of a wire could be measured.

The setting of the time constant of the circuit used to compensate for the thermal lag of the wires required that a square wave be superposed on the hot-wire current. Provision was made to feed square pulses at a frequency of approximately 1 k.c./sec. on to the base of either transistor. A second bridge arm was used in conjunction with the square waves to 'back off' the component of the output voltage due to the square wave current, leaving only the resistance fluctuations.

In this way the square wave setting operation was carried out at constant current as required. Switching ensured that the potentiometer was disconnected during the square wave tests.

The noise level of each channel of this system was less than 10μ.volts root mean square under typical operating conditions.

The two-channel control unit was built on an aluminium chassis with meters and controls to the front and terminals to the rear. The chassis was mounted in a standard 19 inch rack, together with the bridge and potentiometer. Screened cable was used for all interconnections, care being taken to eliminate earth loops.

IV.6. Amplifiers and Compensating Units

a) Amplifiers

Two identical channels were constructed for amplification of the hot-wire outputs and compensation for the effects of thermal lag in the wires.

The basic amplifier in each channel was a Solatron D.C. Decade Amplifier Type No. AA900. This was a stable wide-band D.C. amplifier providing accurate stepped gain amplification of up to 2000 times of low level signals. The output was flat up to a frequency of approximately 40 k.c./sec., and the equivalent input noise over the whole bandwidth was less than 12 μ.volts root mean square.

b) Compensating circuits

The thermal lag of a hot-wire produces an attenuation and a phase shift. It is shown in Appendix II that the frequency response of the wire follows the complex equation $e/e_v = 1/(1 + 2\pi j f M)$ $(j = \sqrt{-1})$ where e_v is proportional to the velocity fluctuations and e is the actual distorted voltage output of the wire. The compensation therefore must have a complex frequency response $1 + 2\pi j f M$. This means that the compensating circuit must also have a characteristic time constant and an amplification which is proportional to the frequency if the frequency is high $(2\pi f M \gg 1)$.

Several circuits with the required frequency response have been used to compensate hot-wire anemometers. The circuits used by the early workers all employed passive components. However, the inductance - resistance circuit of Dryden and Kuethe (1929) and Mock and Dryden (1932), the capacitance-resistance circuit of Schubauer and Klebanoff (1946) and the transformer compensation of Kovasznay (1947) all suffered from serious disadvantages. Improved circuits using negative feedback resistance-capacitance compensation were built by Gould (1945) and Townsend (1947). However, the two-stage circuit of Kovasznay (1953) provided the basis for the present circuit which is shown in Figure IV.9.

With this circuit the ratio between floor (0 - frequency) and ceiling (∞ - frequency) amplification can be as large as 1:250. In this way compensation has been achieved up to frequencies of about 100 K.C./Sec. The time constant $\lambda^{(M)}$ of the circuit could be altered by adjustment of the variable capacitor, one side of which was at earth potential. A further important feature of the circuit was that the basic amplification and the floor to ceiling ratio were both independent of the circuit time constant.

c) Practical compensating amplifier

The circuit diagram of one of the compensating amplifier channels is shown in Figure IV.10.

A low-noise twin triode E.C.C.83 was used in the compensation stage. This provided an uncompensated gain over the stage of approximately 20 times. The floor to ceiling ratio, equal to the feed-back ratio, was set to be approximately 250 by the choice of the resistance in the interstage feedback link.

The time constant was defined by the resistance-capacitance combination in the cathode circuit of the first valve. The resistance was fixed whilst the capacitance could be varied in steps. This capacitance was constructed using precision capacitances in the two lower ranges. In the highest range the capacitances

were selected from a large batch. The use of a Wayne-Kerr capacitance bridge enabled those accurate to ± 1/2 per cent. of their quoted value to be chosen. Capactances from 100 μμF. to approximately 1 μF. in 1000 μμF. steps could be obtained with the variable capacitance. This gave a range of circuit time constants from 0.005 m.sec. to 5 m.sec. approximately.

The frequency response of a compensating amplifier for various time constant settings is shown in Figure IV.11..

The later valve stages of the compensating unit (Figure IV.10) comprised a phase inverter and a push-pull cathode follower output stage. With this system provision was made to drive a passive adding and subtracting circuit for the combination of the outputs from both channels after separate compensation of the hot-wire signals.

The compensating circuits were built in modular units designed to match the Solatron amplifier rack. A photograph of one of the compensating amplifiers is shown in Figure IV.12.

The time constant of the compensating amplifier was set to match that of the hot-wire by the square-wave technique of Kovasznay (1953). The calibration of the compensating amplifiers was achieved using the 'dummy hot-wire' circuit shown in Figure IV.13. This circuit, whose time constant was dependent on the value chosen

for the capacitance, had a frequency response identical to that of a real hot-wire with the same time constant, and thus simulated the behaviour of a real hot-wire. A square wave of frequency approximately 1 k.c./sec. underwent distortion in the circuit. The output from the compensating amplifier coupled after the 'dummy hot-wire' was displayed on a cathode ray oscilloscope. The distorted waveform was restored to its original form when the correct time constant was chosen for the compensating amplifier. This square wave method provided a very sensitive means of adjusting the compensation to the required amount. Figure IV.14 shows the frequency response of the 'dummy hot-wire' and compensating amplifier after setting of the time constant by the square-wave method.

In the work described in the later chapters of this thesis uncompensated hot-wires have been used. This method of operation was chosen as disturbance frequencies of less than 200 cycles/sec. were the only frequencies of interest to the present work, whilst the time constants of the hot-wires used gave an upper cut-off frequency greater than 500 cycles/sec. under all conditions of operation throughout this work.

IV.7. Signal Manipulating Equipment

Only single hot-wires have been used and manipulation of the outputs from these wires has been confined to

harmonic analysis.

For the harmonic analysis a set of filters was constructed following the simplified Q-multiplier circuit of Harris (1951). In this circuit the output of a cathode follower was fed back to the grid of the valve through a tuned circuit. This resulted in an increase in the effective Q-value of the tuned circuit. The practical circuit constructed, which is shown in Figure IV.15., had switching to allow interchange of the capacitances in the tuned circuit. This enabled the filter to be used for three frequencies corresponding to the frequencies of the fundamental, second and third harmonics of the disturbance under observation. Accurate adjustment of the frequency of maximum response of each filter was achieved using trimmer capacitances. A double beam oscilloscope, with a time-base common to both beams, and two signal generators were used in the setting-up procedure. In this way the frequencies of maximum response of a set of filters were adjusted to be accurately in the ratios 1:2:3. A typical response curve is shown in Figure IV.16.

The tuned circuit capacitances were mounted in a box separate from the rest of the circuit. Sets of filters for other fundamental frequencies could be constructed by replacing this plug-in capacitance box by another box with suitably chosen capacitances. Two sets of filters were constructed with fundamental fre-

quencies of 47 cycles/sec. and 65 cycles/sec. respectively.

In the design of the filters the Q-value of each filter was kept below 20. This ensured that a small region of effectively flat response existed about the resonant frequency. However, frequent calibration checks were made on the gain of the filter at the disturbance frequency in use.

The success of the filters described above, in harmonic analysis of hot-wire outputs, resulted in the purchase of a more versatile instrument. The frequency analyzer purchased, a Bruel and Kjaer, Type 2107, proved to be of great value in the later stages of this work.

IV.8. Output Meters

A thermovacuum junction output meter was used during most of the present work. The circuit constructed, incorporating the Cambridge thermovacuum junction, was a simplified version of that described by Bradshaw (1961). This two transistor circuit, shown in Figure IV.17, supplied current to the thermovacuum junction. The output from this, proportional to the mean square of the input voltage, was displayed on a sensitive 'Scalamp' galvanometer. The system was calibrated using a sine wave input from a signal generator.

In the later stages of the work the root mean square meter incorporated in the frequency analyzer was used

as an output meter. The faster response time of this instrument, which had an integrating time to approximately 1 sec. compared to the 15 sec. integrating time of the thermovacuum junction, greatly speeded up the collection of data.

The amplified output signals from the hot-wire, both before and after frequency analysis, were displayed on a Solatron CD1014 oscilloscope. A Cossor oscilloscope with a 35 mm moving film camera was used on occasions to make a linear recording of the amplified hot-wire output.

IV.9. Calibration of the Hot-Wire

In Appendix II it is shown that when the heating current is constant, King's law governing the rate of heat loss from a heated wire normal to an air stream can be simplified to the form $R_w/R_w - R_a = \rho_o + F_1 U^n$ The power n = 0.5 was used by King (1914), and is still valid in many applications of hot-wire anemometry. However, Collis and Williams (1959) have shown that for hot-wires with Reynold's numbers in the range $0.02 < Re < 44$ the value n = 0.45 gives better agreement with experimental results. The Reynold's numbers of the hot-wires used in the conditions of present work all lie within this range.

During preliminary studies it soon became apparent that over the wide range of wind speeds encountered in

boundary-layer work the 0.5 power law did not give sufficient accuracy. Linear calibrations between $R_w/R_w - R_a$ and U^n were obtained however, with n = 0.45 and this value has been used throughout the work.

The equation above shows that a plot of $R_w/R_w - R_a$ against U^n will give a straight line allowing the constants F_1 and ρ_o to be determined. It should be noted that the value of ρ_o obtained in this way differs from the measured value of $R_w/R_w - R_a$ at zero windspeed. Collis and Williams (1959) have shown that the linear relation does not hold at very low windspeeds (less than 0.5 feet/sec.) due to the effects of free convection. However, for all windspeeds encountered in the boundary-layer work described the linear calibration could be applied.

In the calibration procedure adopted values of the hot-wire resistance at the operating current were measured for seven windspeeds at equal intervals in the range from 15 feet/sec. to 45 feet/sec. Care was taken to ensure that the hot-wire was placed in the free stream during calibration. A value of the 'cold' resistance was also determined with the wire in the airstream. Using these values of resistance and windspeed a least-squares best straight line calculation enabled the constants F_1 and ρ_o to be determined. A typical calibration curve is shown

in Figure IV.18. Using the calibration constants F_1 and ρ_o it was possible to obtain values for the fluctuating velocity component from the calibrated output meter readings. The relevant equations are given in Appendix II.

It was found that tungsten wire oxidised in the air at temperatures above 300°C (cf. Schubauer and Klebanoff (1946)). This oxidation resulted in a drift in the calibration of the wire, the hot-wire resistance increasing with time when it was kept for long periods at a high temperature. This calibration drift could be avoided by using smaller hot-wire currents and consequently lower operating temperatures. With the tungsten wire used in this work a current of 45 m.amp. was found to give adequate hot-wire sensitivity without a drift in calibration. Calibration stability was improved also by heating a new wire to near red-heat for several hours before use. Slight changes in the calibration of a wire were found to occur due to the deposition of dust on the wire in the open-circuit tunnel. In practice, as a precaution against drift, a hot-wire was recalibrated each time it was used.

Throughout this work a Ferranti 'Sirius' computer has been used in the determination of the calibration constants from the resistance readings and in the reduction of data. This facility has resulted in a great saving in the amount of labour involved in obtaining meaningful information from the hot-wire anemometer.

IV.10. Determination of the y-position of the Hot-wire

The traversing mechanism using a clock-gauge to make relative measurements of the hot-wire position in the y-direction accurate to 0.0005 inches has been described already in Section II.3.. It was necessary, however, to find some means of setting the hot-wire absolutely with reference to the plate, so that the actual y-distance of the wire from the plate surface was known at any position.

The optical method used to determine the zero position of the hot-wire is shown in Figure IV.19.. A small plane mirror was placed on the floor of the tunnel, lying between the guide rail of the traversing mechanism and the plate, at an angle of approximately 45° to the plate. With the mirror immediately below the hot-wire probe and suitable background illumination the probe and its reflextion in the flat plate were viewed by a telescope mounted on a rail outside the tunnel. With this system it was possible to judge when the tips of the needle supports just touched the surface of the flat plate and the clock-gauge reading at this position could be noted.

The only remaining uncertainty in the estimation of the y-position of the wire was the distance of the wire itself from the plate where the tips of the needle

supports touched the surface. Using the apparatus shown in Figure IV.20. this distance for each wire could be measured outside the tunnel with the calibrated eyepiece of the microscope. The difficulties associated with the mounting of the wire on the supports resulted in slight variations in this distance for different wires, but in general the closest distance of approach of a wire to the plate surface was approximately 0.003 inches.

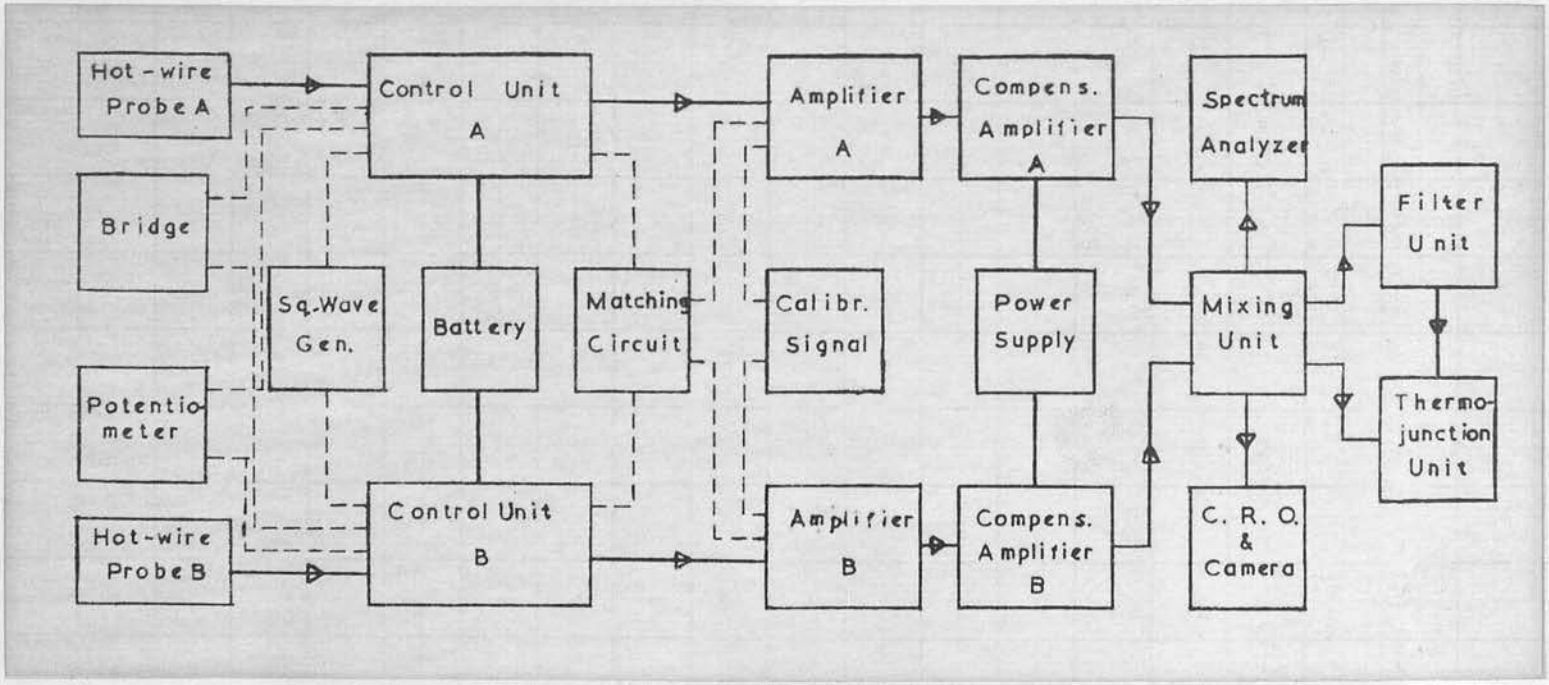

Figure IV.1. Block Diagram of Hot-wire System.

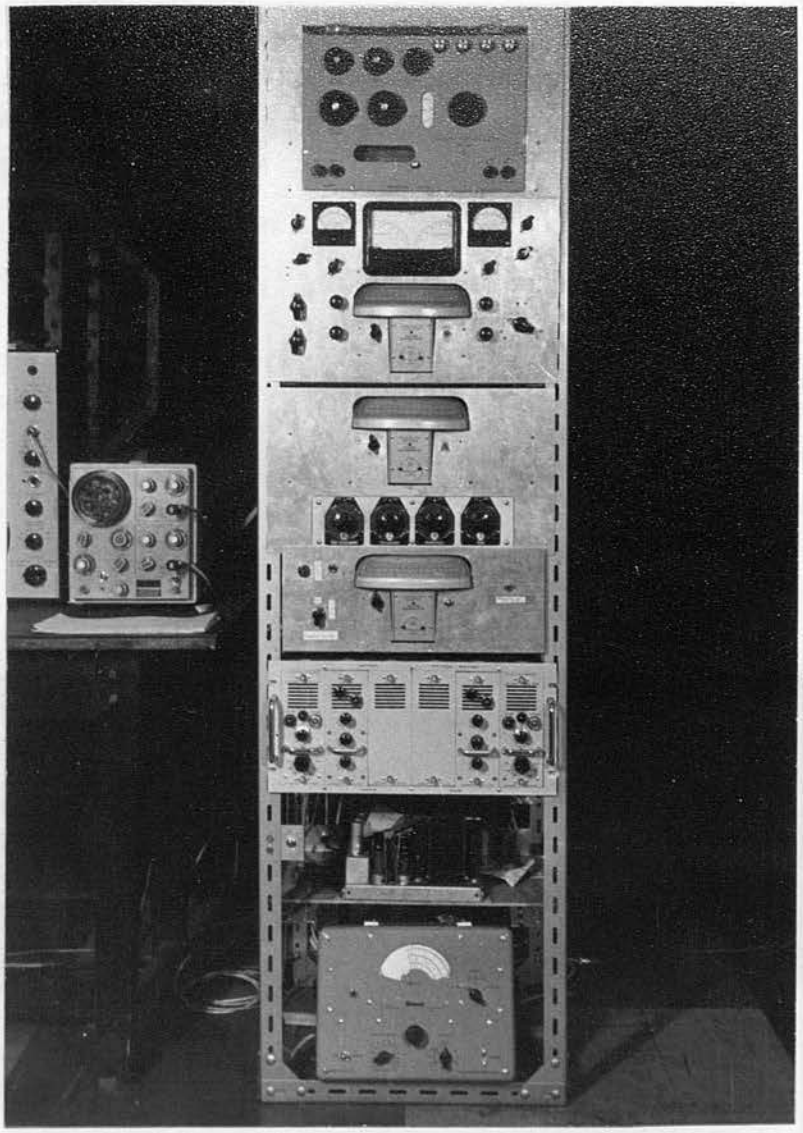

Figure IV.2. Photograph of Hot-wire System.

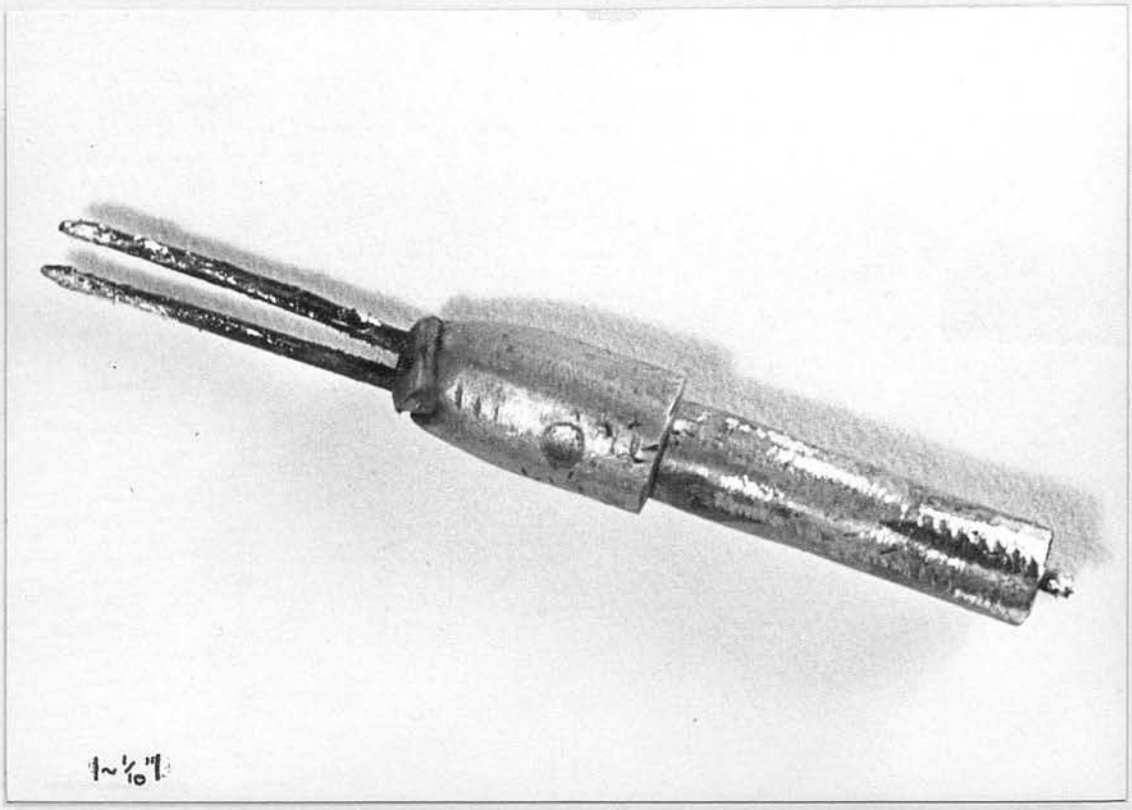

Figure IV.3. Photograph of Hot-wire Probe.

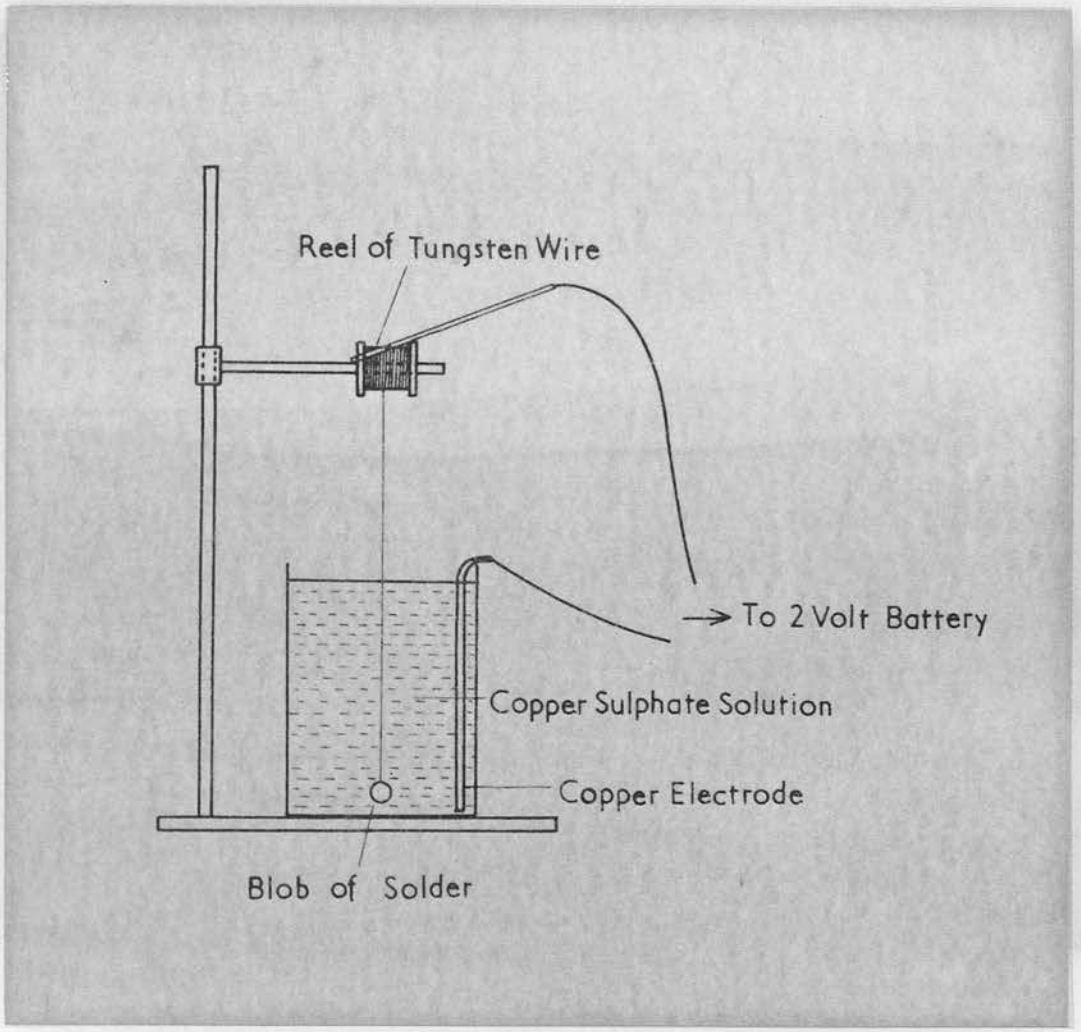

Figure IV.4. Diagram of Copper Plating Bath.

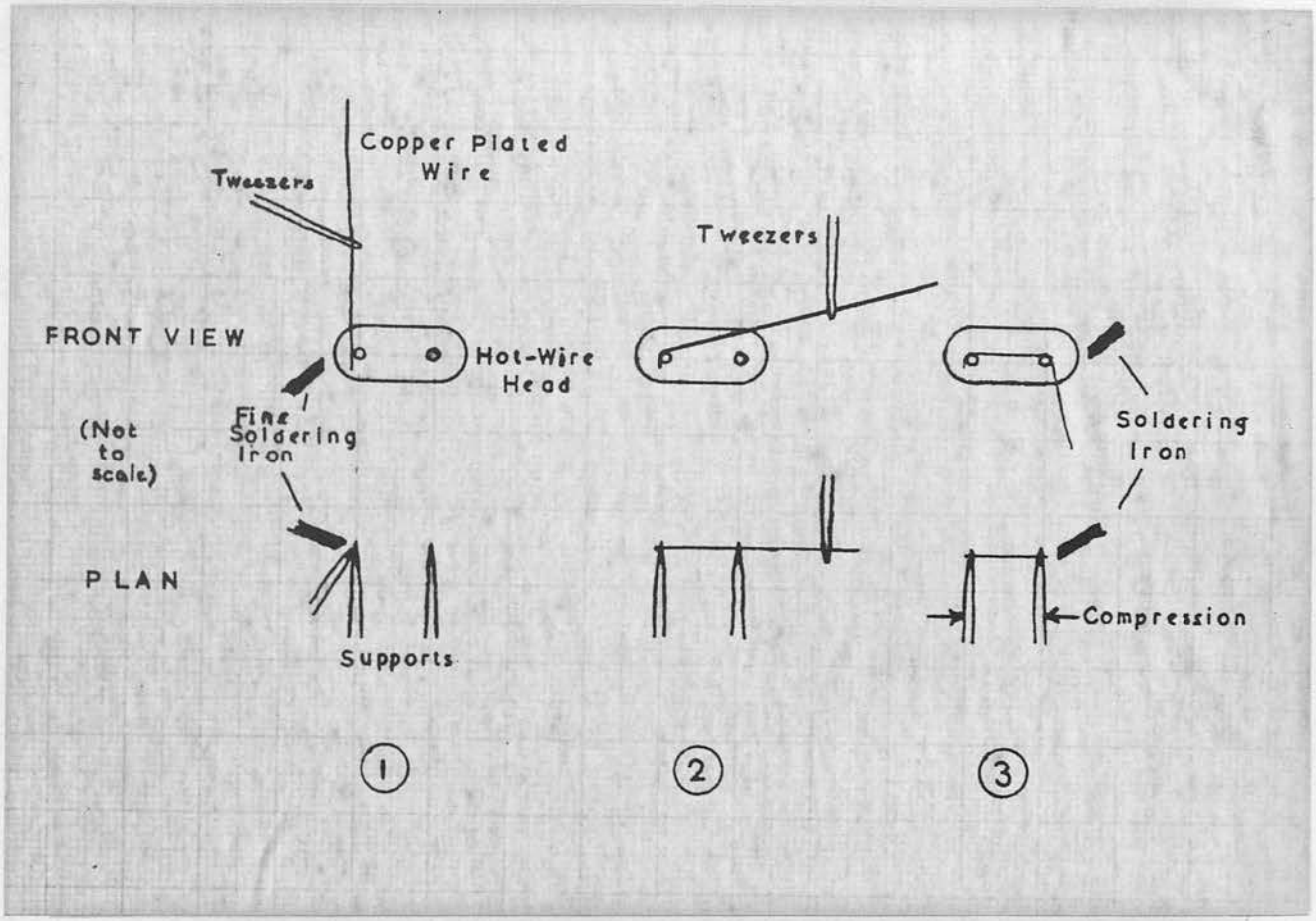

Figure IV.5. Sequence of Operations in Mounting Wires.

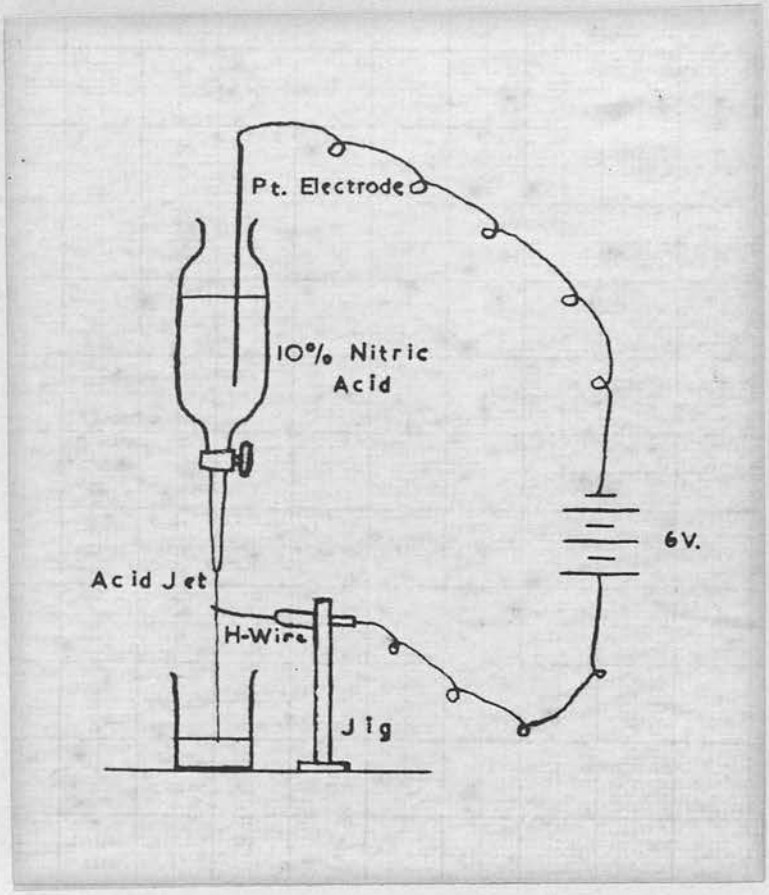

Figure IV.6. Diagram of Etching Apparatus.

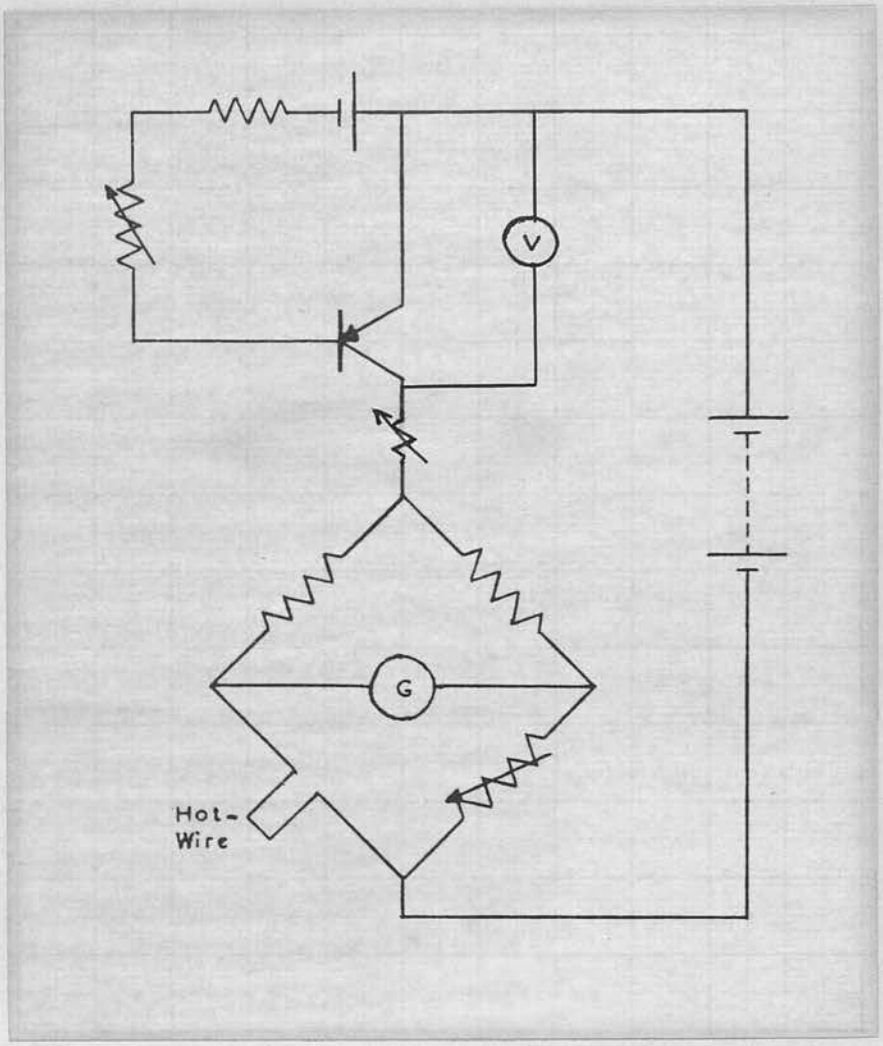

Figure IV.7. Basic Hot-wire Circuit.

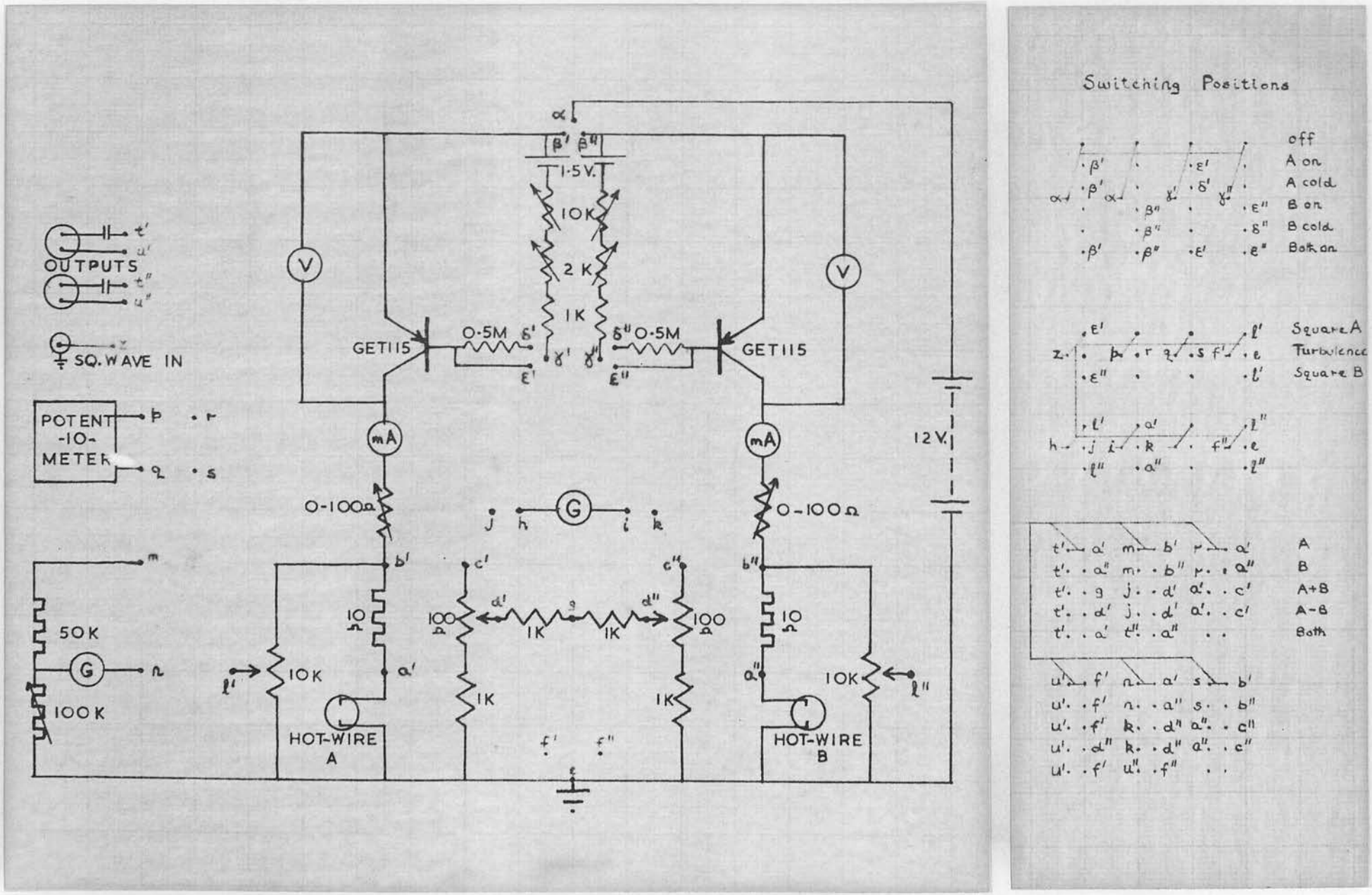

Figure IV.8. Two-channel Hot-wire Circuit.

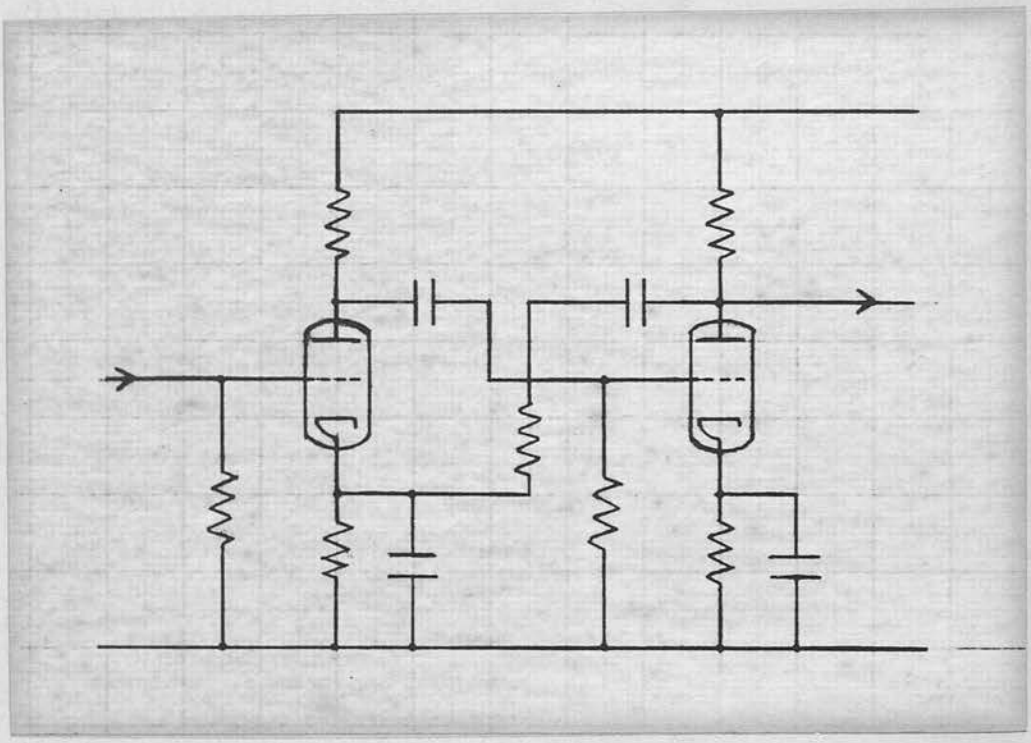

Figure IV.9. Basic Compensating Circuit.

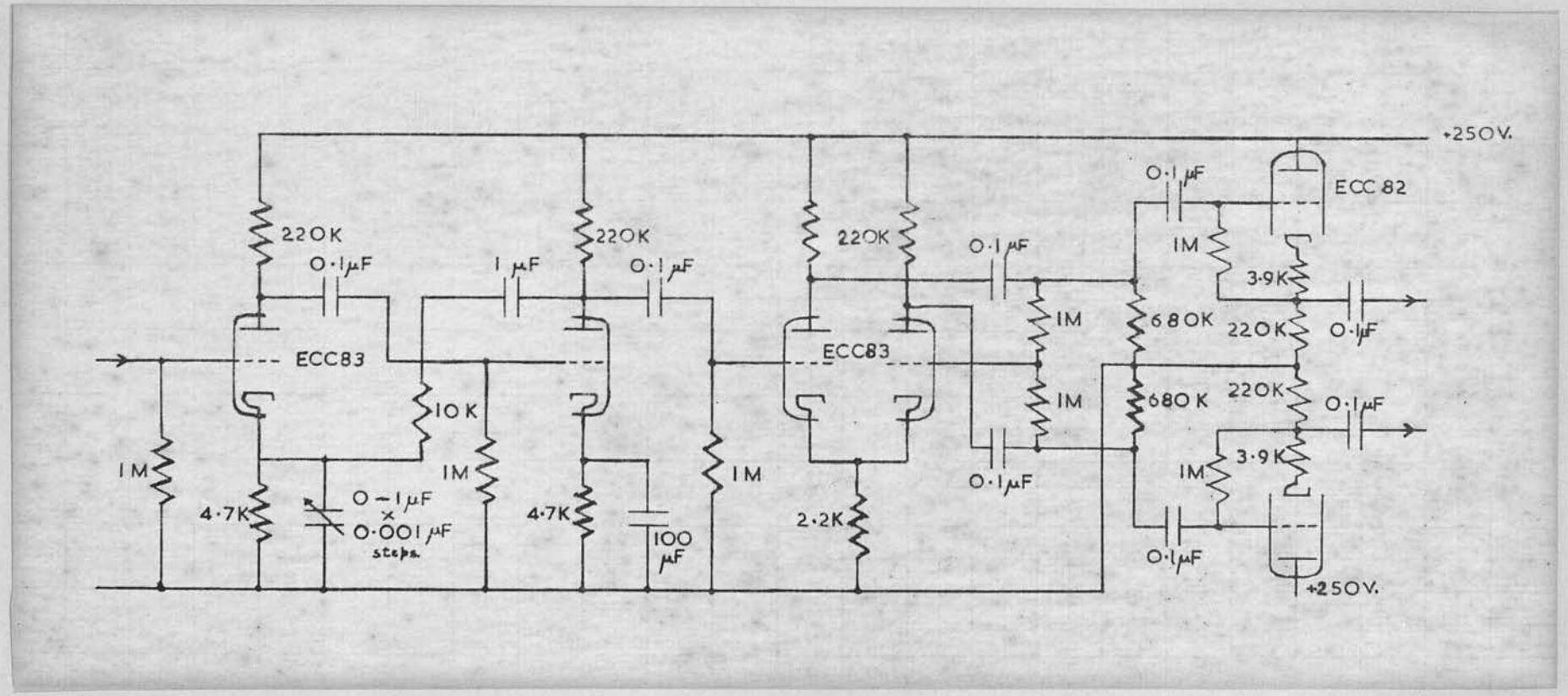

Figure IV.10. Compensating Amplifier Circuit.

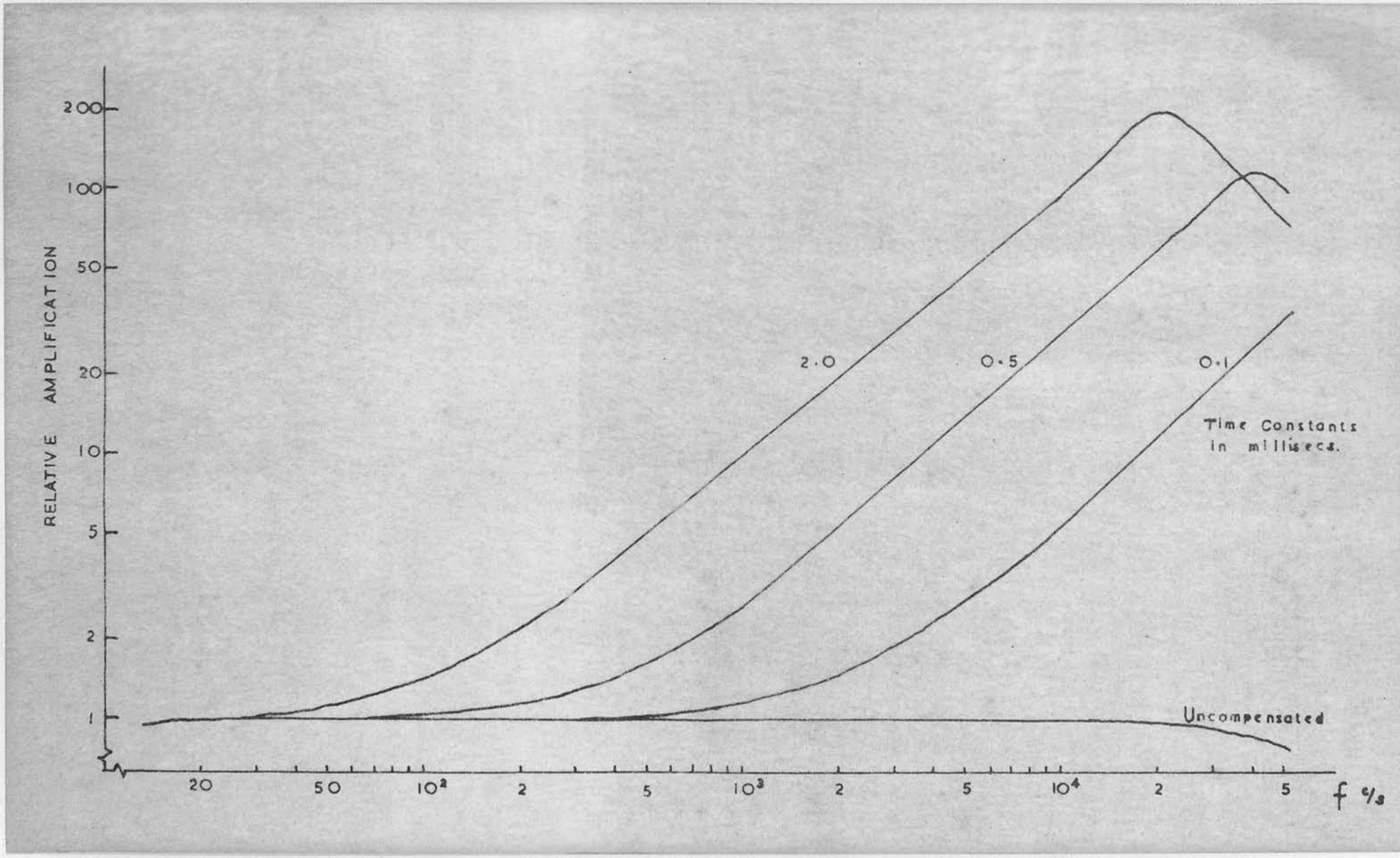

Figure IV.11. Frequency Response of Compensating Amplifier for Various Time Constants.

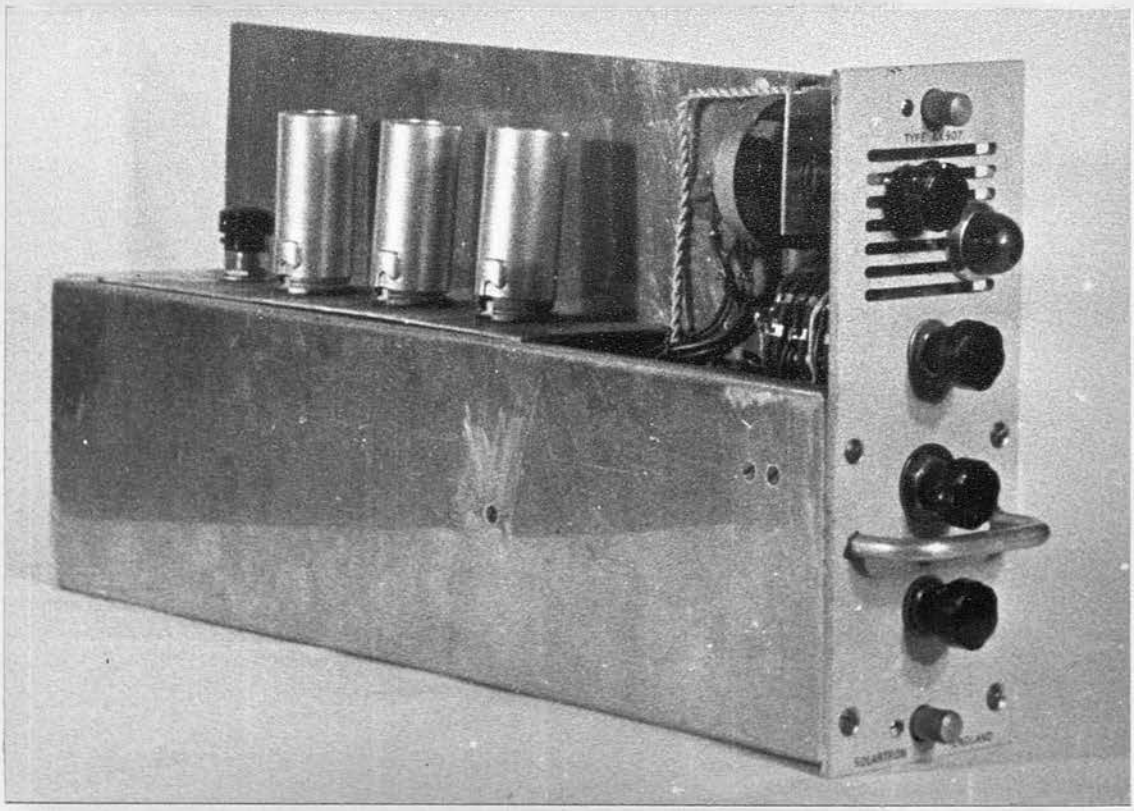

Figure IV.12. Photograph of Compensating Amplifier Module.

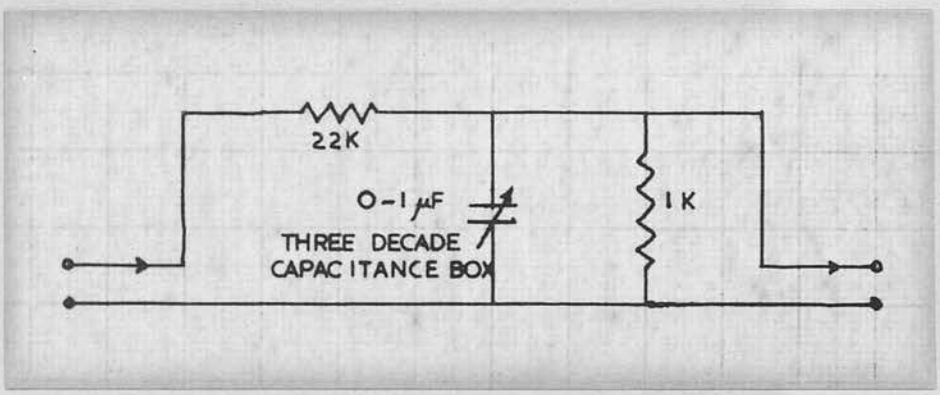

Figure IV.13. Dummy Hot-wire Circuit.

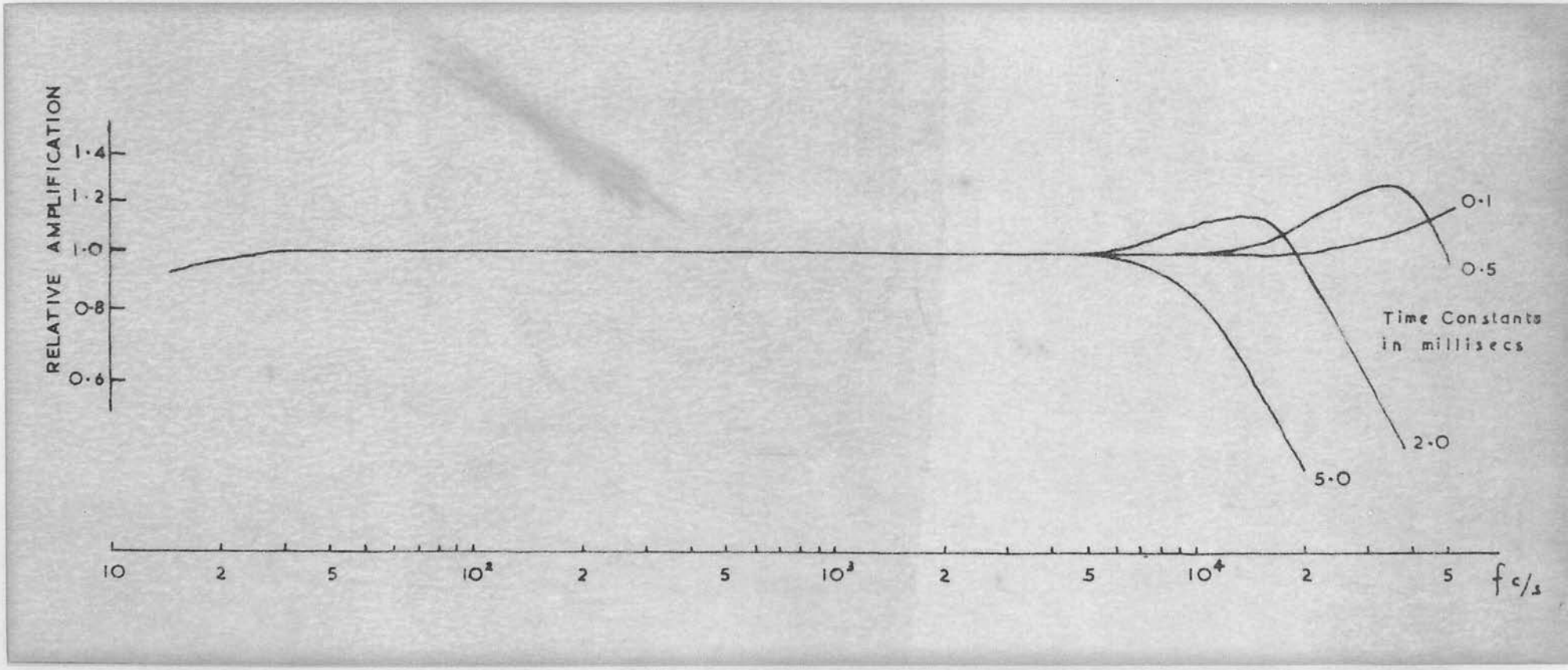

Figure IV.14. Frequency Response of Dummy Hot-wire and Compensating Amplifier for Various Time Constants.

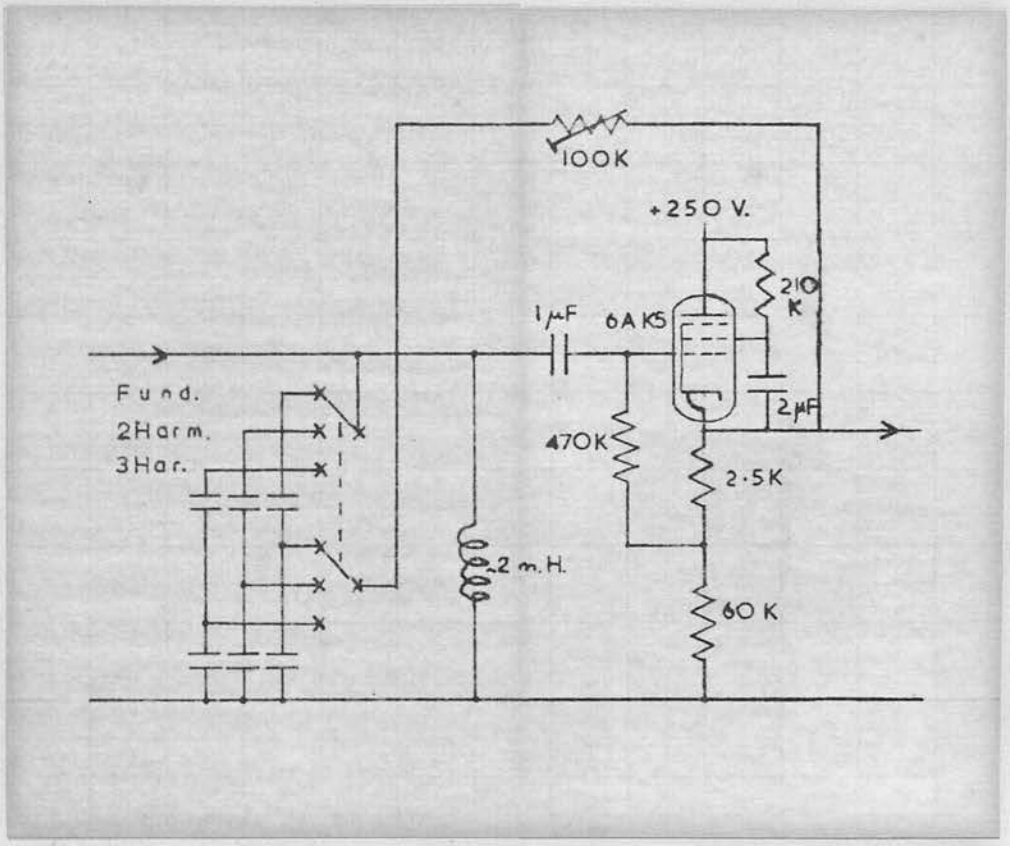

Figure IV.15. Filter Circuit.

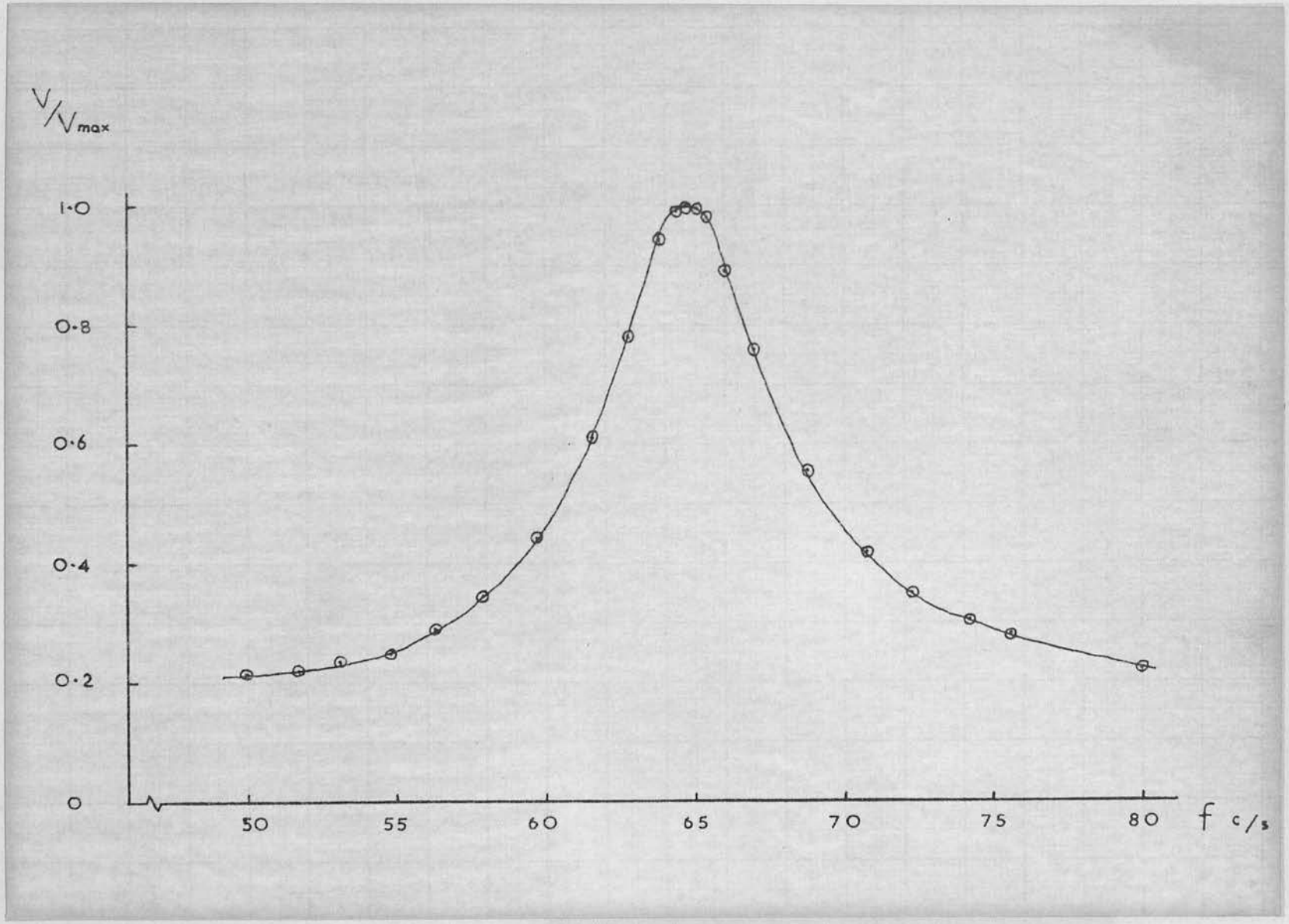

Figure IV.16. Frequency Response of Typical Filter.

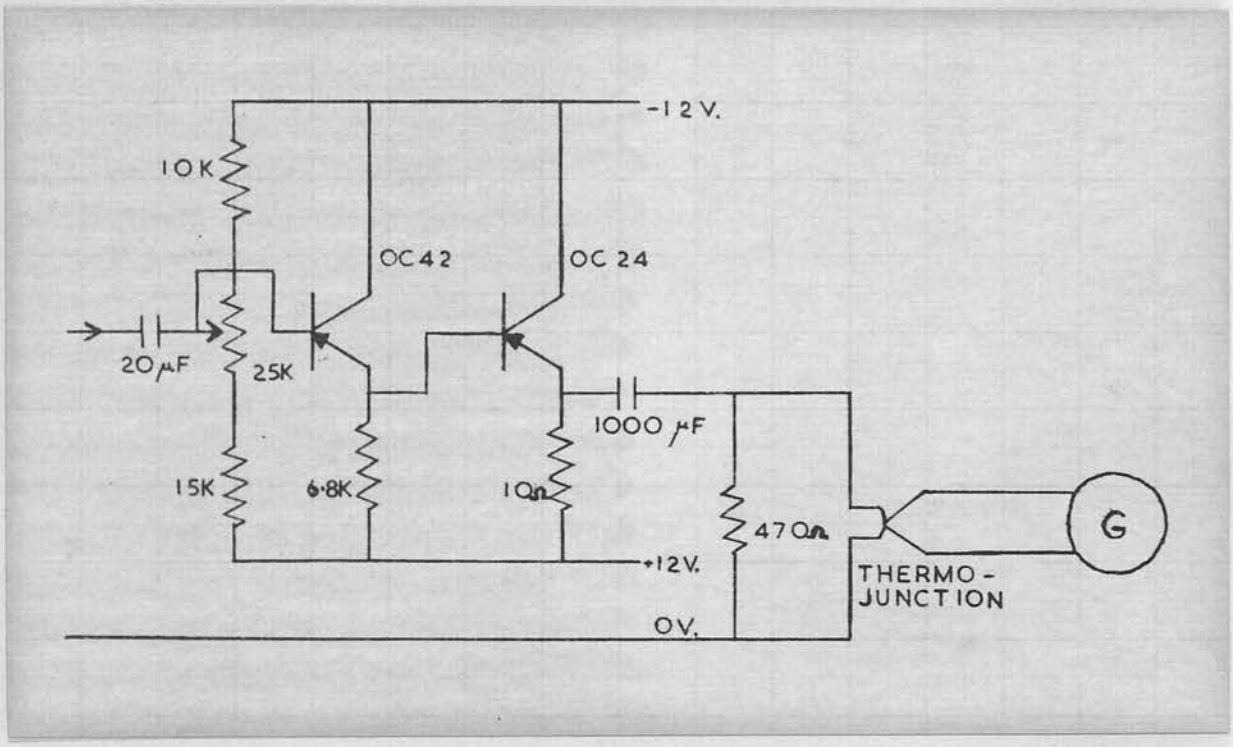

Figure IV.17. Thermovacuum Junction Circuit.

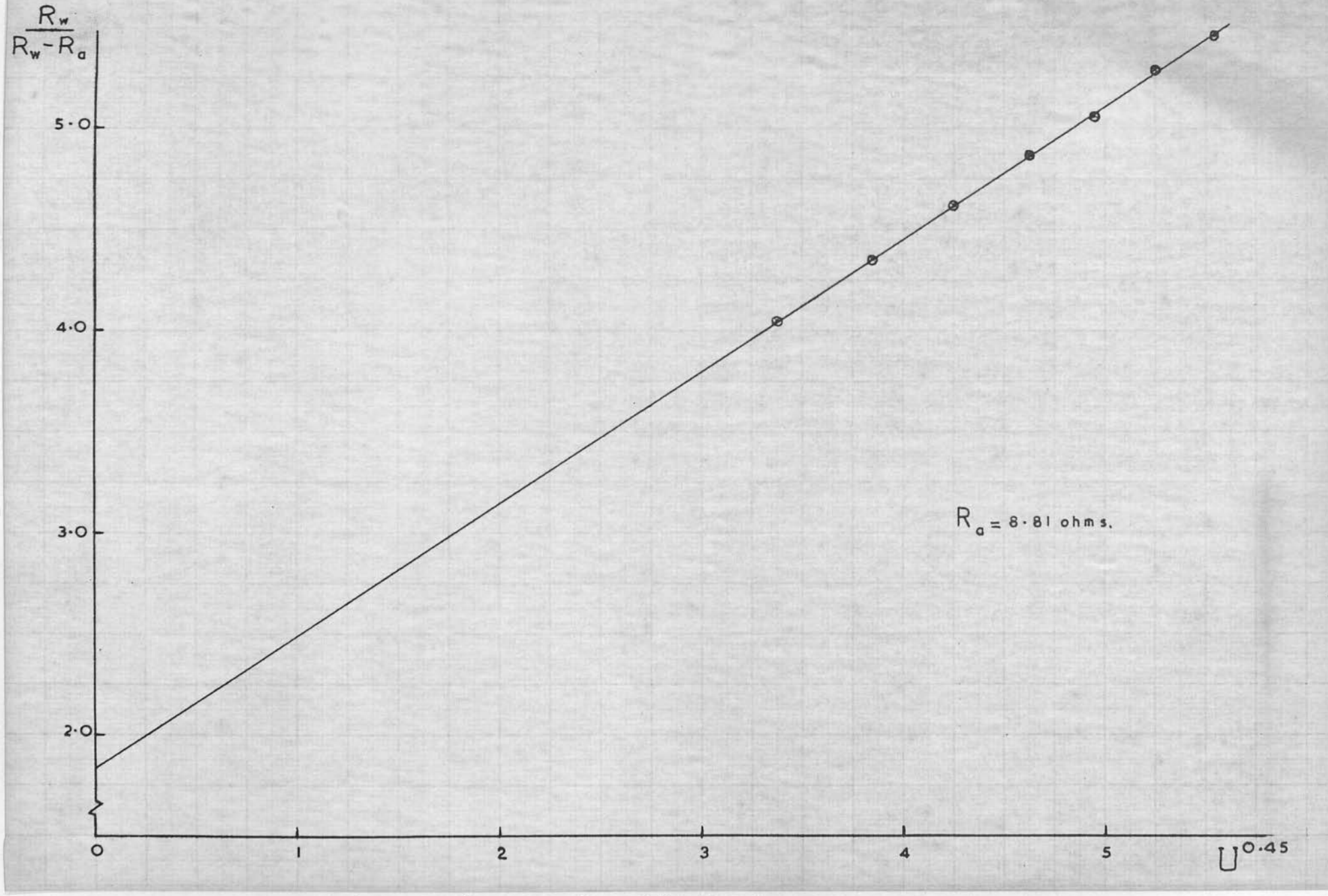

Figure IV.18. Hot-wire Calibration Curve.

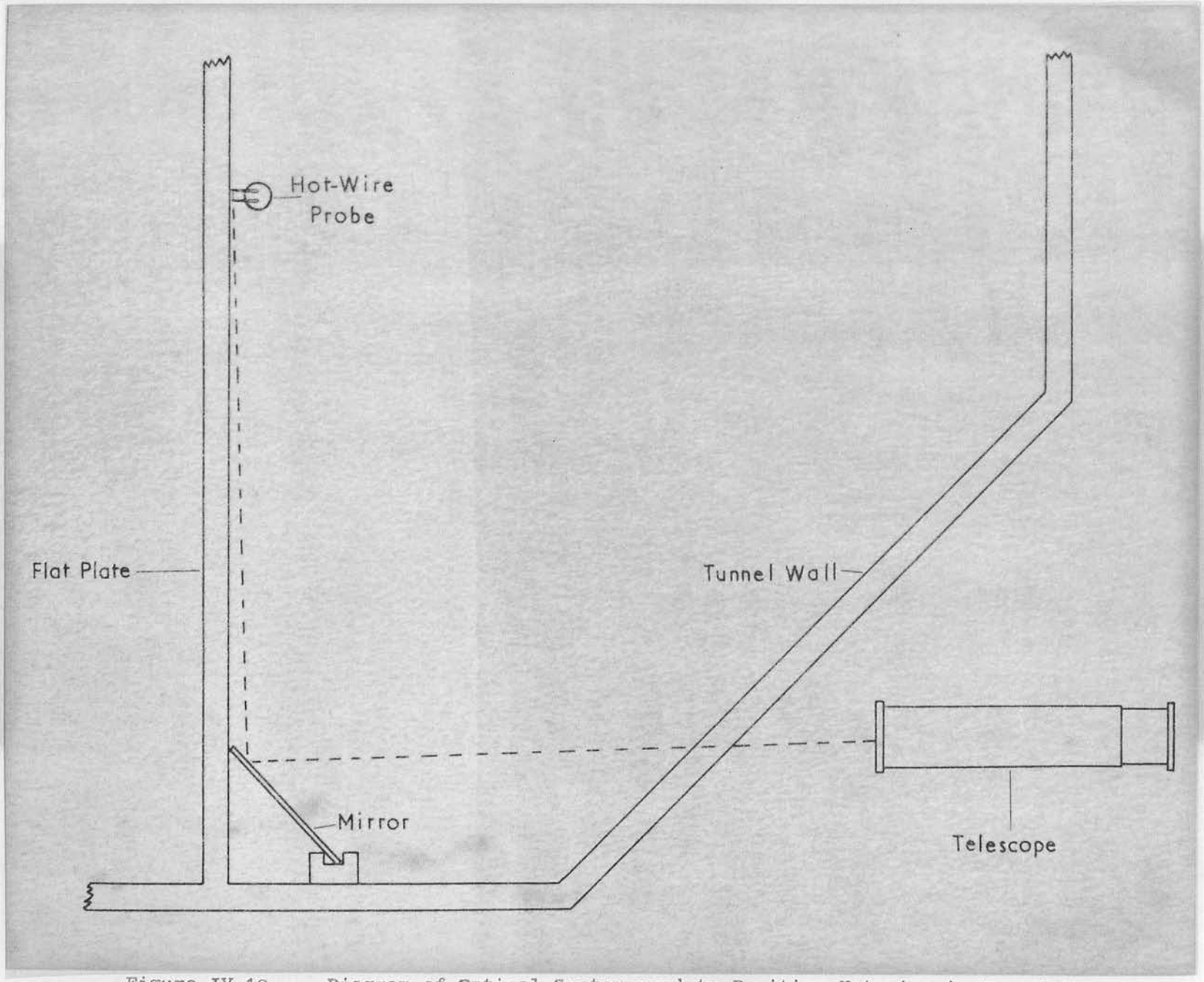

Figure IV.19. Diagram of Optical System used to Position Hot-wire in Tunnel.

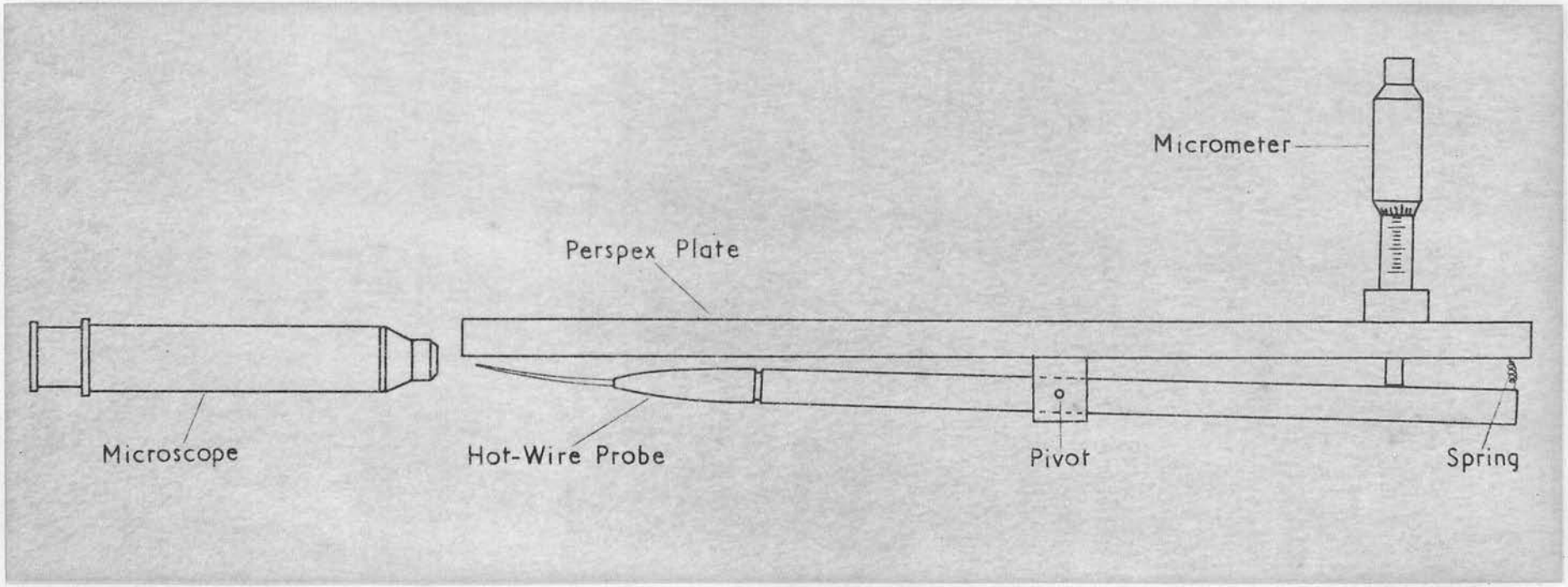

Figure IV.20. Diagram of Optical Method used to Determine Position of Hot-wire on Supports.

CHAPTER V

PRELIMINARY STUDIES OF BOUNDARY-LAYER PHENOMENA

V.1. Mean Flow Measurements

As a preliminary check on the hot-wire system and the traversing equipment it was decided to make some measurements of the mean flow in the boundary layer.

Previous workers with the Heriot-Watt tunnel (Burns (1958) and Whitelegg (1961)) had used pitot tubes to show that the boundary layer profile on the flat plate in the laminar region was in good agreement with the Blasius profile. It was felt that similar agreement using the hot-wire anemometer would be a vindication of this technique in mean flow measurements.

A hot-wire was traversed through the boundary layer in steps of 0.01 inches from the free stream to the surface of the plate. A hot-wire resistance reading was taken at each y-position and the local mean velocity calculated from the calibration. The boundary-layer thickness (δ) was calculated by numerical integration using the formula

$$\delta = 1/0.341 \int_0^{\delta} (1 - U/U_0)\, dy.$$

and the boundary layer profile plotted on a non-dimensional scale. From a series of boundary-layer traverses at

various x- positions along the tunnel centre line in the laminar region, considerable experience was acquired in the techniques of hot-wire anemometry. The resulting boundary-layer profiles were found to be in good agreement with the Blasius profile, a typical graph being shown in Figure V.1.

V.2. Distribution of the Intensity of the Disturbance through the Boundary Layer

The next step was to extend the scope of the hot-wire observations to measurements of longitudinal fluctuating components of velocity.

Studies were made of the distribution through the boundary layer of the intensity (R.M.S. value) of artificially introduced disturbances of the Tollmein-Schlichting type. The disturbances were introduced into the boundary layer by the vibrating ribbon technique described in Chapter III. A wide range of amplitudes of ribbon vibration was tried so that information for use in future studies could be obtained regarding the optimum range of ribbon amplitudes. The windspeed and frequency were chosen so that Branch I of the neutral stability diagram lay close to the ribbon position, x = 1' 0", observations being made along the plate centre line. Disturbances were thus in an amplifying zone immediately downstream of the ribbon. A hot-wire, at x = 1' 2", was traversed from the free stream to the surface of the

plate in steps of 0.01 inches. Readings of hot-wire resistance and total signal hot-wire output were taken at each ȳ- station for a series of seven ribbon vibration amplitudes. Only relative values of ribbon amplitude are quoted as no accurate method of the estimation of the absolute ribbon amplitude had been developed at this time.

The resulting disturbance intensity distributions, shown in Figure V.2., illustrate the features of the intensity distribution through the boundary layer of a Tollmein-Schlishting disturbance close to Branch 1 of the neutral stability curve. The main features observed were the intensity peak close to $Y/\delta = 0.2$ and the minimum intensity in the region of $0.7 < Y/\delta < 0.85$. The oscilloscope display of the hot-wire output signal showed that a phase change of approximately 180 degrees occurred at this minimum. These features were in good general agreement with the predictions of the linear theory and with the experimental observations of Schubauer and Skramstad (1946).

With the same conditions as above, the distribution of intensities through the boundary layer was studied at five other x-stations from 1' 4" to 2' 0". The results are presented in Figures V.3.a-e. The disturbance from a given ribbon amplitude was followed downstream until the output trace on the oscilloscope showed the presence of tubulent spots. The intensity of the peak at this position was approximately 7 per cent. of the free-stream velocity.

The curves in Figure V.3. illustrate further features of disturbances in the boundary layer and of their growth up to the point of breakdown. The disturbance intensities resulting from the smaller ribbon amplitudes grow slowly and show a movement, towards the plate, of the intensity peak and the position of the minimum of intensity as they progress downstream. Larger amplitudes show an initial slow growth of the intensity peak followed by a rapid increase in intensity with increasing x - position. Associated with this rapid increase in intensity are the outwards shift of the maximum intensity to approximately $Y/\delta = 0.3$ and of the minimum to about $Y/\delta = 0.8$. The increase in intensity in the region $0.5 < Y/\delta < 0.7$ is in agreement with the observation of Tani and Komoda (1962) of an outwards shift of the centre of gravity of the intensity distribution in the region of non-linear downstream growth of the disturbance. The largest ribbon amplitude resulted in disturbances which grew rapidly immediately downstream of the ribbon, turbulent spots being apparent at x = 1' 6".

The following main conclusions, in agreement with those of previous workers, were drawn from the observations described above.

a) An increase in ribbon amplitude resulted in an upstream movement of the entire pattern of the breakdown process.

b) A small disturbance near Branch 1 of the neutral stability curve grew slowly, apparently following the predictions of linear theory as it moved downstream. At a certain stage in the growth a rapid increase in intensity resulted and the distribution of the disturbance through the boundary layer was modified. This increase in the growth rate was quickly followed by the appearance of a turbulent spot and a catastrophic breakdown of the boundary layer to full turbulence.

c) For large initial disturbances there was no region of 'linear' growth downstream of the ribbon.

d) In the early stages of development of the disturbance, that is, in the 'linear' region, the distribution through the boundary layer of the disturbance intensity agreed with the results of Schubauer and Skramstad (1946).

e) The behaviour of the wave in the region of rapid growth preceding the birth of the first turbulent spot was essentially similar to that observed by Klebanoff and Tidstrom (1959) and Tani and Komoda (1962).

The results of the boundary-layer traverses described above showed the power of the hot-wire method in the detailed study of boundary-layer phenomena and led to further use of the hot-wire anemometer in the study of the growth of disturbances in the boundary layer.

V.3. Reduction of Boundary-Layer Traverse Data

During the work described in Section V.2. above it was quickly realised that the reduction of data obtained from boundary-layer traverses was a time consuming process. Throughout most of the work described above and all later work involving boundary-layer traverses the Ferranti 'Sirius' digital computer, belonging to the Heriot-Watt College, was used for data reduction.

The program developed calculated the calibration constants for the hot-wire and used these to calculate disturbance intensities from the mean hot-wire resistance and the fluctuating voltage inputs. A further feature of the program was the calculation of the boundary layer thickness from the mean resistance readings, by a numerical integration process using the formula quoted in Section V.1., a print out of the Y/δ value of each station being given.

This program written in Sirius Autocode language is given in Appendix III.

V.4. The Growth of Disturbances in the Boundary Layer

In the next phase of the work, the growth of artificially introduced disturbances in the boundary layer was studied.

Previous workers, notably Klebanoff, Tidstrom and Sargent (1962) had found it convenient to use instruments mounted at a fixed distance from the plate (i.e. at constant y) in their observations of the downstream growth

of injected waves. However, Laufer and Vrebalowich (1960) have studied the growth of disturbances in a supersonic boundary layer by placing the hot-wire at the same local velocity at each x - position (i.e. at constant y/δ). In the present work it was decided to keep the hot-wire at constant y/δ during traverses in the downstream direction. The nature of the traversing mechanism, together with the fact that it did not run in the x direction accurately parallel to the plate, made the setting of the wire at a given y - position to an accuracy of $\pm$ 0.0005 inches a very difficult process. However, by observing mean resistance of the hot-wire the sensing element could be set very easily at the position of a given value of local velocity. Traverses were then made following the development of the disturbances along a streamline. The streamlines followed during most of these observations were in the region of the critical layer, near y/δ = 0.2, where the intensity of the disturbance through the boundary layer had its maximum value.

The procedure consisted of setting the hot-wire at the y/δ position chosen at an x - position immediately downstream of the ribbon. During this operation the current in the ribbon circuit was switched off. Observations with the hot-wire anemometer of the disturbance intensity were made for a number of ribbon currents.

Subsequently, with the ribbon current off, the hot-wire was moved to a downstream position (the interval was usually 2 inches) and its position in the boundary layer adjusted until its mean resistance had the same value as at the previous position. The sensing element was thus set at the same local velocity at each x - position.

Using this precedure the growth of the wave disturbances produced by a series of ribbon amplitudes was studied. The region on the neutral stability diagram under observation was varied within small limits by using several windspeeds and frequencies of ribbon vibration.

Typical graphs showing wave growth observations taken along the plate centre line by the above method are illustrated in Figure V.4. These are plotted with the intensity axis normalized to the value of the intensity at x = 1' 2" resulting from the smallest ribbon amplitude. The ribbon amplitudes are quoted as ratios of the smallest amplitude, which was approximately 0.0004 inches. No reliable method was available at this stage of the work for determination of the absolute ribbon amplitude.

The results shown in the graph can be classified into three groups depending on the ribbon amplitude.

For the smallest ribbon amplitudes the disturbances decreased in intensity immediately downstream of the

ribbon. The position of mimimum intensity was found to be close to the position of Branch I of the neutral stability curve as predicted by the linear theory of Shen. Further downstream a slow increase in intensity was observed followed by a rapid amplification associated with the breakdown process of the unstable laminar boundary layer.

The disturbances produced by the largest ribbon amplitudes (of order 0.0035inches) showed entirely different behaviour, and under certain conditions were observed to amplify rapidly even upstream of the predicted position of Branch I of the neutral stability curve. It thus appears that disturbances produced by the large ribbon amplitudes were not small enough, even immediately downstream of the ribbon, to behave according to the predictions of linear theory.

This observation of amplification of disturbances upstream of Branch I of the neutral stability curve would seem to be in accord with the theoretical work of Stuart (1960c). In a study of the stability of plane Poiseuille flow he concluded that it was possible for disturbances of sufficiently large amplitude to be amplified even before the critical Reynold's number was reached. No experimental support for this observation of amplification before Branch I has been reported in the writings of other workers, possibly because most observations have been made in the region of Branch II and only small amplitude effects have been studied near

Branch I. It thus appears that for large disturbances upstream of Branch I the mechanism of the instability and breakdown process is different from that normally associated with the growth of small disturbances. Bennett (1953) has produced some evidence to show that, for large disturbances introduced into the boundary-layer from a high level of free stream turbulence, the transition process may be controlled by the laminar separation process suggested by Taylor. It could be that breakdown initiated before Branch I of the neutral curve is controlled by a similar type of mechanism.

The disturbances introduced by ribbon amplitudes in an intermediate range showed features different from those already described for large and small amplitudes. Immediately downstream of the ribbon, disturbances of intermediate size followed the predictions of linear theory, being damped till they reached Branch I of the neutral curve and then amplified. Further downstream, however, they broke away from the pattern set by the disturbances of smaller ribbon amplitudes and showed a region of less amplification, and in some instances a region of damping, before the final rapid amplification leading to breakdown.

This phenomenon of less amplification than expected or damping in an amplifying zone had previously been observed by Klebanoff and Tidstrom (1959). In the

three-dimensional situation existing in their tunnel this reduction in amplification was observed to be associated with a spanwise transfer of energy.

The observations described above and the conclusions of Klebanoff and Tidstrom prompted investigations into the three-dimensional nature of the boundary layer in the Heriot-Watt tunnel.

V.5. Observations in the Spanwise Direction

a) Mean flow variations

The first step taken in the study of the three-dimensional nature of the boundary layer was the observation of the variation of boundary-layer thickness in the spanwise direction.

With the traversing mechanism described in Section II.3. it was not possible to move instruments in the z-direction without removing and re-positioning the entire boom arrangement. Consequently a new method was devised for traversing instruments in the spanwise direction. In this method the instrument (e.g. a hot-wire probe) was mounted on a boom protruding vertically downwards into the tunnel from its roof. A micrometer screw outside the tunnel was used to move the boom, and thus the instrument mounted on it, in the z-direction. The total range of travel, in the spanwise direction, possible using this method was just over 2 inches.

In the early studies of spanwise variations of boundary-layer thickness the instrument employed was a boundary-layer pitot tube constructed from a length of hypodermic tubing. Later, the instrument shown in Figure V.5. incorporating both a pitot tube and a hot-wire probe, was used. This instrument was constructed so that, when it was mounted on the boom, the pitot tube and the hot-wire were kept at a fixed distance from the plate (a constant $\bar{y}$ of approximately 0.035 inches for the hot-wire), and yet could be moved over the 2 inch range in the spanwise direction. The traverses using this instrument were carried out at a distance of 1' 3" from the leading edge of the plate.

Pressure changes in the boundary layer detected by the pitot tube and an inclined- tube manometer, together with the hot-wire resistance readings showed that the local velocity in the boundary layer at a fixed distance from the plate was not constant in the spanwise direction. This result implied the existence of spanwise variations in the boundary-layer thickness of the type observed by Klebanoff and Tidstrom. A graph of the observed spanwise variations in local velocity in the boundary layer is shown in Figure V.6.

These variations in the mean flow were found to be completely independent of the ribbon vibration and were in fact still present when the ribbon and its mounting were removed from the plate. The 'wavelength'

of these variations in the y-direction was found to be about 1 inch. The difference in boundary-layer thickness between maximum and minimum was of the order of 8 per cent. of the mean boundary-layer thickness. The 'wavelength' of 1 inch was the same as that observed by Klebanoff and Tidstrom. No definite explanation of this similarity can be given. However, Bradshaw (1964) has shown that periodic variations in boundary-layer thickness are associated with the damping screens used in the tunnel. As no information is available on the mesh size and wire diameter of the screens in the National Bureau of Standards tunnel it can only be assumed that some similarity between these screens and those used in the present work resulted in the same spanwise 'wavelength' being detected in both cases.

Periodic checks on the distribution of the spanwise variations in boundary-layer thickness throughout the course of this work have shown that the pattern was liable to shift in the z - direction although the 'wavelength' remained constant. These shifts were observed only after the cleaning of the screens, the pattern remaining fixed at other times. The process of cleaning the screens involved their removal with subsequent replacement, not necessarily in exactly the same position. This dependence of the spanwise boundary-layer thickness pattern on the orientation of the tunnel screens was in accord with the observations of Bradshaw (1964). Care

was taken to ensure that after cleaning the screens were replaced in the same order and with the same orientation as before, but even with these precautions changes in the spanwise pattern were noted.

In consequence of this, there has been no control throughout this work of the three-dimensional nature of the boundary layer, and this had to be carefully re-examined subsequent to each time the screens were cleaned.

b) Variations in disturbance intensity

Using the instrument, incorporating the hot-wire probe, described in the previous section it was found that there were spanwise variations in the intensity of the fluctuating part of the flow when disturbances were introduced in the boundary layer using the vibrating ribbon. Figure V.7. shows these variations. Comparison of this graph with that of Figure V.6. showed that the largest intensity of disturbance was associated with the region where the boundary layer was thickest. The windspeed and ribbon frequency were such that this observation was made at a position close to Branch I of the neutral stability curve. This result was in agreement with that of Klebanoff and Tidstrom who noted that near Branch I the largest intensity was associated with the thickest boundary layer.

V.6. Downstream Growth of Disturbances at Several Spanwise Positions

A hot-wire study was made of the downstream growth of artificially introduced disturbances at spanwise positions corresponding to maximum and minimum boundary-layer thickness using the traversing mechanism described in Section II.3. It was found that the pattern of growth differed at the two positions. Figure V.8. shows a typical set of growth curves taken at constant y/δ in the region of the critical layer at spanwise positions $\bar{z}$ = 0.5 inches and $\bar{z}$ = 1.0 inches. The windspeed and ribbon frequency were such that Branch I of the neutral curve lay close to the ribbon position, x = 1' 0", and the ribbon amplitude was small enough to ensure that the growth followed a linear pattern for some distance immediately downstream of the ribbon.

Figure V.8. shows that over the early part of the development the growth rates at both $\bar{z}$ - positions were essentially the same, as would be expected when linear theory holds. However, further downstream the growth of the disturbance was found to be more rapid at $\bar{z}$ = 0.5 inches, a position of maximum boundary layer thickness, than at $\bar{z}$ = 1.0 inches, a position of minimum boundary-layer thickness. It would appear that the disturbance at the $\bar{z}$ = 0.5 inches position grew at the expense of that at $\bar{z}$ = 1.0 inches, although the three-dimensional effect would not appear to be strong enough under these

conditions to produce a region of damping of this wave. The appearance of a turbulent spot, a burst of high frequency disturbance, was observed on the oscilloscope first at the z = 0.5 inches position. The first turbulent spot at z = 1.0 inches occurred some 2 inches downstream of this position. The disturbance intensity when a spot appeared was some 7 per cent. of the free stream velocity.

The features of the disturbance growth at spanwise positions of differing boundary-layer thickness were essentially similar to those observed by Klebanoff and Tidstrom and found to be associated with a spanwise energy transfer. Exact comparison cannot be made however due to the different methods of observation, growth at constant y/δ in the present case and growth at constant $\bar{y}$ in the studies of Klebanoff and Tidstrom, and also the different degrees of three-dimensionality in the two experimental situations.

V.7. Comparison of Experimental and Linear-Theory Growth Rates

Shen (1954) using linear theory calculated the amplitudes of disturbances with certain discrete values of $\beta_r \nu / U_o^2$ as the disturbances crossed the amplifying region from Branch I to Branch II of the neutral curve. These results are shown in Figure A.I.2., the amplitude being plotted in terms of the amplitude

of the disturbance at Branch I. From this graph points of constant $\ln A/A_0$ were obtained and used to plot curves of constant amplification in the ($\beta_r \nu / U_0^2$, R) plane. These are shown in Figure V.9. Using this graph it was possible to obtain growth curves for values of $\beta_r \nu / U_0^2$ not specifically calculated by Shen.

It was decided to compare the growth curves of linear theory obtained in this way with the disturbance growths measured experimentally. A further aim of this part of the work was to locate the point at which the growth of the disturbance diverged from linear theory and to measure the amplitude of the disturbance at this point. Klebanoff and Tidstrom had suggested that amplitude of disturbance might form a criterion for departure from linear theory.

Four ribbon frequencies were used, 65 cycles/sec., 80 cycles/sec., 90 cycles/sec. and 103 cycles/sec. corresponding to non-dimensional frequency parameters ($\beta_r \nu / U_0^2$) of 100×10^{-6}, 125×10^{-6}, 140×10^{-6} and 160×10^{-6} respectively. With a windspeed of 25 feet/sec. and the lowest frequency, Branch I of the neutral curve lay close to the ribbon position, while for higher frequencies the disturbances were injected into an amplifying zone of the boundary layer. The z- position was chosen to correspond to the maximum growth rate in the streamwise direction. Three ribbon amplitudes were

used at each frequency, 0.0004 inches, 0.0007 inches and 0.001 inches. At the highest frequency the amplitude of 0.0002 inches was used to show damping downstream of Branch II of the neutral curve.

The method of operation was the same as that described in Section V.4., where the hot-wire probe was traversed downstream at constant y/δ in the region of the critical layer. The growth curves obtained from the experimental points were similar to those already described where a slow rate of growth gave way to a rapid amplification followed by a turbulent spot when the disturbance intensity reached approximately 7 per cent. of the mean flow velocity.

By fitting the experimental intensity at a given Reynold's number to Shen's theoretical growth curve at this Reynold's number it was possible to estimate the disturbance intensity at Branch I of the neutral curve. The experimental intensities were then non-dimensionalized in terms of the intensity at the neutral curve and values of $\ln A/Ao$ obtained for comparison with the theoretical curve. This was done using the experimental values at x = 1' 4" (R = 795) as a basis for fitting the experimental results to the theoretical curves. The results, to beyond the point of departure from the linear region, are plotted together with the theoretical curves in

Figures V.10.a-d.

The experimental points, in general, showed fairly good agreement with the theoretical curves in the early stages of the development of the disturbance. Further downstream, a marked point of departure of the experimental values from the theoretical curve was observed. An increase in ribbon amplitude caused this point of departure to move to lower Reynold's number, as expected.

Discrepancies between theory and experiment are apparent for the two smallest ribbon amplitudes at the lowest frequency. The ribbon position at this frequency was close to Branch I of the neutral curve so that the amplification immediately downstream of the ribbon was small. Thus, for small ribbon amplitudes, disturbances of low intensity were detected by the hot-wire at the several stations immediately downstream of the ribbon. The resulting voltage fluctuations were difficult to distinguish from the noise produced by the residual turbulence in the tunnel. It was thus possible that the measurements of intensity made in this region, under these conditions, were rather high. As x = 1' 4", the point fitted to the theoretical curves, was one of the stations where the intensity may have been underestimated, the resultant points showing disturbance growth further downstream could be expected to fall below the theoretical growth curve. Even with this explanation,

further experimental work with a low turbulence wind tunnel is needed to examine the shape of the growth curve in the immediate vicinity of Branch I of the neutral stability diagram.

The disturbance growth produced by smallest ribbon amplitude at a frequency of 103 cycles/sec. is plotted in Figure V.10.d. This shows the growth and subsequent damping of a disturbance as it crosses Branch II of the neutral curve together with the theoretical growth curve which is available only for the amplifying region. Low signal levels again made measurements difficult. However, the position of the experimentally observed turning value is certainly close to the position of Branch II predicted by Shen.

Klebanoff and Tidstrom produced some evidence to suggest that departure from the linear theory was associated with a critical wave intensity for a given disturbance frequency. A more general suggestion was that when a critical disturbance energy level was reached departure from linear theory results. From the graphs plotted in Figures V.10 a-d. it was possible to estimate the Reynold's number for departure from linear theory. Using this and the original experimental data an estimate was obtained of the disturbance intensity at this point Table V.1. shows that there was no critical intensity of disturbance associated with departure. For a given

frequency the intensity at departure from linear theory appears to decrease with increasing Reynold's number. It is also apparent that for a constant ribbon amplitude the disturbance intensity at departure decreases with increasing frequency. However, no simple relationship has been found to link these facts. It should be noted that the above results were obtained at constant Y/δ while those of Klebanoff and Tidstrom were at constant y.

Morgan (1964) has suggested that the breakdown process is initiated when the parameter ($a\beta_r R / U_o$), where a is a linear function of ribbon amplitude, reaches a critical value. The present results would seem to indicate that for departure from linear theory a parameter involving a product of powers of a, β_r and R would be required. Dependence on windspeed has not been checked. However, it seems that the simple linear dependence of the three quantities predicted by Morgan will not fit the present results and no simple relationship is apparent for the limited data available.

V.8. Distortion of the Mean Flow

A further result of the experiments on the downstream growth of disturbances in the boundary layer was the observation of the distortion of the mean flow under the action of the growing fluctuations. Figure V.11., a typical graph of non-dimensionalized local mean velocity against Reynold's number illustrates this phenomenon. This graph, for a disturbance frequency of 90 cycles/sec.

and a ribbon amplitude of 0.0004 inches, shows the mean flow conditions as determined by the mean resistance of the hot-wire corresponding with Figure V.10. c(1). Up to a boundary-layer Reynold's number of 930 the local velocity remained constant, as expected for a hot-wire set at constant y/δ . At the station immediately downstream of this however, the local velocity at the hot-wire position was slightly less than expected. As the hot-wire was set at the same local velocity, with the ribbon unactivated at this station, as at the positions of lower Reynold's number it must be concluded that the distortion of the mean flow pattern was a direct result of the action of the disturbance on the boundary layer. Moving to higher Reynold's numbers (above 1020) in Figure V.11. it is seen that the wave caused increasing distortion of the mean flow, but now in such a way that the local velocity at the hot-wire was greater than that with no disturbance present.

Comparison of the mean flow graphs like Figure V.11. with the corresponding growth curves of disturbance intensity showed that distortion of the mean flow first occurred at small disturbance intensities (in some cases less than 1 per cent. of the mean flow velocity.). However, it has not been possible to identify a single value for this disturbance level or to find a parameter with a critical value determining this point of mean flow distortion. It should also be noted that the first

distortion of the mean flow leading to a decrease in local velocity occurred at a Reynold's number immediately below that for which significant departure from linear theory was observed. This implied that the effect of this distortion of the streamlines on the growth of the disturbance was, in the early stages at least, very small, predictions of the linear theory, which neglected this effect, still being followed.

Profiles of the mean velocity distribution through the boundary layer were measured by the method described in Section V.1. The x-stations were chosen to correspond to positions where observations at constant Y/δ had shown that the local velocity with the disturbance present was (a) the same as, (b) slightly less than, and (c) greater than the local velocity detected with the ribbon not vibrating. The profiles obtained are plotted in Figures V.12.b-d. For case (a) the profile agreed with the Blasius profile as expected. The action of the growing wave was to cause a slight distortion of the profile towards lower local velocities in the region $0.1 < Y/\delta < 0.4$ at station (b), while at (c) the distortion of the profile was towards higher local velocities in this region, the form tending towards a turbulent boundary layer profile. In case (b) the departure from the Blasius profile was not great and, in view of the experimental uncertainty, taken alone would not have been considered sufficient evidence for mean flow distortion. The observations at constant

y / δ as described, proved to be a much more accurate method of detecting distortion of the streamlines than studies of the boundary-layer profile.

The distortion of the mean flow profile and the action of the Reynold's stresses of the disturbance has been treated theoretically by Meksyn and Stuart (1951) and Stuart (1958). The departures from the Blasius profile at station (b) were in broad agreement with the results of these workers. The general shape of the boundary layer profile at this station was similar to their predictions. It would thus appear that in the early stages of the transition process a mechanism of the type studied by Meksyn and Stuart has a disturbing influence on the flow.

The experimental work of Klebanoff, Tidstrom and Sargent (1962) on a three-dimensional boundary layer has shown the complexity of the mean flow distortion mechanism. However, their conclusion was that other mechanisms dominate the later stages of the transition process to such an extent that the Reynold's stress effects become relatively unimportant among the various non-linear effects. The present experimental observations, where mean flow distortion was present but was small, would seem to agree with this conclusion of these workers.

V.9. Conclusions

In this chapter the results of preliminary studies of flow features in the boundary layer have been described. These raise many questions to which answers could only be given after much more experimental evidence was available.

Some of the detailed flow features which on the basis of the preliminary results would appear to warrant further study are:

1) The amplification of large disturbances upstream of Branch I of the neutral stability curve.

2) The exact nature, scale and origin of the spanwise variation in mean flow conditions.

3) The establishment of a criterion for departure from linear theory.

4) The distortion of the mean flow profile under the action of the Reynold's stresses and the effect this has on local flow behaviour.

All these are topics which might prove rewarding to future workers, and which require further study before the nature of the transition process can be fully understood.

Ribb Amp \ Freq	65 c/s		80 c/s		90 c/s		103 c/s	
	R_D	$u'/U_o\%$	R_D	$u'/U_o\%$	R_D	$u'/U_o\%$	R_D	$u'/U_o\%$
0.0004"	1170	1.2	1020	1.0	950	0.70	900	0.5
0.0007"	1090	1.7	970	1.25	900	1.0	850	0.7
0.001"	1040	1.9	930	1.4	880	1.2	-	-

R_D is the approximate Reynold's number for departure from linear theory.

Table V.1.

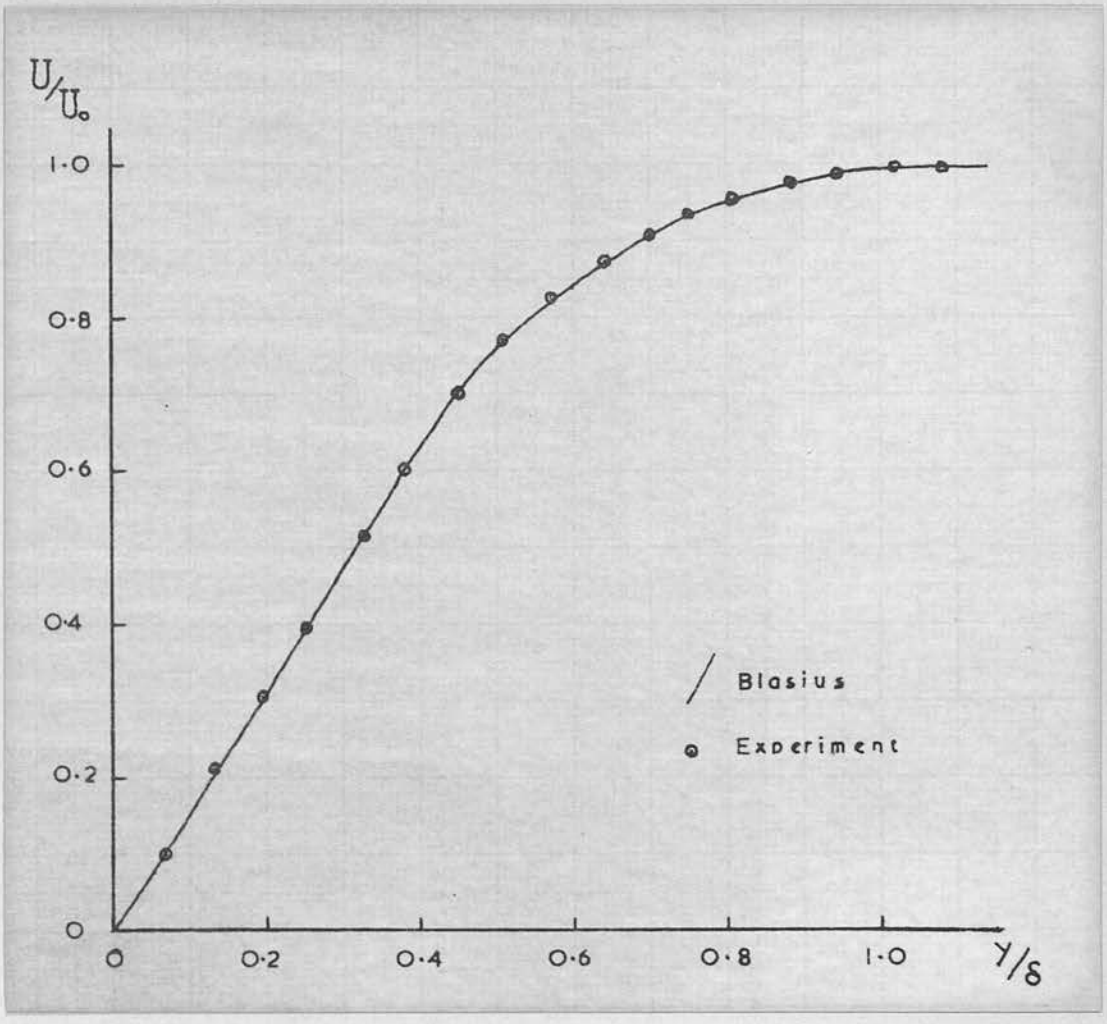

Figure V.1. Boundary-layer Profile.

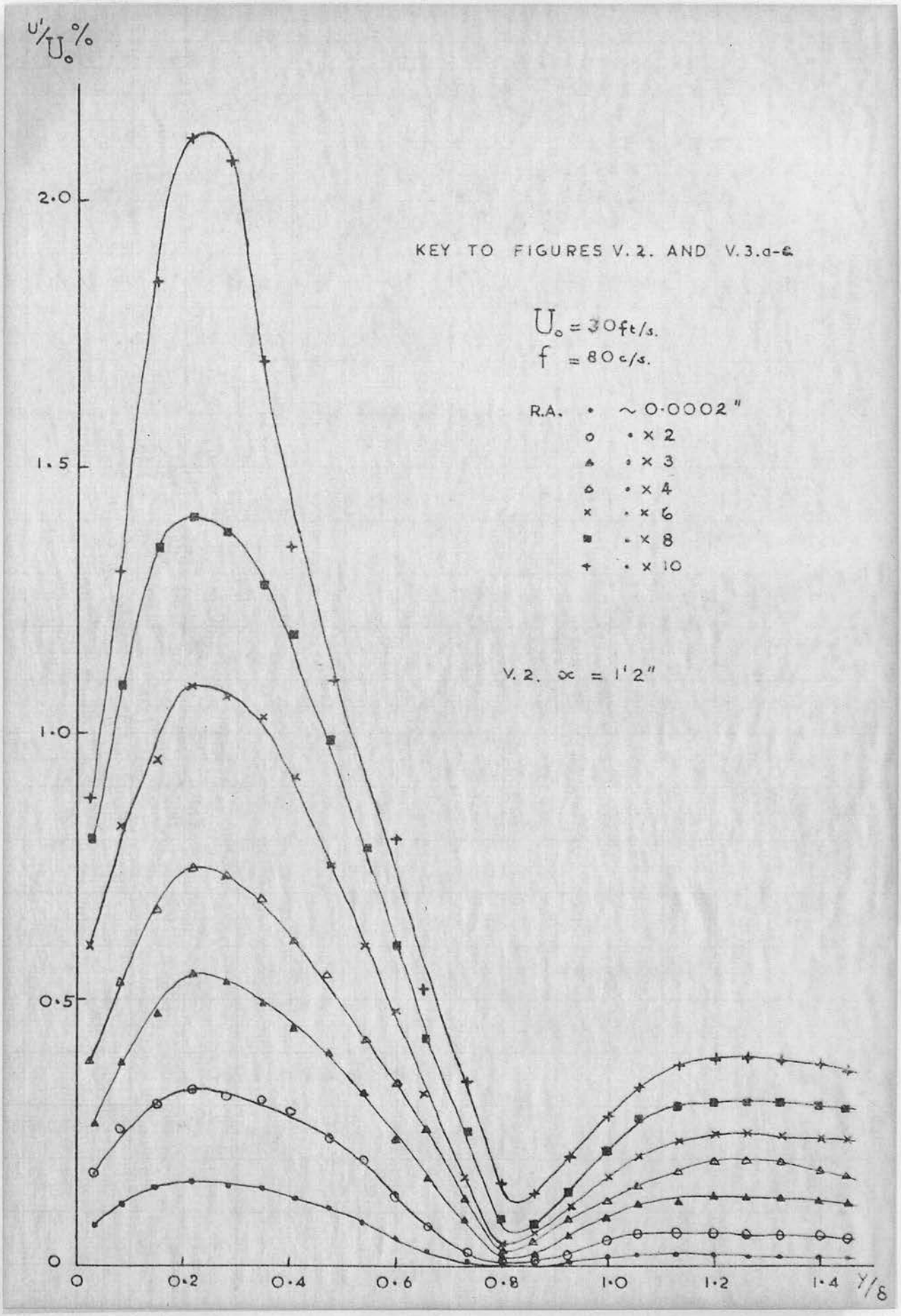

Figure V.2. Distributions of Intensity through the Boundary Layer.

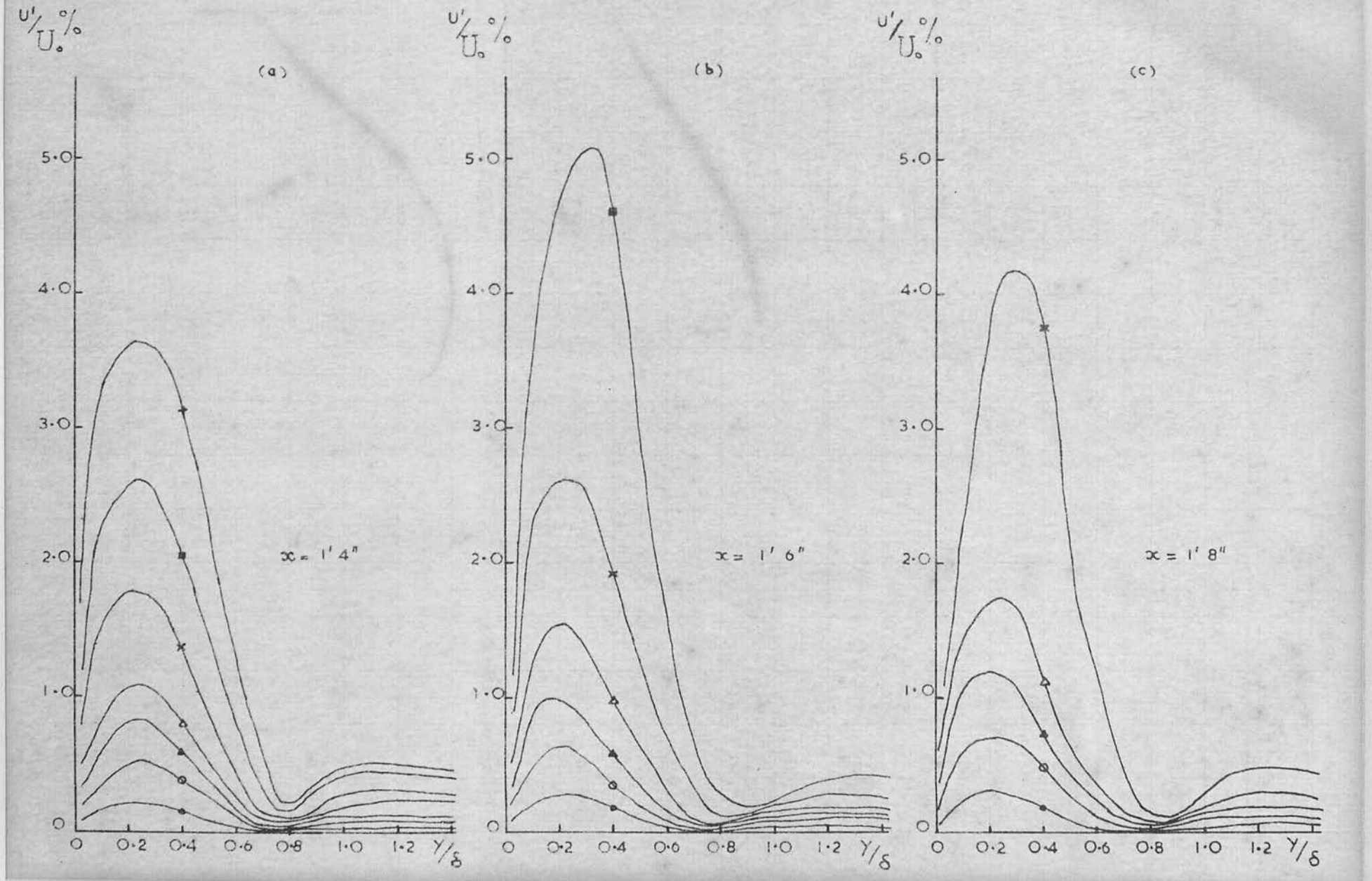

Figure V.3.a-c. Distributions of Intensity through the Boundary Layer.

Figure V.3.d-e.

Distributions of Intensity through the Boundary Layer.

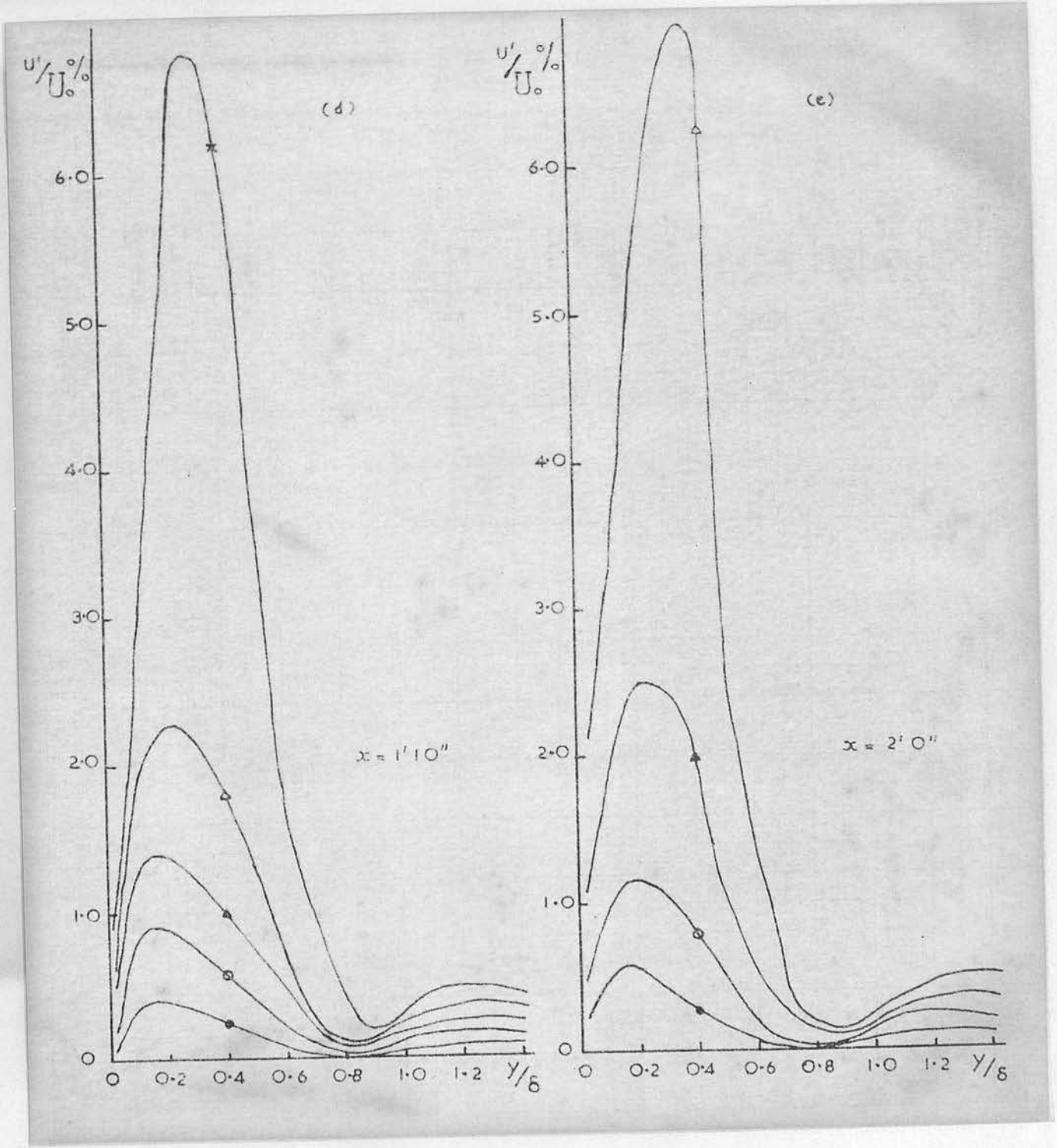

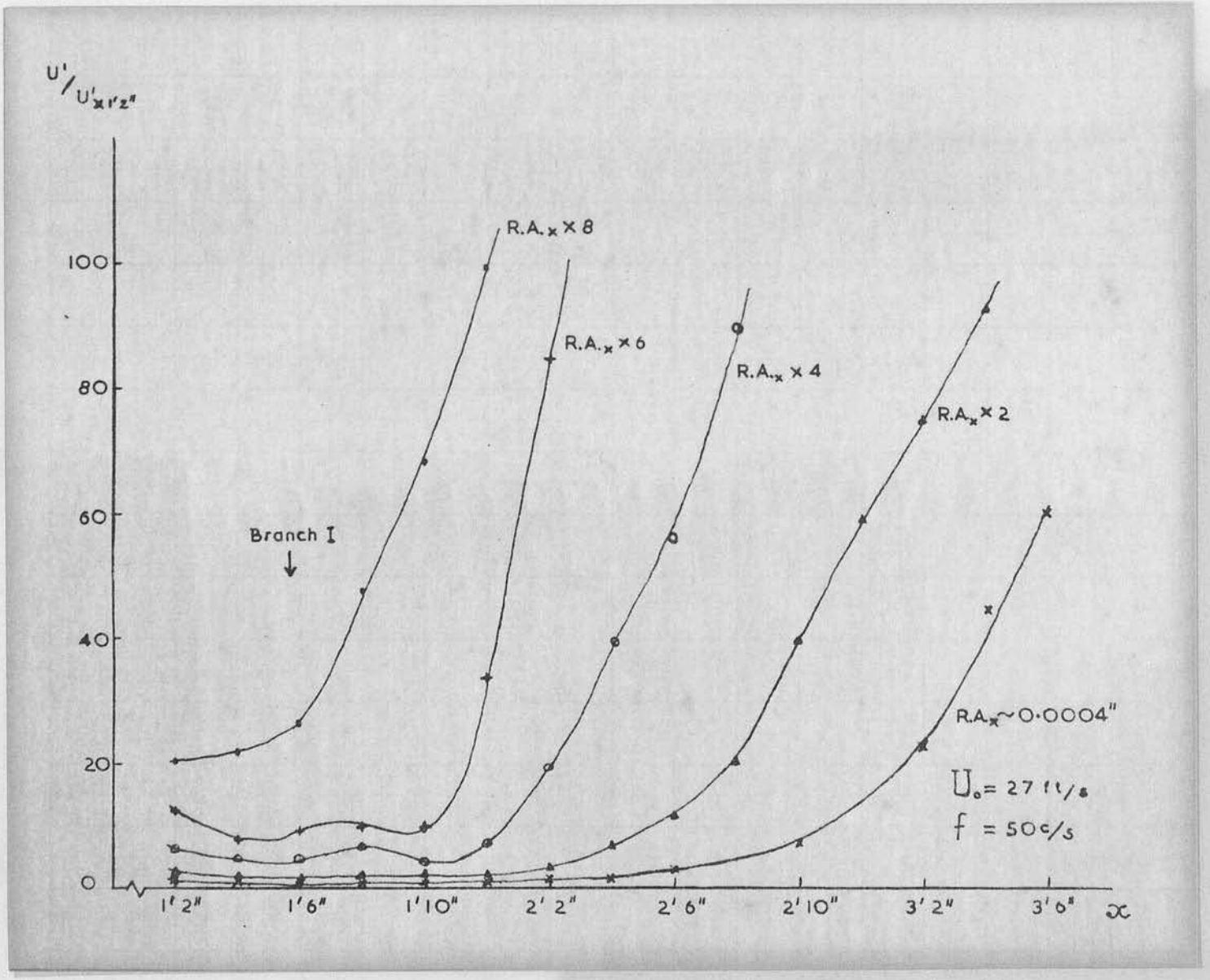

Figure V.4. Downstream Development of Disturbance Intensity.

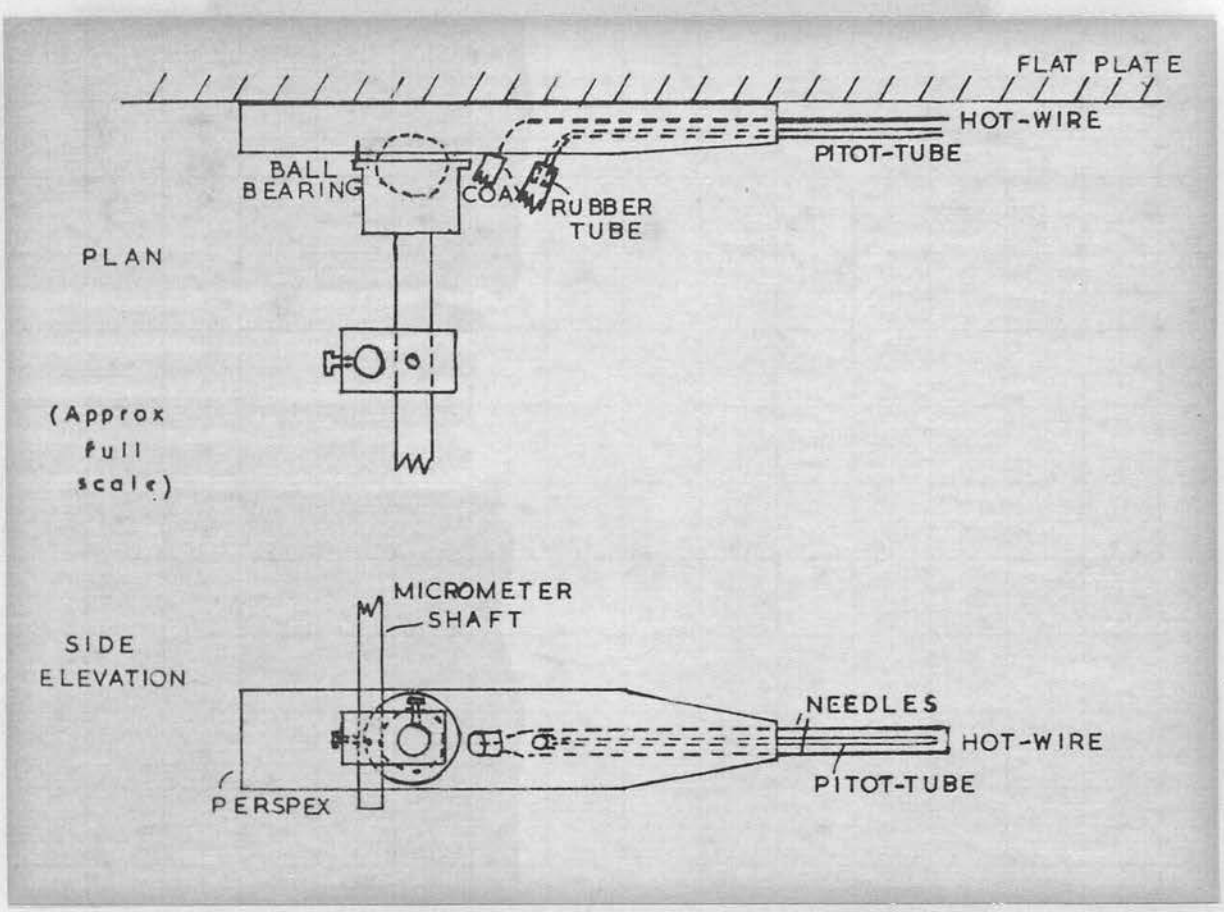

Figure V.5. Diagram of Probe for Traversing in the z-direction.

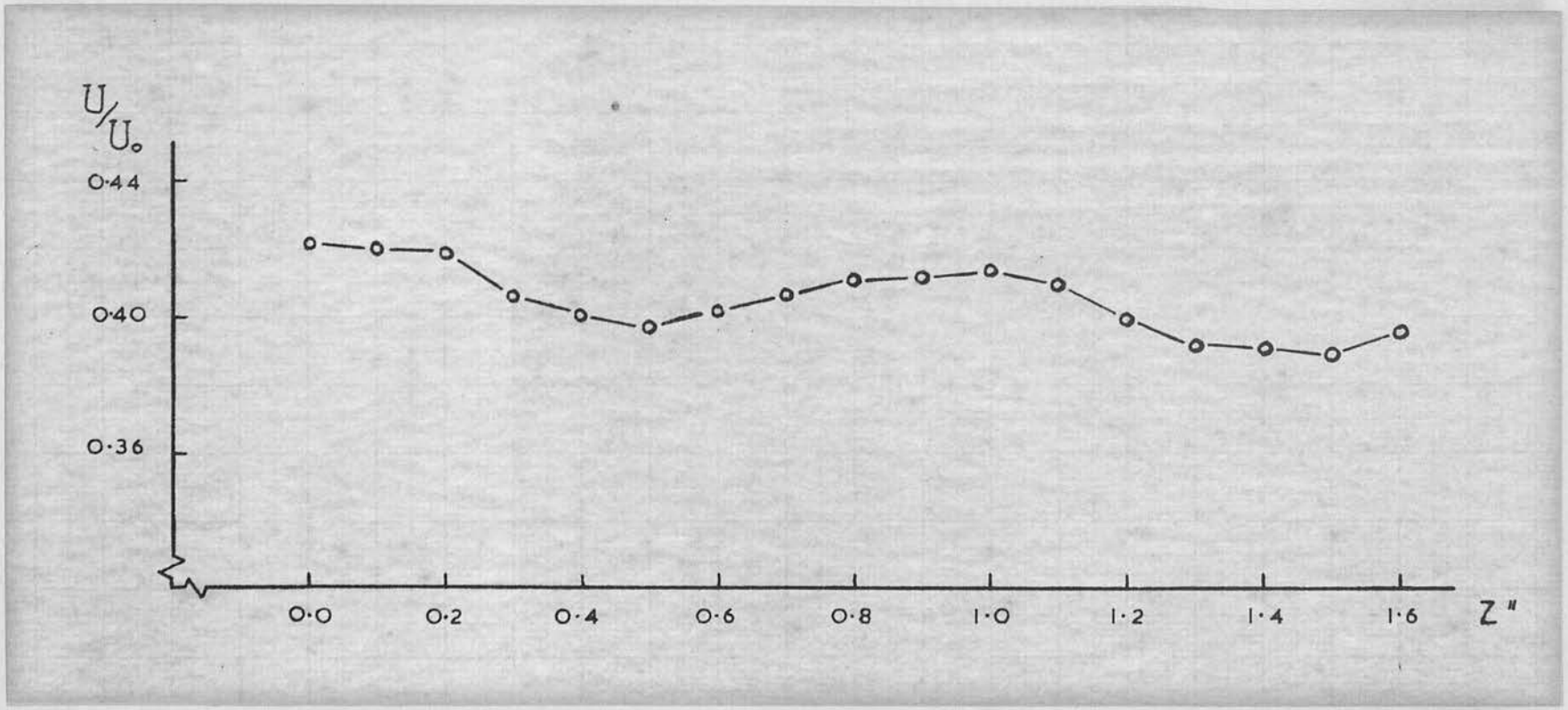

Figure V.6. Spanwise Variations in Mean Velocity at a Fixed Distance from the Plate.

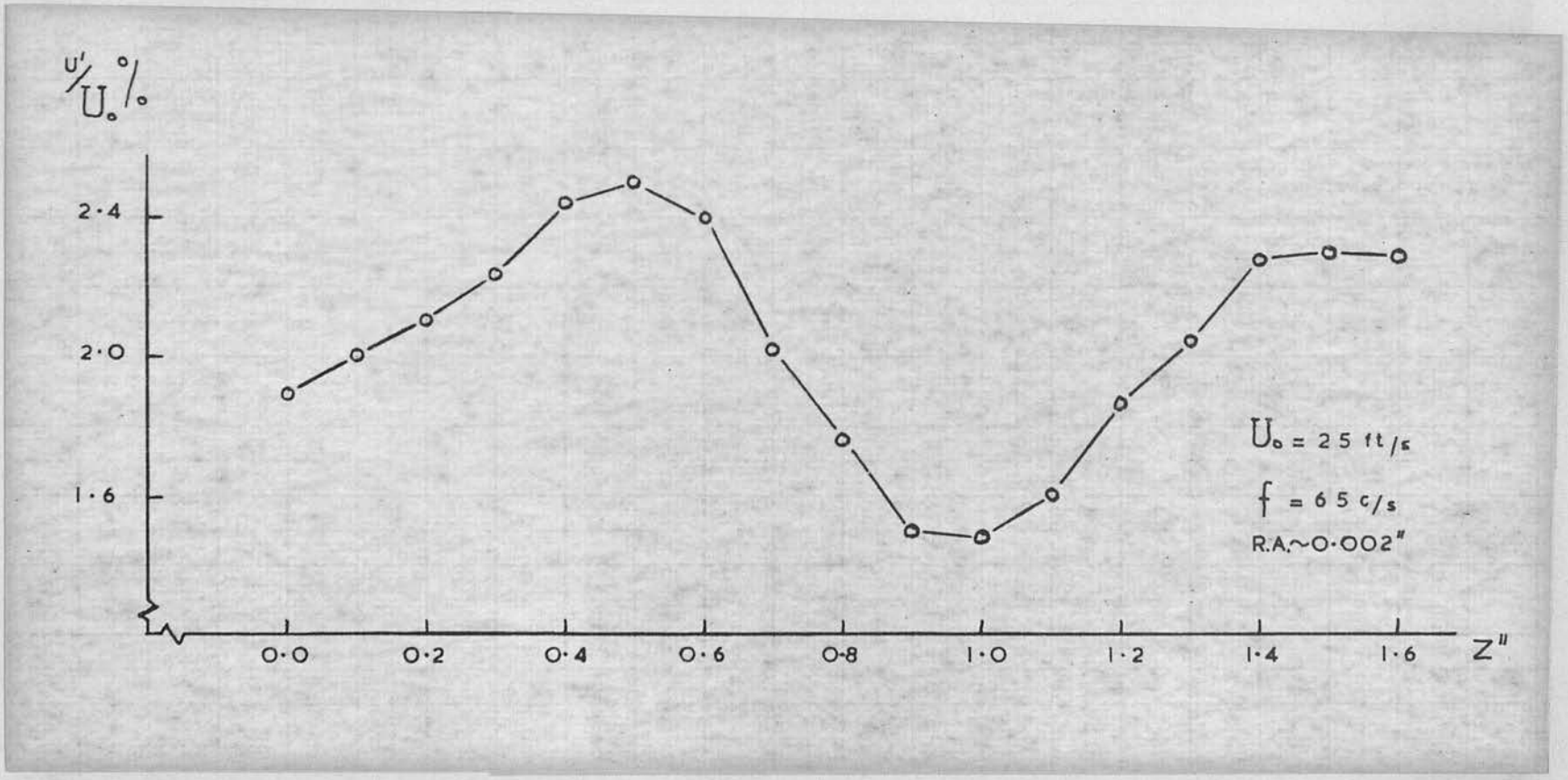

Figure V.7. Spanwise Variations in Disturbance Intensity at a Fixed Distance from the Plate.

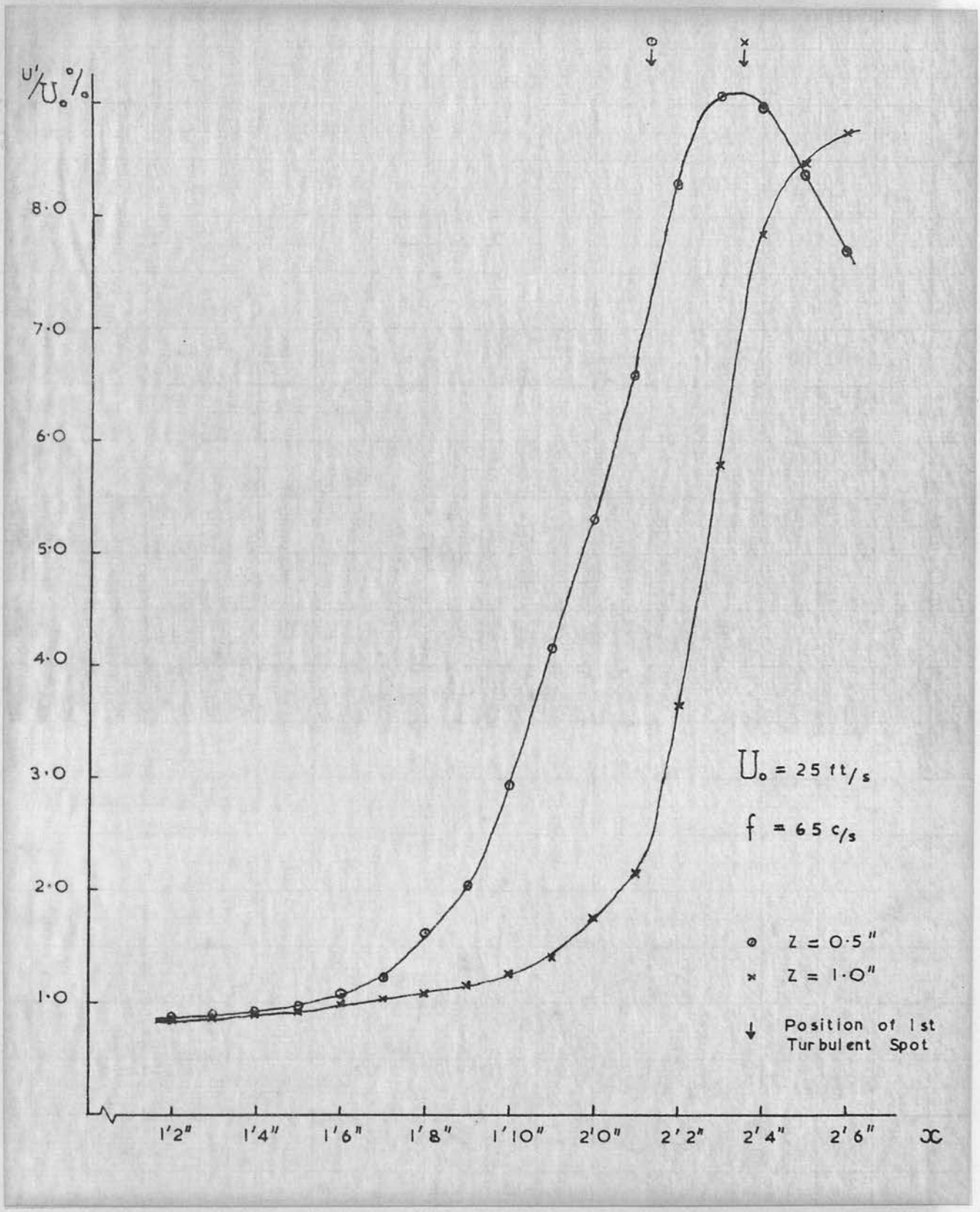

Figure V.8. Downstream Development of Disturbance Intensity at Two z-positions.

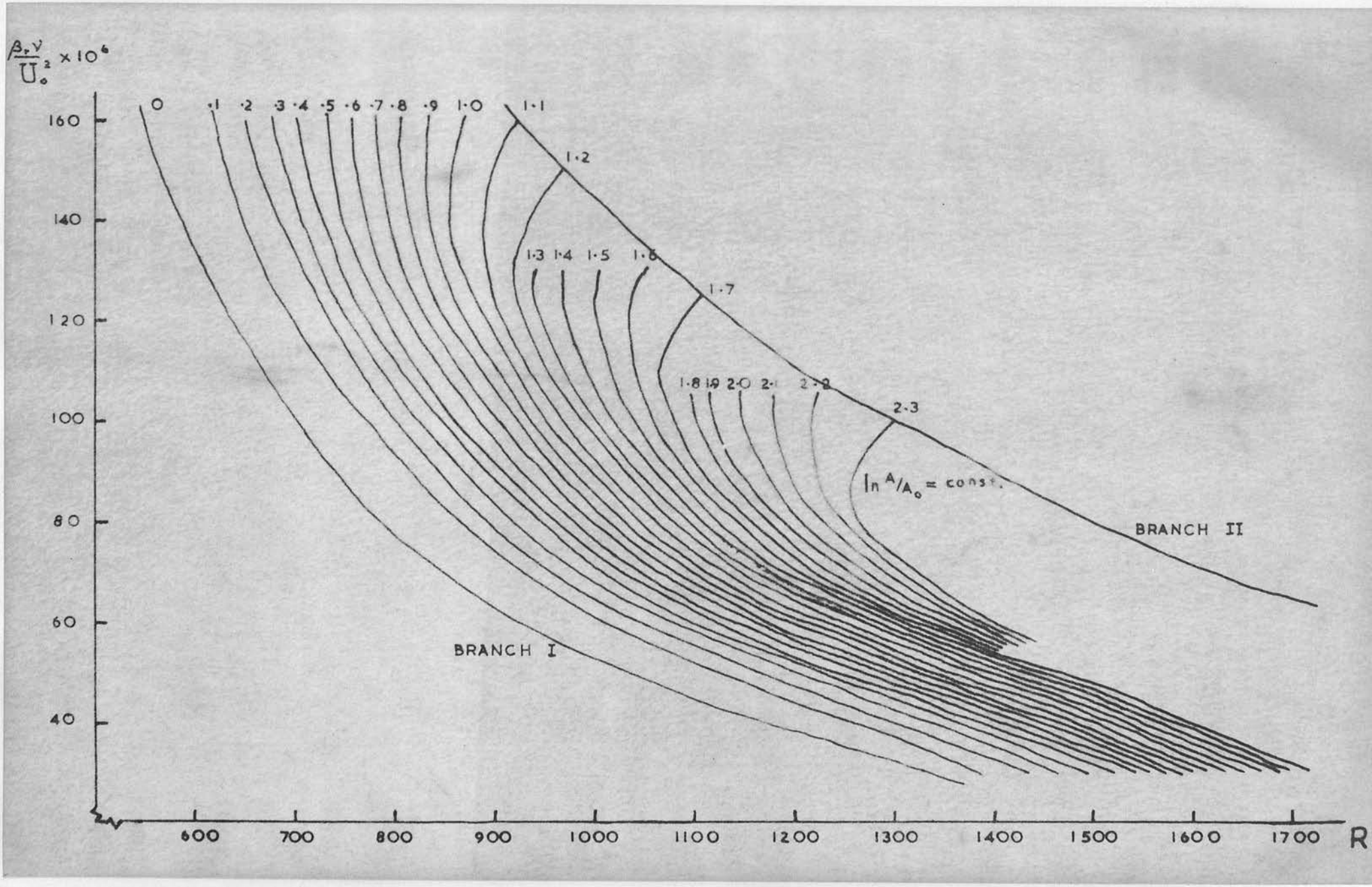

Figure V.9. Theoretical Curves of Constant Amplification with respect to Branch I of Neutral Curve (after Shen).

KEY TO Figures V.10.a-d.

/ Theoretical growth after Shen.

o Experimental points fitted to theoretical curve at R = 795.

Windspeed: 25 ft./sec.

Ribbon Amplitudes:

(o)	0.0002 inches
(1)	0.0004 inches
(2)	0.0007 inches
(3)	0.0010 inches

Frequencies:

Figure V.10a.	65 cycles/sec.
Figure V.10b.	80 cycles/sec.
Figure V.10c.	90 cycles/sec.
Figure V.10d.	103 cycles/sec.

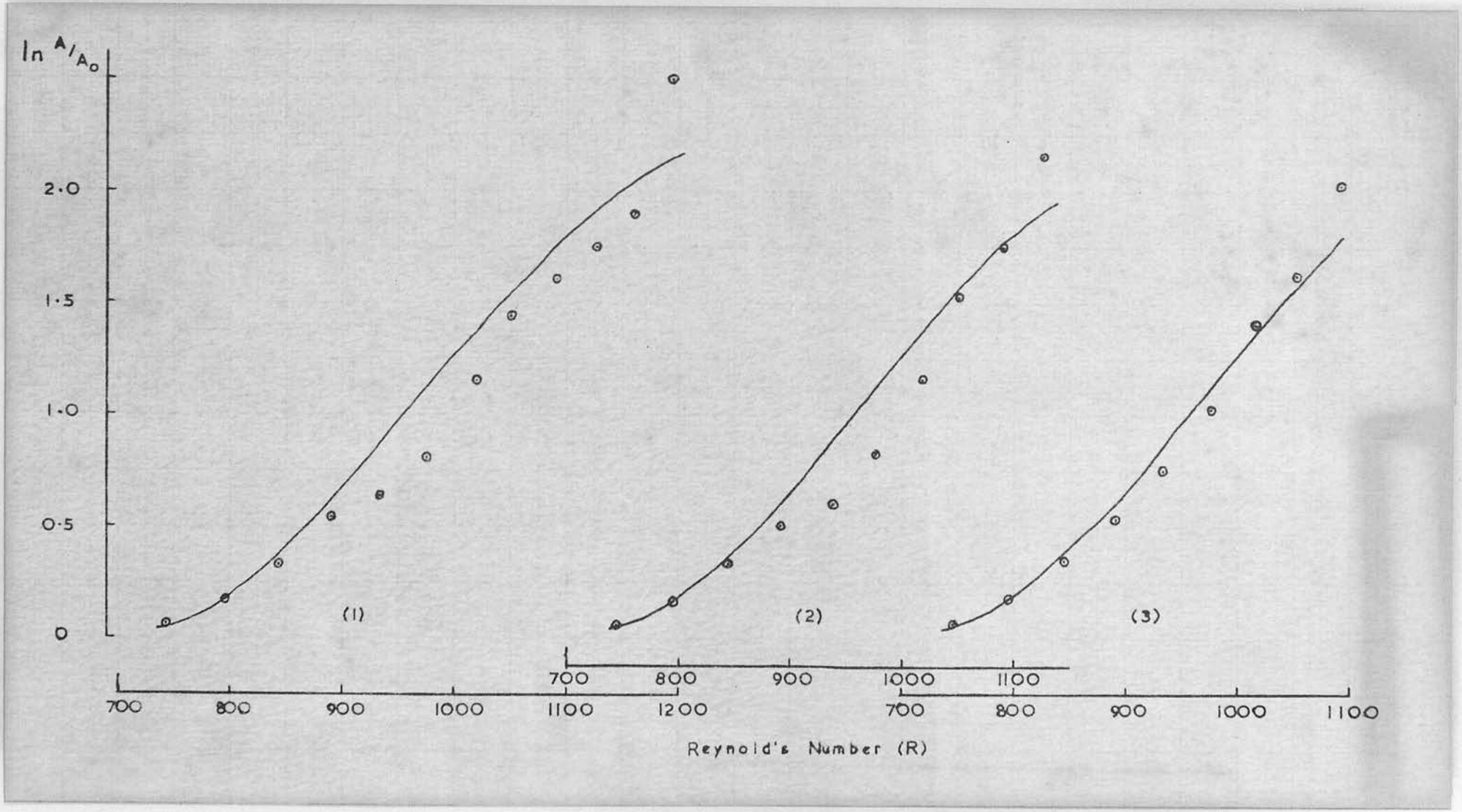

Figure V.10a. Downstream Growth of Disturbances (Linear Theory and Experiment).

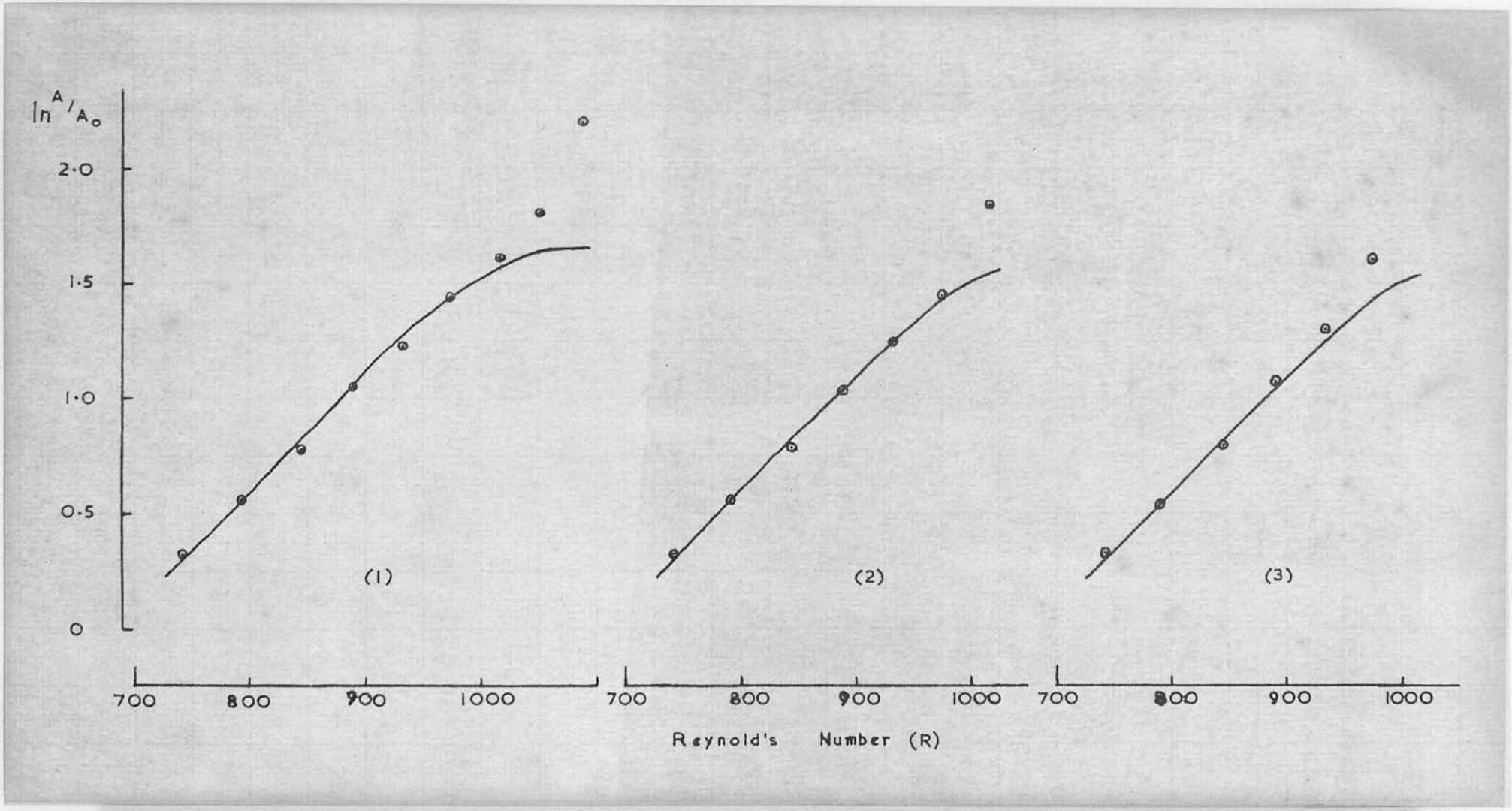

Figure V.10b. Downstream Growth of Disturbances (Linear Theory and Experiment).

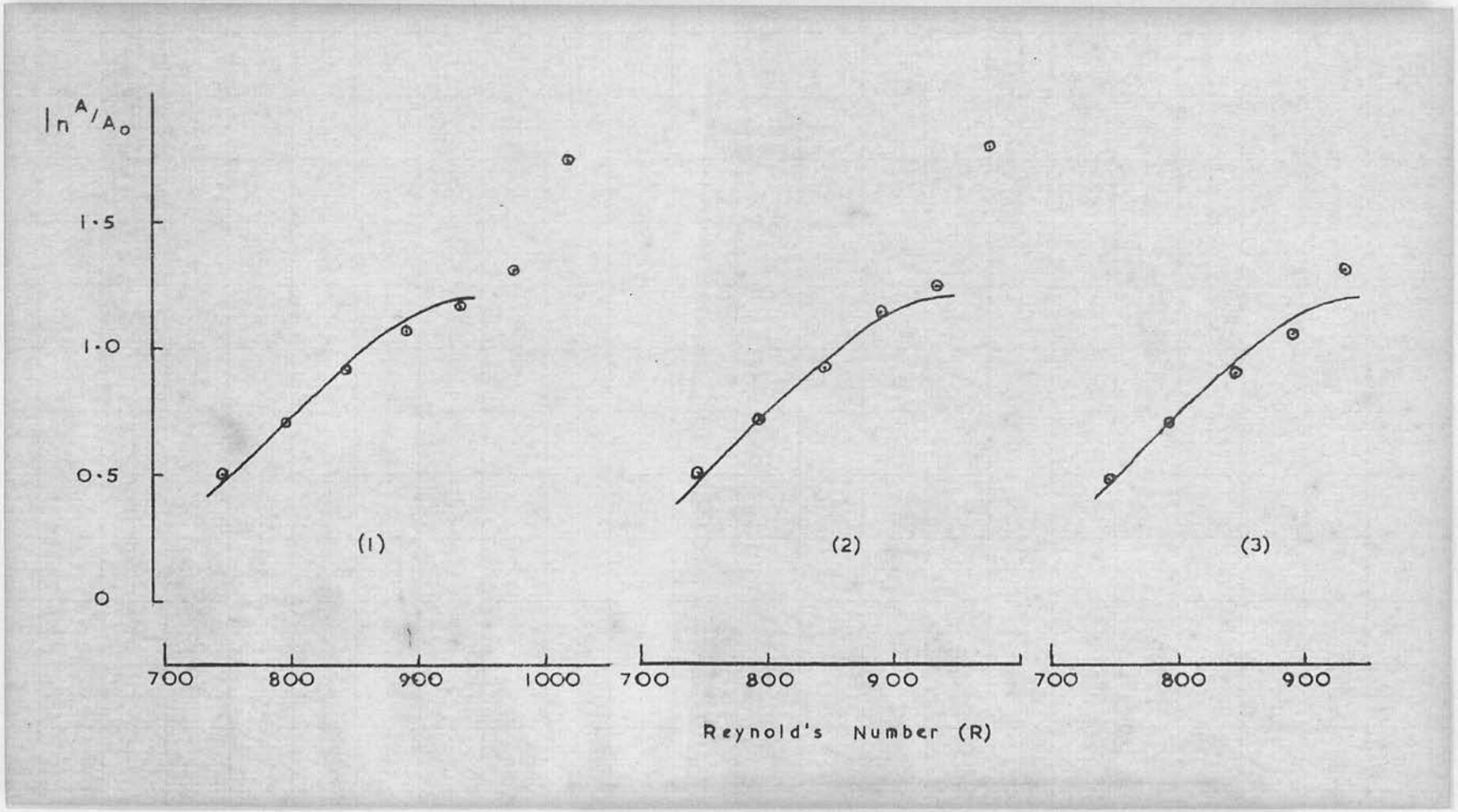

Figure V.10c. Downstream Growth of Disturbances (Linear Theory and Experiment).

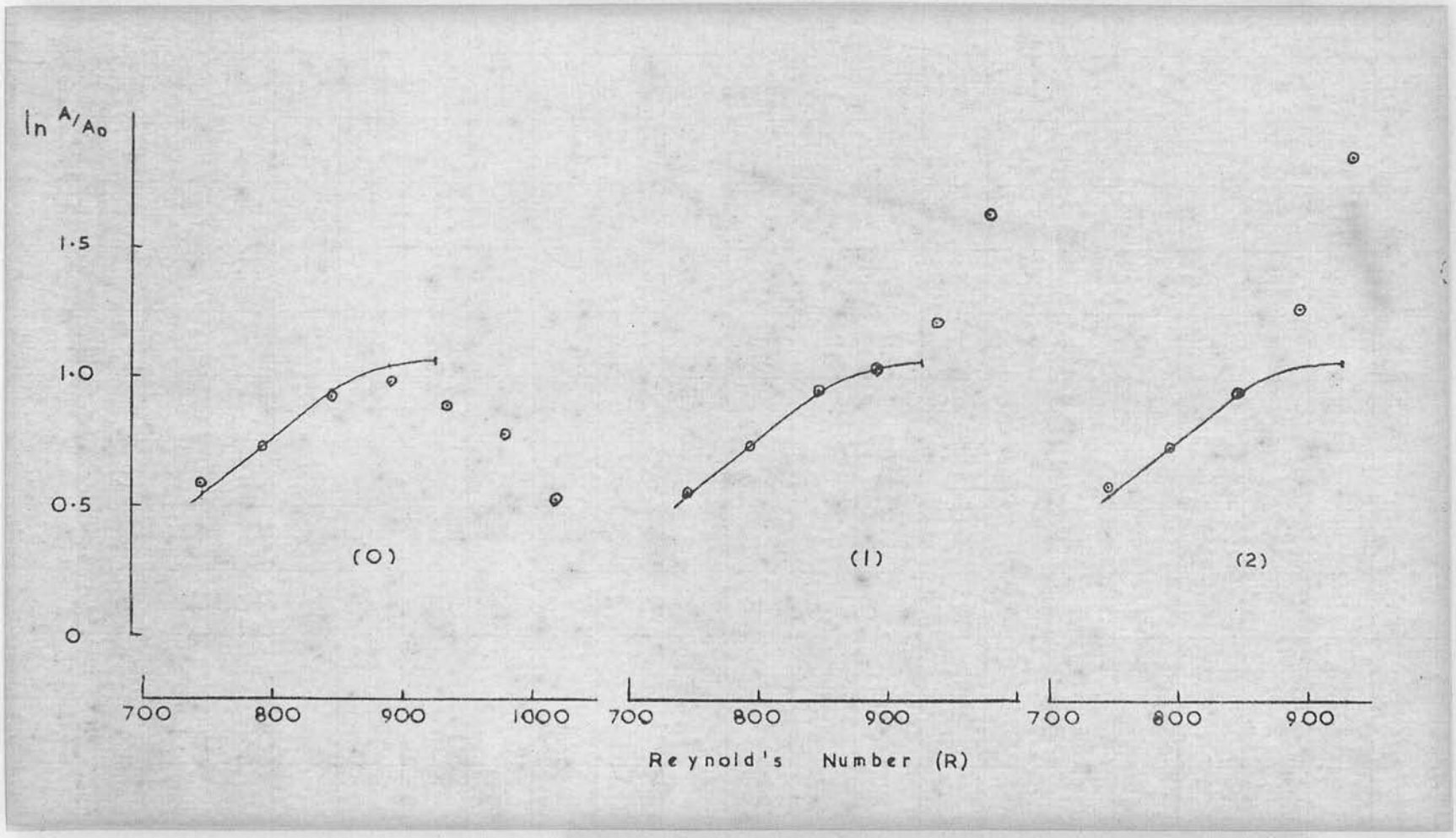

Figure V.10d. Downstream Growth of Disturbances (Linear Theory and Experiment).

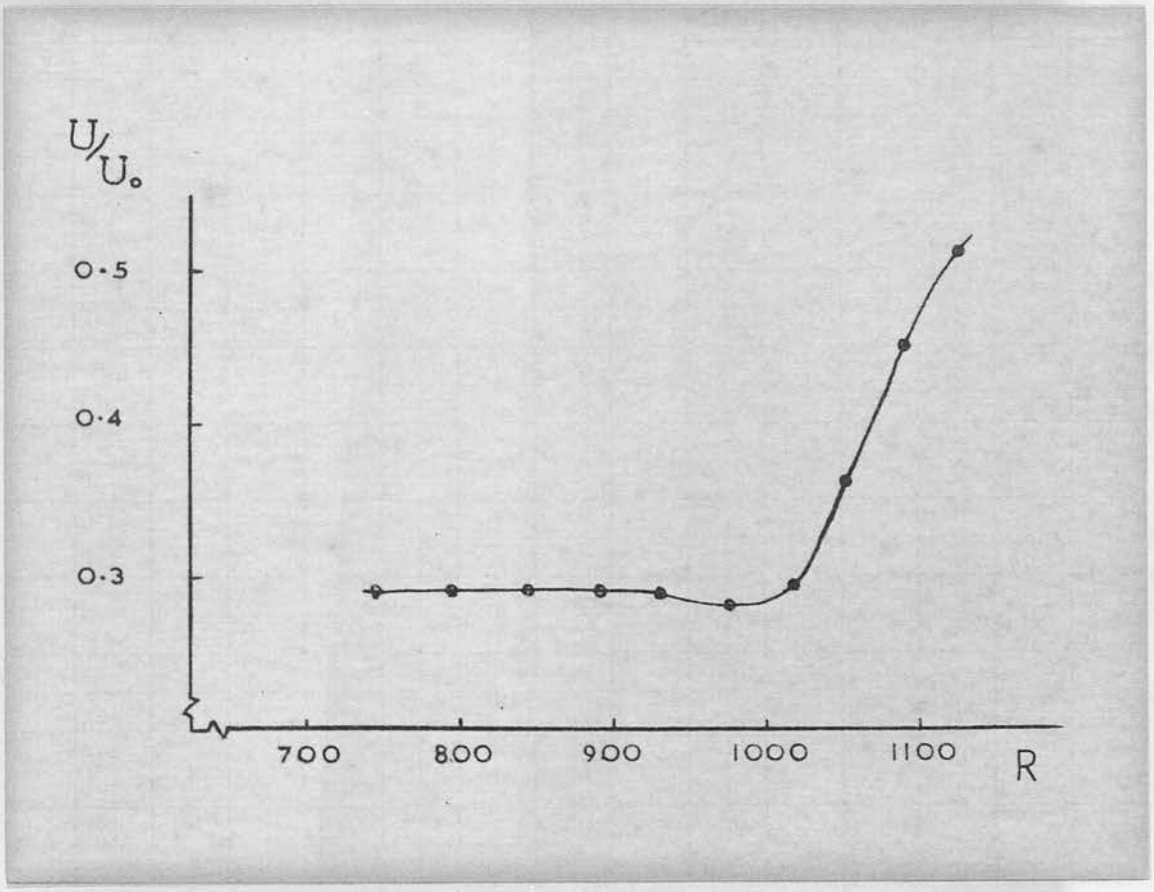

Figure V.11. Downstream Change in Local Mean Velocity.

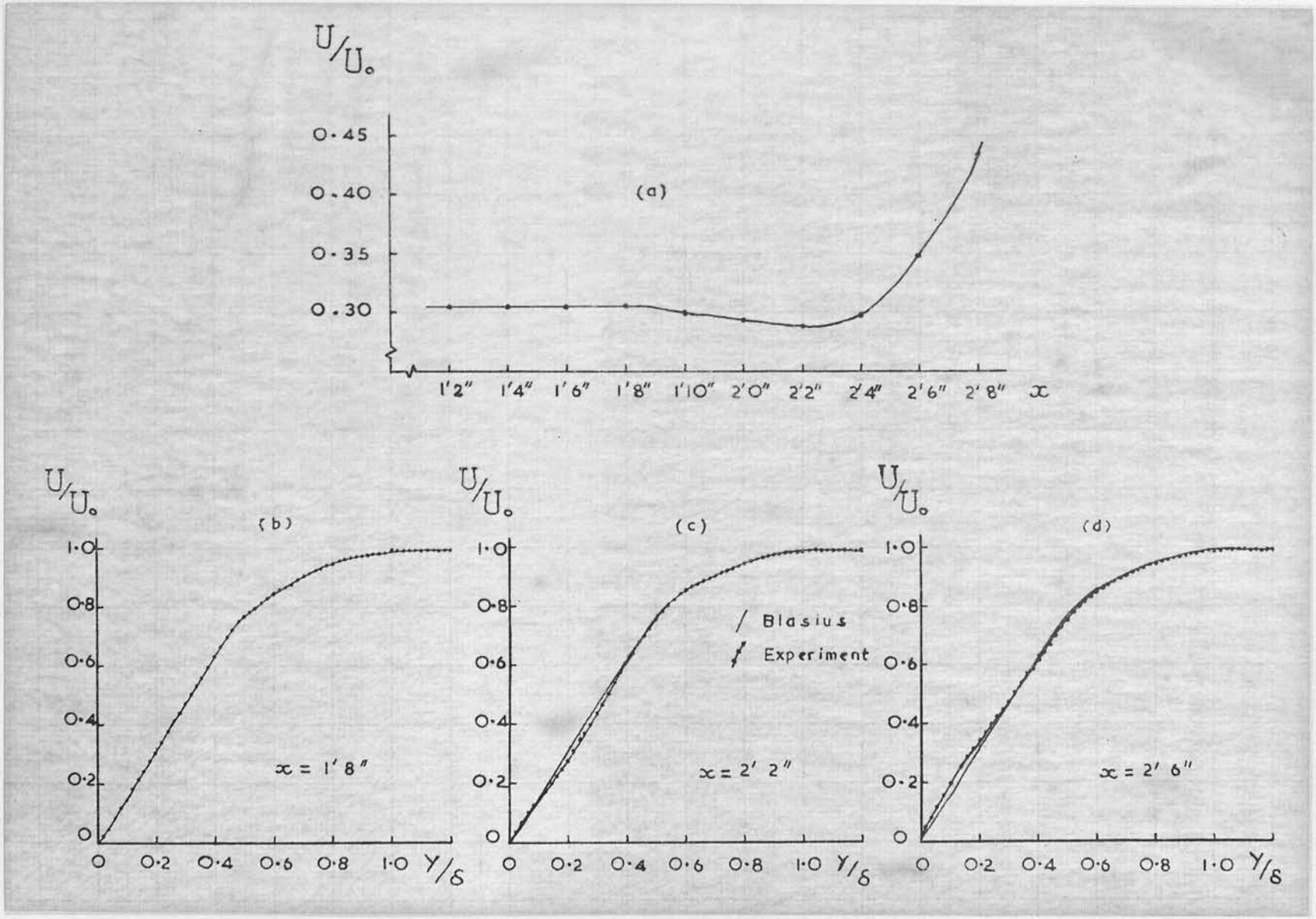

Figure V.12a. Downstream Change in Local Mean Velocity.
Figure V.12.b-d. Distortion of the Mean Flow Profile.

CHAPTER VI

HARMONIC CONTENT OF WAVE DISTURBANCES IN THE BOUNDARY LAYER

VI.1. Introduction

At this stage of the work it was felt that future interest should be confined to the study of some particular feature of flow behaviour rather than to continue with the more general studies already described. It was hoped that such a study would yield detailed information about some mechanism which was present in the transition process but which had received only superficial attention from other workers on account of its relative unimportance in their systems.

The generation of components of higher harmonic frequencies of a wave disturbance in the boundary layer had been considered theoretically by Lin (1958) in an order of magnitude analysis. His conclusion, already mentioned in Section I.2e, was that all harmonic components simultaneously become important around the critical layer before there is significant distortion of the mean flow. This conclusion is at variance with the work of Stuart reported by Bradshaw, Stuart and Watson (1960) where the mean motion distortion and second harmonic component are shown to be of order A^2 if the basic

perturbation is of small order A, while higher harmonic components are of order A^n ($n \geq 3$).

Experimental work on the generation of higher harmonics has been restricted to that of Klebanoff, Tidstrom and Sargent (1962). These workers made measurements of the harmonic content associated with wave growth in the vicinity of the critical layer. After a brief study they concluded that harmonic generation played an unimportant role in the breakdown process, and consequently made no further study of this phenomenon.

During the preliminary studies described in the previous chapter the presence of components of higher harmonic frequencies in the wave disturbance had been observed in oscilloscope displays of hot-wire output. In view of this, together with the theoretical conflict and the lack of existing experimental information, it was felt that the topic of the harmonic content of disturbances in the boundary layer was suitable for further study with the instrumentation and other resources available.

VI.2. Analysis of Linear Recordings

The first method employed to measure the magnitudes and phases of the harmonic components of the wave disturbances involved the filming of oscilloscope traces of hot-wire output signal with subsequent analysis of the filmed records.

The oscilloscope camera used was a 35mm moving film type with a gearbox to give a wide range of film speeds from 1 inch/sec. to 81 inches/sec.. A film speed suitable to the disturbance frequency was chosen and a film record made of the velocity fluctuations in the boundary layer, as detected by the hot-wire, by moving the film past a dual-beam oscilloscope which had its time-base switched off. In this way a linear recording of the hot-wire output together with a reference trace from the ribbon input was obtained.

After processing the film the recording of the hot-wire signal was analysed. In the method of analysis finally adopted a magnified projection of a length of film was cast on to squared paper by means of an epidiascope. The displacement of the trace was noted at twelve points per cycle of the fundamental disturbance separated by equal time intervals. A numerical Fourier analysis was carried out using these readings. A full description of the method has been given by Whittaker and Robinson (1946). An outline of the arithmetical computations is given in Appendix IV. The arithmetical analysis proved to be very time consuming when calculations were carried out by hand. To ease this burden the 'Sirius' digital computer was used in the numerical analysis. The Sirius Autocode program, based on the analysis of twelve consecutive cycles of filmed hot-wire trace, is given in Appendix V. This analysis gave values of the

amplitude and phase of the first five harmonics although only the first two of these can be regarded as significant as the amplitude of the others was comparable in magnitude to the background noise.

This method of determining the harmonic content of a wave disturbance had the disadvantage of taking a very long time since it involved filming, developing, processing, projection and analysis of the film and the preparation of punched data tapes for the computer.

VI.3. Downstream Development of the Second Harmonic

In the first experiments the harmonic content of the wave was studied by using a hot-wire at constant y/δ in the region of the critical layer. Filmed records of the hot-wire output were obtained at stations downstream of the ribbon from x = 1' 2" to breakdown of the wave at intervals of 2 inches in the x-direction. The spanwise position corresponded to a maximum of boundary-layer thickness. The windspeed was 25 feet/sec. and the ribbon vibration frequencies were in the range 40 cycles/sec. to 65 cycles/sec. These low frequencies were chosen because visual observations of the oscilloscope traces of hot-wire outputs had shown that the harmonic content appeared to be greater for low frequencies than for frequencies above the range chosen.

From the results of these studies it was immediately apparent that the decay and growth of the second harmonic

at constant y/δ did not necessarily follow that of the fundamental at this position. A typical result is shown in Figure VI.1. This shows that the fundamental had minimum intensity near x = 1' 6" which was close to Branch I of the neutral curve with the conditions listed. The second harmonic, which was an order of magnitude smaller than that of the fundamental, however increased in intensity up to x = 1' 10" then decreased before increasing rapidly in the region, just before a turbulent spot was detected, where the fundamental was amplifying rapidly. This graph is in conflict with one shown by Klebanoff, Tidstrom and Sargent (1962) for a downstream traverse at constant y in the neighbourhood of Branch II of the neutral curve. This graph shows that the second harmonic intensity was amplified downstream and no region of damping was noted.

In the present work increasing the ribbon amplitude caused the final rapid amplification of the second harmonic intensity to move upstream until no region of damping of the second harmonic could be detected, whereas it might have been expected that an upstream shift of the entire pattern would result. It would thus appear that the damping of the second harmonic was not an integral part of the breakdown process but was associated with some property of the second harmonic wave itself.

It should be noted here that Branch II of the neutral curve (after Shen) for a fundamental wave with a frequency the same as that of the second harmonic in Figure VI.1 occurred near x = 2' 3", but the first maximum of second harmonic intensity was found in the region of x = 1' 10".

From the computations of phase angles the wave velocity of the components of the disturbance was calculated. It was found that the second harmonic was travelling down the boundary layer with a wave velocity greater than that of the fundamental.

Observations at other y-positions showed that the second harmonic content of the wave was not constant through the boundary layer. In the region of the minimum of the fundamental intensity the second harmonic intensity was observed to be comparable in magnitude to that of the fundamental, a result which is at variance with the conclusion of Lin that the harmonics would become important around the critical layer. The above result, however, appeared to be also in conflict with the observation of Klebanoff et. al. that the percentages of second harmonic present at two y-stations near 0.2δ and 0.6δ were comparable in magnitude.

In view of this apparent conflict it was felt that more information about the second harmonic content would be gained by studying its intensity distribution through the boundary layer at several x- and z- positions rather than continuing with the traverses at constant Y/δ.

As one traverse through the boundary layer at fixed x - and z - position involved making observations at up to 40 y-stations the time consuming nature of the film analysis method made its use impracticable. In consequence another approach to harmonic analysis was sought. This resulted in the construction of the band-pass filters described in Section IV.7..

VI.4. Preliminary Observations of Second Harmonic Intensity Distributions

In the first series of traverses through the boundary layer the second harmonic intensity was studied as a fraction of the fundamental wave intensity. Windspeed and frequency were chosen so that Branch I of the neutral curve was near the ribbon position and the Z - position was one of maximum boundary-layer thickness. It was found that this ratio did not remain constant as the y-position was altered. A graph typical of those obtained is shown in Figure VI.2. From a value of about 15 per cent. at $y/\delta < 0.1$ the ratio of second harmonic to fundamental intensities fell as y increased to approximately $0.6\,\delta$. A rapid rise followed, values sometimes in excess of 100 per cent. being found near $y = 0.8\,\delta$ with a steady fall in the ratio for y values above this into the free stream. A dependence on x-position was noted particularly in the region $0.2 < y/\delta < 0.5$,

where an increase in the second harmonic content was observed in the region of non-linear amplification of the fundamental. The magnitude and width of the maximum near 0.8 δ was found also to be dependent on downstream position.

The next step was to study the distribution of the second harmonic intensity through the boundary layer in the y-direction as the previous results had indicated that this must differ from the fundamental intensity distribution. Observations of first and second harmonic intensity were made through the boundary layer at stations separated by an interval of 0.01 inches in the y-direction. The fundamental frequency of 65 cycles/sec. allowed one of the sets of filters to be used. The windspeed chosen was 25 feet/sec. The ribbon amplitude of 0.001 inches was kept constant throughout this series of experiments.

The distributions of first and second harmonic intensities through the boundary layer at x = 1' 6" and at a spanwise position of maximum boundary-layer thickness are plotted in Figure VI.3. It can been seen that the second harmonic intensity distribution differed significantly from that of the fundamental, this latter being in general agreement with the predictions of linear theory. For the second harmonic the intensity reached a maximum value close to the plate for $y/\delta < 0.1$.

A minimum intensity was noted in the region of $y/\delta = 0.6$. At the minimum intensity of the fundamental near $y/\delta = 0.8$ the second harmonic content was large compared to the fundamental.

Traverses through the boundary layer at other stations further downstream showed that the second harmonic intensity increased in the region $0.2 < y/\delta < 0.5$ with increasing x - position until a second maximum of second harmonic intensity appeared at $y/\delta = 0.3$.

Boundary-layer traverses at other spanwise positions gave second harmonic intensity distributions essentially similar to those at the position of maximum boundary-layer thickness. The main features of a maximum intensity close to the plate and a minimum near $y/\delta = 0.6$ were the same at all spanwise positions, differences occurring in the region $0.2 < y/\delta < 0.5$.

There was no theoretical evidence available regarding the distribution of the second harmonic through the boundary layer nor had any experimental work been reported. Consequently, it was decided to investigate this feature more fully under as carefully controlled conditions as were possible with the Heriot-Watt tunnel. The purchase of the Brüel and Kjaer frequency analyzer to replace the filter and thermojunction units allowed for much greater flexibility in the choice of frequency and also greatly reduced the time taken to make an observation.

VI.5. Distribution of the Second Harmonic Intensity through the Boundary Layer

Before the commencement of this phase of the work the mesh screens were removed from the tunnel to be cleaned. On replacing these screens after cleaning a traverse in the spanwise direction was made at a fixed distance from the plate using the instrument described in Section V.5a. This showed that any variation in boundary-layer thickness in the spanwise direction was masked by the fluctuations in windspeed resulting from the natural unsteadiness of the tunnel. From the readings of local mean velocity at the probe position in the boundary layer it was concluded that any variation in boundary-layer thickness in the z - direction was less than 5 per cent.

Although it was not possible to detect three-dimensionality in the boundary layer by mean flow measurements it was found that an artificially introduced two-dimensional disturbance had differing rates of growth in the streamwise direction at various z-positions. The growth curves obtained from hot-wire readings taken at a constant y/δ in the region of the critical layer, showed that the rapid amplification of the wave preceding breakdown occurred at a position further upstream at $Z = 0.5$ inches than at $Z = 1.0$ inches. This indicated that the boundary layer was three-dimensional, energy being transferred in the spanwise direction as the wave was amplified while moving downstream. It was thus

concluded that z = 0.5 inches, where the rapid growth occurred furthest upstream, was in the vicinity of the spanwise position for maximum growth rate of the disturbance, whilst z = 1.0 inches was in the vicinity of the spanwise position for minimum growth rate.

The ribbon vibration frequency used in these studies was 55 cycles/sec. and the ribbon amplitude was 0.0012 inches. This was the amplitude used almost exclusively throughout this phase of the work. With the windspeed of 25 feet/sec. Branch I of the neutral curve was near x = 1' 4".

From values of local mean velocity at each downstream position obtained from hot-wire resistance readings it was found that, with the conditions listed above, the distortion of the mean flow occurred first in the region of x = 2' 0".

Distributions through the boundary layer of the intensities of the first and second harmonics of the longitudinal fluctuations were found by traversing the hot-wire outwards from the surface of the plate in steps of 0.0005 inches. Figures VI.4a.-f. show the results of these traverses at z = 0.5 inches for x = 1' 4" to z = 2' 2" with 2 inch interval.

For the first harmonic, the distribution showed the familiar features of a maximum of intensity in the region of Y/δ =0.2, whilst the minimum was at Y/δ = 0.85, for x = 1' 4" moving in to about Y/δ =0.75 for x = 2' 2", a phase change of 180 degrees being noted on an oscilloscope when passing through the minimum.

The distribution of the intensity of the second harmonic also showed a maximum and a minimum, but these were closer to the plate than in the case of the first harmonic, results which confirmed the earlier observations (Section VI.4.). The maximum intensity occurred at $Y/\delta < 0.1$, whilst the minimum was at Y/δ = 0.7 for x = 1' 4" moving to Y/δ = 0.55 for x = 2' 0". It would appear from Figure VI.4f. that the minimum had moved to a higher value of Y/δ at x = 2' 2". Observations on an oscilloscope of the output from the frequency analyzer revealed that a phase change of 180 degrees occurred on passing through the position of minimum second harmonic intensity. At all x - positions the second harmonic intensity peak was about an order of magnitude smaller than that of the first harmonic.

The shape of the second harmonic intensity distribution in the region $0.15 < Y/\delta < 0.5$ is of interest. For x = 1' 4" the distribution exhibited a slight 'fullness' in this region. Two inches further downstream this

'fullness' had become more evenly distributed over this region so that the shape of the second harmonic intensity distribution through the boundary layer closely resembled the Tollmein-Schlichting distribution of the first harmonic intensity, but had a lateral shift towards the plate. At x = 1' 8" the second harmonic intensity distribution was concave in shape between the maximum and the minimum, but two inches further downstream, the 'fullness' had reappeared in the region of $y/\delta = 0.3$. A further growth of the second harmonic content in this region was observed at x = 2' 0". At x = 2' 2" the second harmonic content had increased to such an extent in this region that the intensity distribution through the boundary layer showed twin maxima, one close to the plate at $y/\delta < 0.1$ and the other at $y/\delta = 0.2$.

The intensity of the second harmonic in the outer region of the boundary layer had a maximum value at x = 1' 6", thereafter decreasing further downstream to a minimum at x = 2' 0". The height of the peak close to the plate also showed changes with downstream position.

A ribbon vibration frequency of 70 cycles/sec. was used later in this work. With a windspeed of 25 feet/sec., Branch I of the neutral stability curve lay at about x = 1' 0" so that the disturbance of fundamental frequency was in an amplifying region immediately downstream of the ribbon. Mean flow distortion under these conditions was first apparent at about x = 1' 9".

A boundary layer traverse made at x = 1' 8" with this ribbon frequency and amplitude (0.0012 inches) showed that the shape of the second harmonic intensity was similar to that at x = 1' 8" for a frequency of 55 cycles/sec.; a sharp maximum close to the plate with concave form for $0.1 < y/\delta < 0.6$ was noted (Figure VI.5a.) Further downstream, at x = 2' 2", in the region of mean flow distortion resulting in lower local mean velocity than expected from the Blasius profile, the intensity distribution of the second harmonic through the boundary layer had two maxima (Figure VI.5b.). The maximum closer to the plate occurred for $y/\delta < 0.1$ whilst the other was near $y/\delta = 0.3$. This outer peak was some three times larger than the other. At x = 2' 6", with the boundary layer profile tending towards turbulent shape, this outer peak in the second harmonic intensity distribution had grown and spread to such an extent that the maximum close to the plate had been absorbed by it (Figure VI.5c.). At this position, a large maximum of nearly 20 per cent. of the fundamental intensity was apparent for $y/\delta \sim 0.5$, the minimum had moved towards the edge of the boundary layer. There was evidence that another maximum of second harmonic intensity occurred in the region of $y/\delta = 0.65$ at this x - position (Figure VI.5c.). However, the scatter in the experimental points was large in this region, and additional information

would be required to definitely establish the existence of this peak.

A further series of boundary layer traverses was made for the spanwise position z = 1.0 inches. It was found that there were twin maxima in the second harmonic intensity distribution through the boundary layer for all x - positions. The magnitude of the second harmonic intensity in the outer region of the boundary layer was found to be larger in general at z = 0.1 inches than at z = 0.5 inches

Figure VI.6. shows the distributions of the first and second harmonic intensity through the boundary layer at x = 1' 8" for a frequency of 55 cycles/sec. The small peak in the second harmonic intensity near $y/\delta = 0.3$ for this z - position can be contrasted with the concave shape in the region at z = 0.5 inches shown in Figure VI.4c.

Figures VI.7a -f, show the growth of this outer peak in the second harmonic intensity distribution for the frequency 70 cycles/sec. at z = 1.0 inches. For x = 1' 4" to x = 1' 8" the magnitude of this secondary peak was small, being only some 2 per cent. of the first harmonic intensity. However, further downstream this peak grew and spread rapidly until at x = 2' 2" it had almost absorbed the inner peak and now had a magnitude of approximately 15 per cent. of the first harmonic intensity in the vicinity of the critical layer.

The distribution through the boundary layer of the third harmonic intensity for a ribbon frequency of 70 cycles/sec., $z = 0.5$ inches and $x = 1'\ 6''$ is shown together with first and second harmonic intensities in Figure VI.8.. This shows that the third harmonic intensity had a maximum, closer to the plate surface than $y/\delta = 0.1$, which was an order of magnitude smaller in size than that of the second harmonic, that is, less than 1 per cent. first harmonic intensity.

VI.6. Note on Errors

A close quantitative analysis of the graphs in the above section will show apparent minor inconsistancies. It should be realised that large quantitative errors were present in certain aspects of this experimental work. However, these do not detract from the importance of the qualitative aspect of the results.

The largest uncertainty arose in the assessment of ribbon amplitude. The accuracy of this procedure in an absolute measurement was certainly no better than $\pm$ 10 per cent. The effect of even a 10 per cent. increase in ribbon amplitude on the boundary layer was marked and under certain conditions could result in an upstream movement of several inches of the transition process.

VI.7. Further Experiments on the Nature of the Harmonic

To ensure that the harmonic intensity distributions obtained were peculiar to the second harmonic and were not common to an injected disturbance of the same frequency, the distribution of the intensity of the fundamental was found for a disturbance whose frequency was 110 cycles/sec. The ribbon amplitude was adjusted so that the intensity of the disturbance was of the same order of magnitude as the intensity of the second harmonic at the x - and z - position chosen, x = 1' 8", z = 0.5 inches, with a ribbon frequency of 55 cycles/sec.

The distribution of the intensity of the second harmonic of 110 cycles/sec. (Figure VI.5c) was different from the distribution of the intensity of the fundamental of the same frequency (Figure VI.9.). The shape of the distribution of the fundamental intensity agreed well with the linear theory, whilst that of the 110 cycles/sec. second harmonic has already been described.

By observing the phase of the signal output from the frequency analyzer relative to that of a reference trace displayed on a double beam oscilloscope, measurements were made of the wavelengths of the first and second harmonic waves in the boundary layer for several fundamental frequencies. The wave velocities of the first and second harmonics were calculated from these wavelengths.

It was found that the wave velocity of the first harmonic was in fairly good agreement with the predictions of linear theory. The wave velocity of the second harmonic had a higher value than that of the fundamental and was within 5 per cent. of the wave velocity measured for a fundamental of the same frequency. It should be noted however, that the wave velocity of the second harmonic was always slightly lower even though within 5 per cent. of that of the fundamental of the same frequency.

The downstream growth of the second harmonic wave was studied at a constant y/δ value of approximately 0.1 in the region of the peak of the second harmonic disturbance intensity. With a small ribbon amplitude, the x-position of maximum second harmonic intensity was noted in the region where the fundamental had not significantly departed from linear theory. These positions are plotted on the ($\beta_r \nu / U_o^2$, R) plane in relation to the neutral curve in Figure VI.10. for as wide a range of conditions as could be conveniently attained with the tunnel. It can be seen that in general these points lie close to Branch II of the neutral curve.

From analysis of filmed oscilloscope traces of second harmonic and a reference trace it was found that, for x = 1' 6" and $y/\delta \sim 0.1$ the harmonic wave was in phase at z = 0.5 inches and z = 1.0 inches. However,

further downstream in the region of the rapidly developing second harmonic intensity peak at $y/\delta \sim 0.3$ a phase difference of approximately 120 degrees was observed between the second harmonic at z = 0.5 inches and that at z = 1.0 inches.

Bradshaw, Stuart and Watson (1960) have suggested that the conclusion of Lin (1958) on the generation of higher harmonics in the critical layer before mean flow distortion could possibly be applied to large disturbances. To test this suggestion the ribbon amplitude was increased and traverses made through the boundary layer at a downstream position just before distortion of the mean flow. A graph, for approximately doubled ribbon amplitude shown in Figure VI.11. illustrates the general result that the ratio of second harmonic intensity to first harmonic intensity increased with increasing ribbon amplitude. The intensity of the second harmonic in the boundary layer, therefore, appeared to be a function of the amplitude of the initial disturbance, though in no case could this disturbance be made large enough to satisfy Lin's predictions.

VI.8. Non-linearity of the Hot-Wire

It was realised that the non-linearity of the hot-wire would produce distortion of the signal which would tend to contribute to the measured second harmonic content.

The effects of this non-linearity could be expected to be greatest in regions where the disturbance velocities were not small in comparison with the mean velocity. A region of low mean velocities and relatively large disturbance velocities occurs in the boundary layer close to the plate for $y/\delta < 0.1$. As this was the region where the measured second harmonic intensity had a maximum it was felt that an analysis of the contribution to the second harmonic intensity resulting from hot-wire non-linearity would be necessary to establish the validity of the results obtained.

A numerical analysis of second harmonic content resulting from hot-wire non-linearity was carried out using the Manchester University 'Atlas' digital computer. The program for this analysis in Atlas Autocode given in Appendix VI.

It was found that, under typical conditions in the region of the boundary layer for $y/\delta < 0.2$ the second harmonic intensity contributed by hot-wire non-linearity was at most some 3 per cent. of the fundamental intensity.

After deduction of the hot-wire contribution to second harmonic intensity from the measured intensity in no instance was the resulting intensity distribution significantly different from that measured. Thus the results of this numerical analysis showed that in the present work the second harmonic contribution from hot-wire non-linearity could be neglected.

VI.9. Harmonic Content of the Ribbon Vibration

The output from the capacitance electronics used to monitor the ribbon performance was analysed for harmonic content. It was found that under typical conditions the second harmonic content was some 4 per cent. of the fundamental. Part of this second harmonic must undoubtedly have been contributed by the non-linearity of the capacitance electronics. The input signal to the ribbon was found to contain approximately 2 per cent. second harmonic.

As nothing is known about the coupling between the ribbon and the boundary layer it must be assumed that some of this second harmonic distortion present in the ribbon motion was transmitted to the boundary layer. Thus, at least part of the harmonic content measured in the boundary layer may have come from the ribbon and not from a non-linear distortion of the fundamental disturbance by the boundary layer. The fact that the second harmonic in the boundary layer may have been at least partially generated by the ribbon however in no way detracts from the importance of the results obtained for the intensity distributions of the second harmonic through the boundary layer.

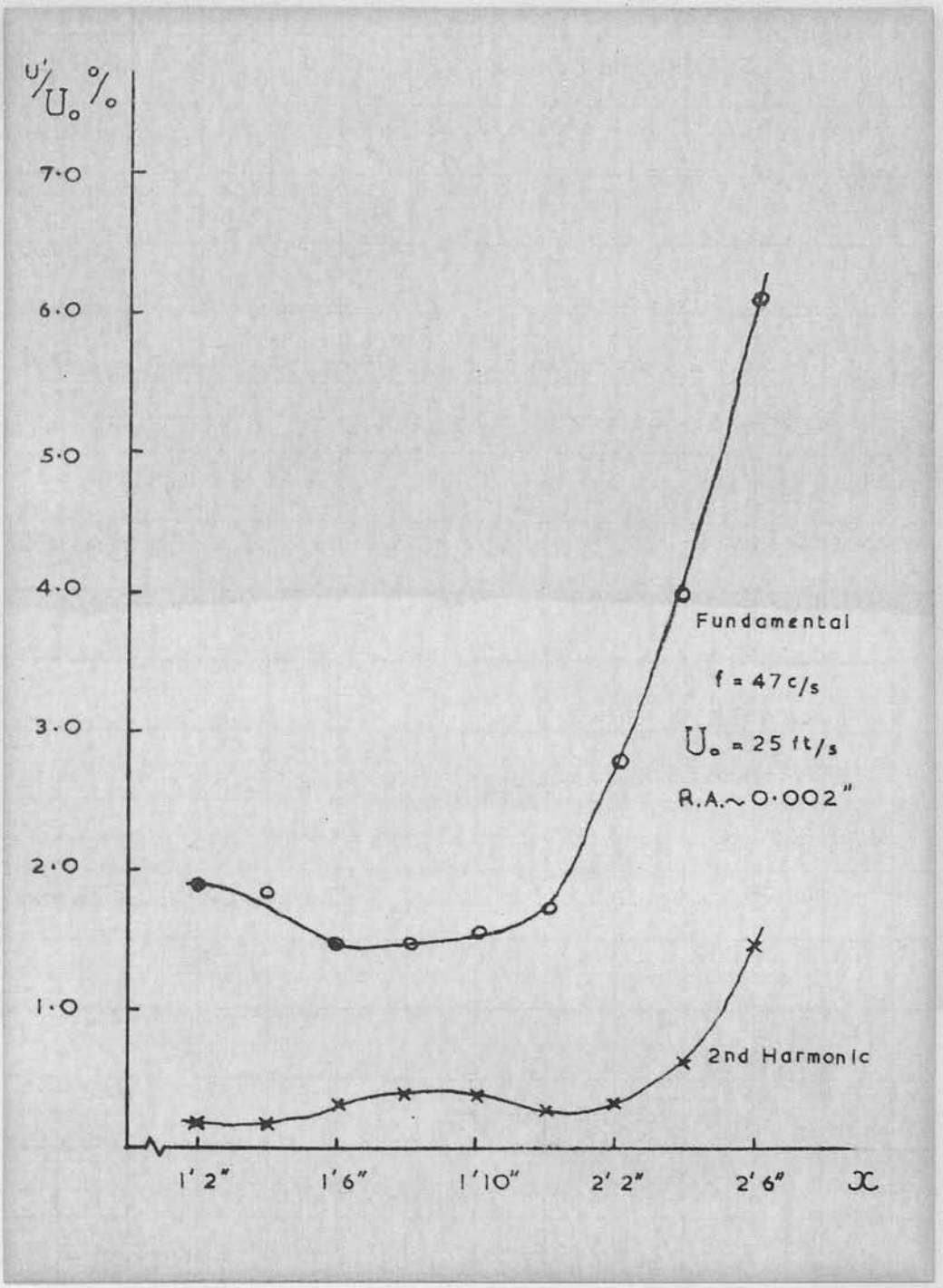

Figure VI.1. Downstream Development of Fundamental and Second Harmonic Intensities.

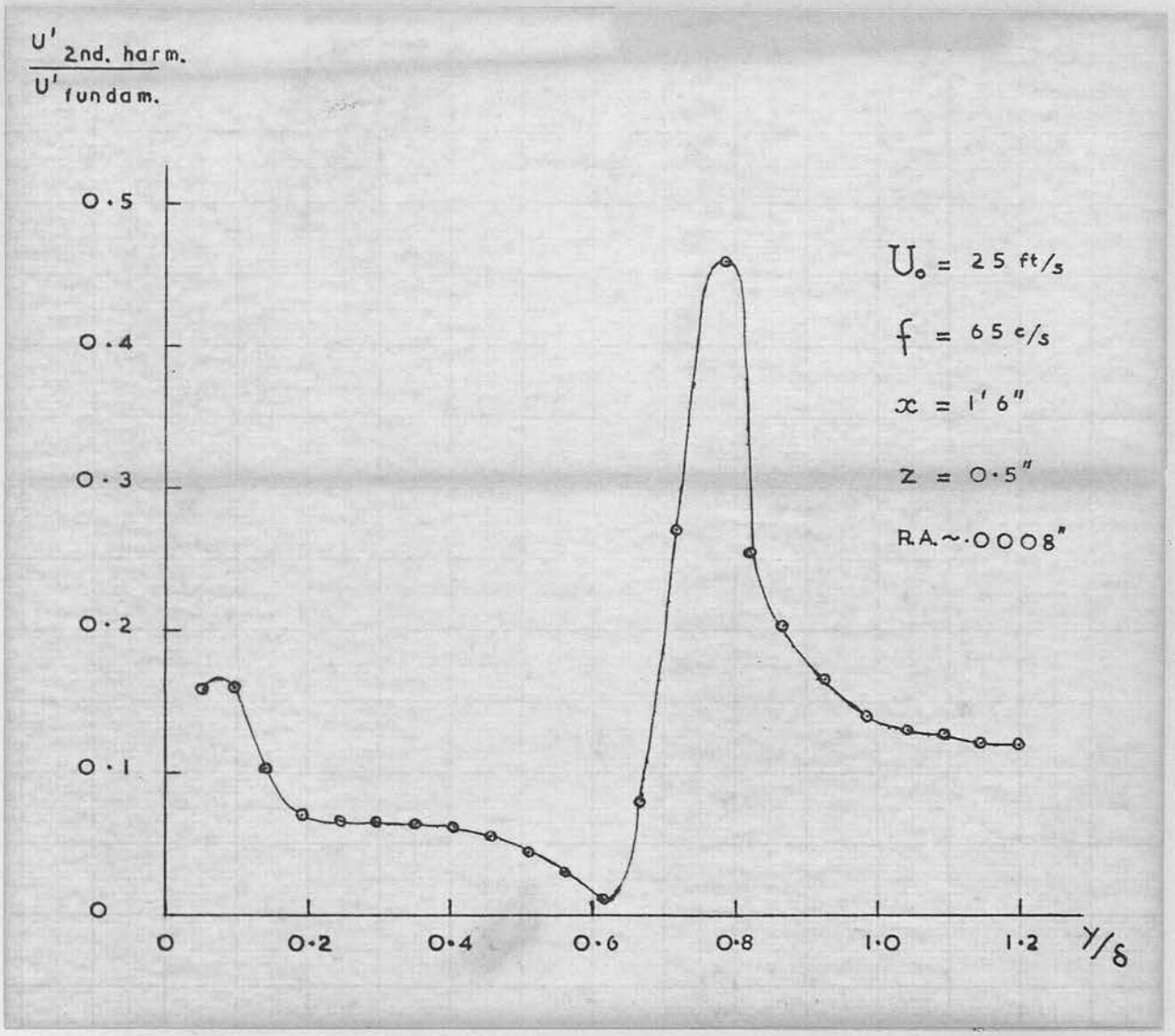

Figure VI.2. Ratio of Fundamental to Second Harmonic Intensities through the Boundary Layer.

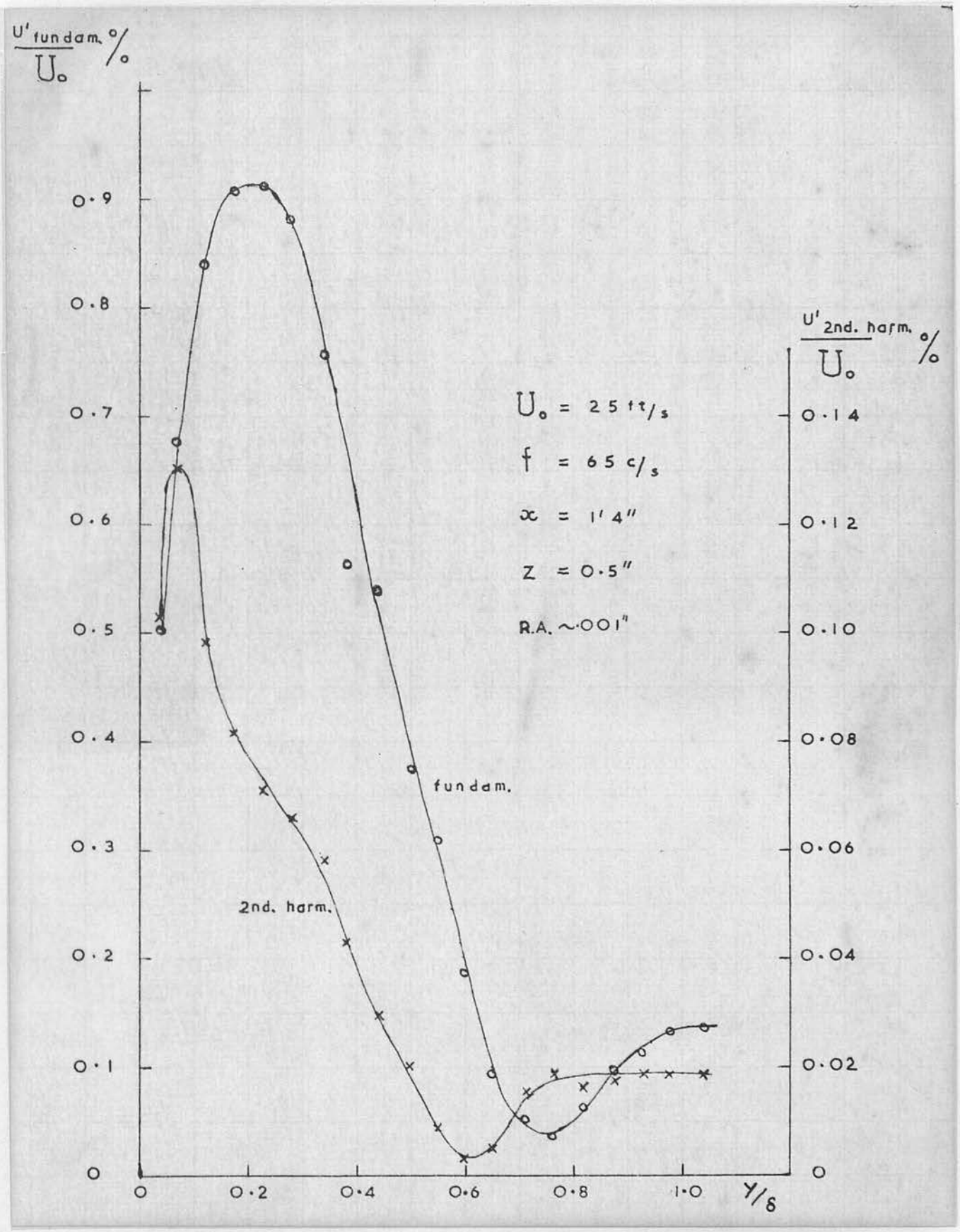

Figure VI.3. Distribution of Fundamental and Second Harmonic Intensities through the Boundary Layer.

NOTE

In Figure VI.4. to Figure VI.9. and Figure VI.11.

① denotes Fundamental Intensity

② denotes Second Harmonic Intensity x 10

③ denotes Third Harmonic Intensity x 10

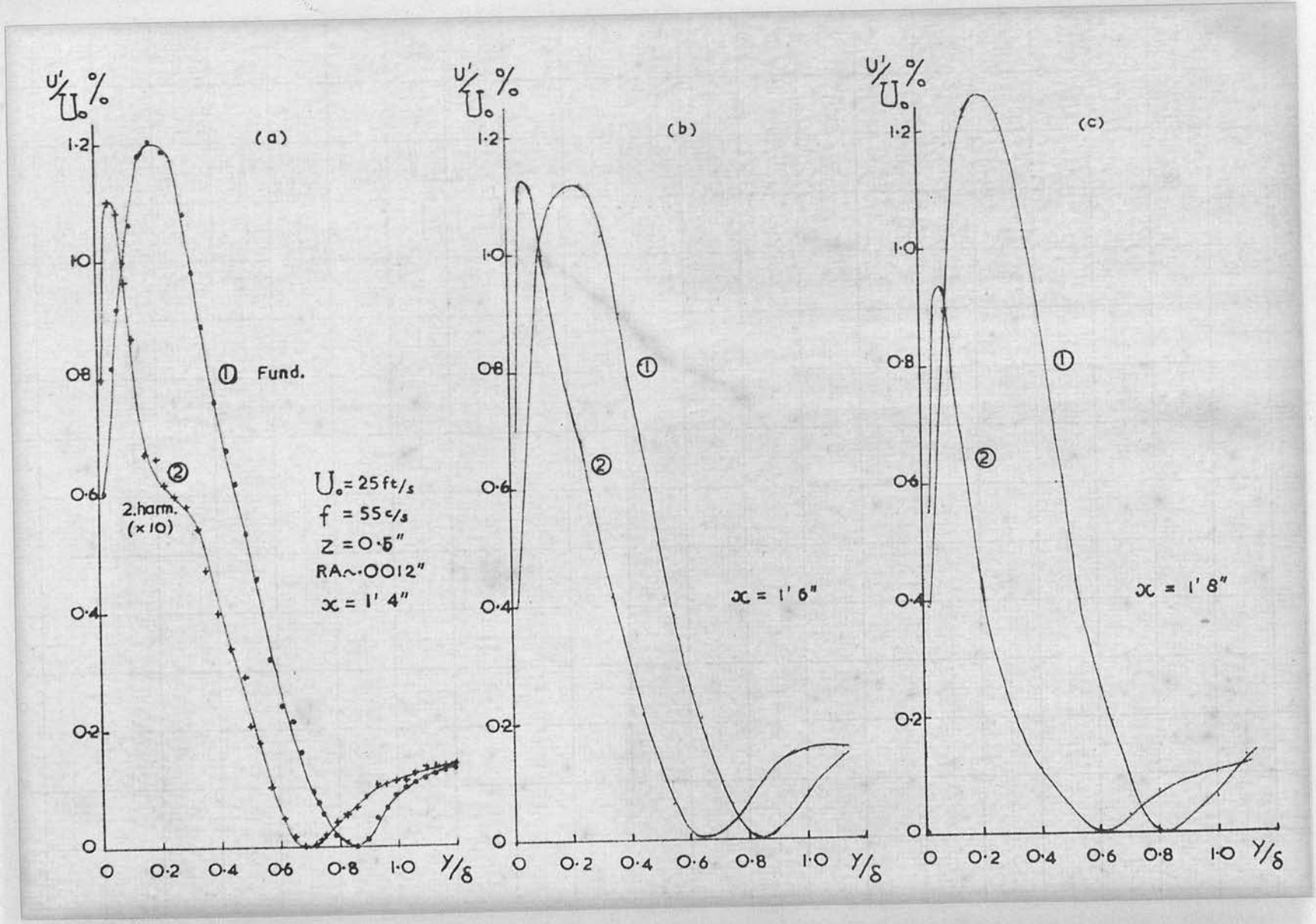

Figure VI.4.a-c. Distribution of Fundamental and Second Harmonic Intensities through the Boundary Layer.

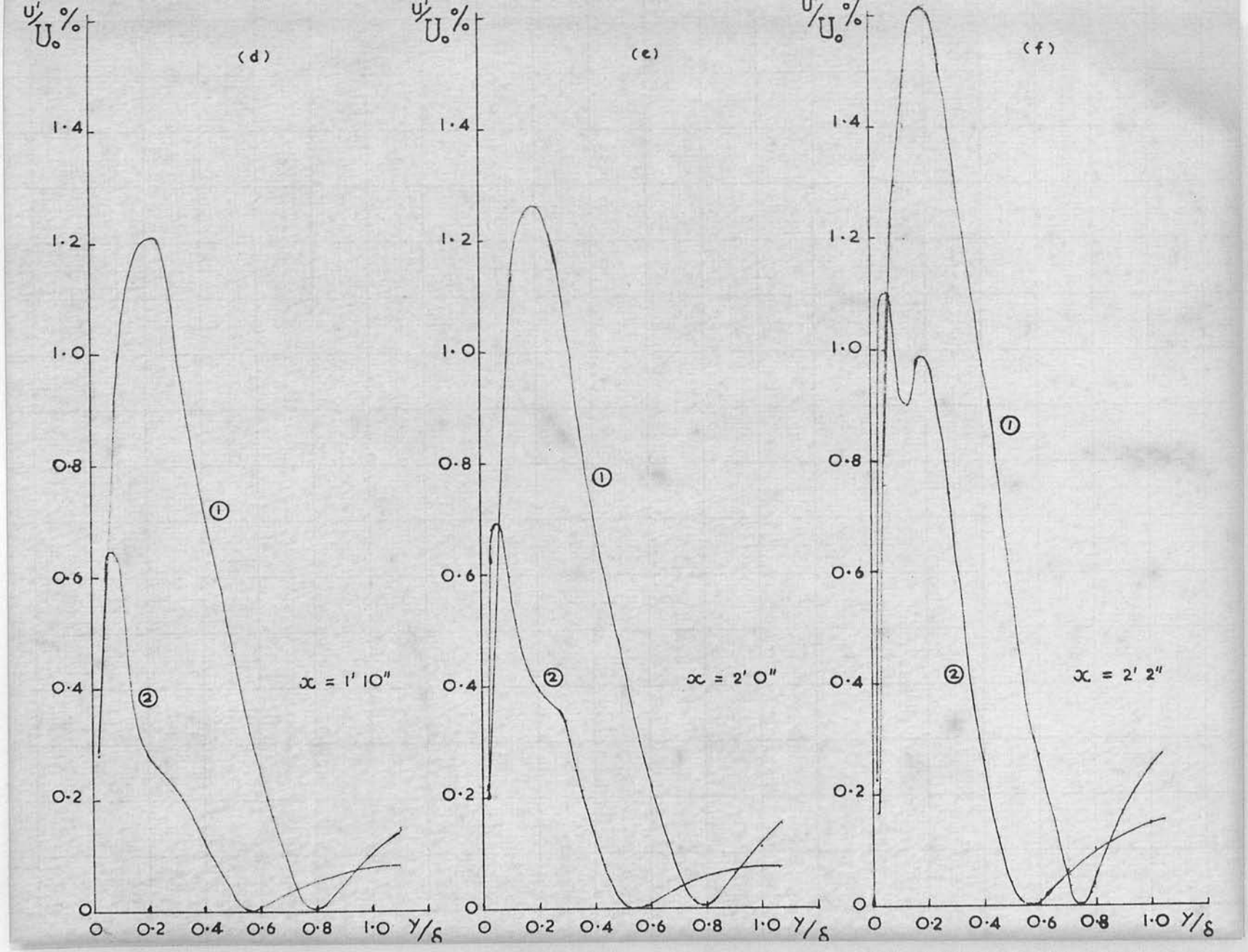

Figure VI.4.d-f. Distribution of Fundamental and Second Harmonic Intensities through the Boundary Layer.

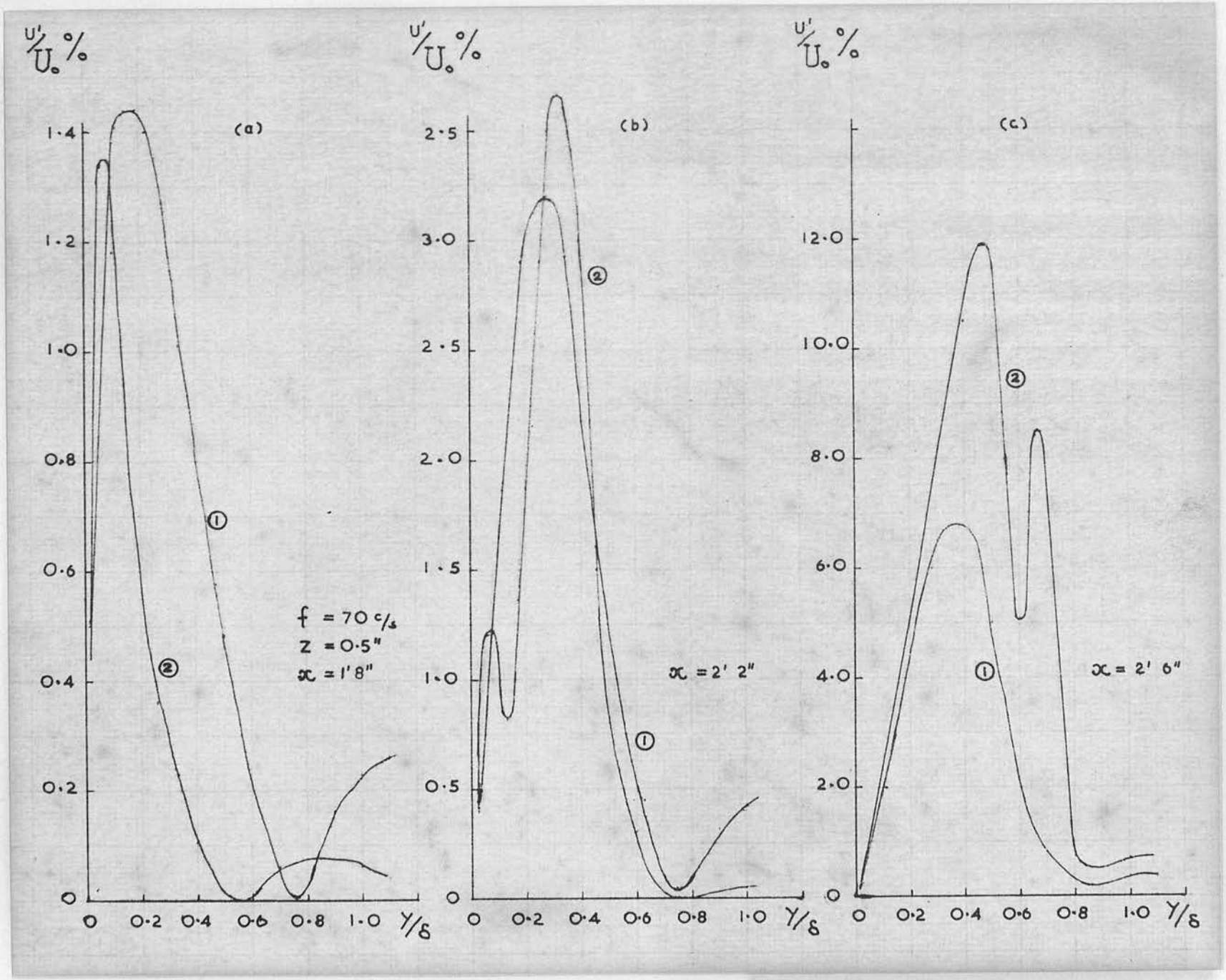

Figure VI.5.a-c. Distribution of Fundamental and Second Harmonic Intensities through the Boundary Layer.

Figure VI.6. Distribution of Fundamental and Second Harmonic Intensities through the Boundary Layer.

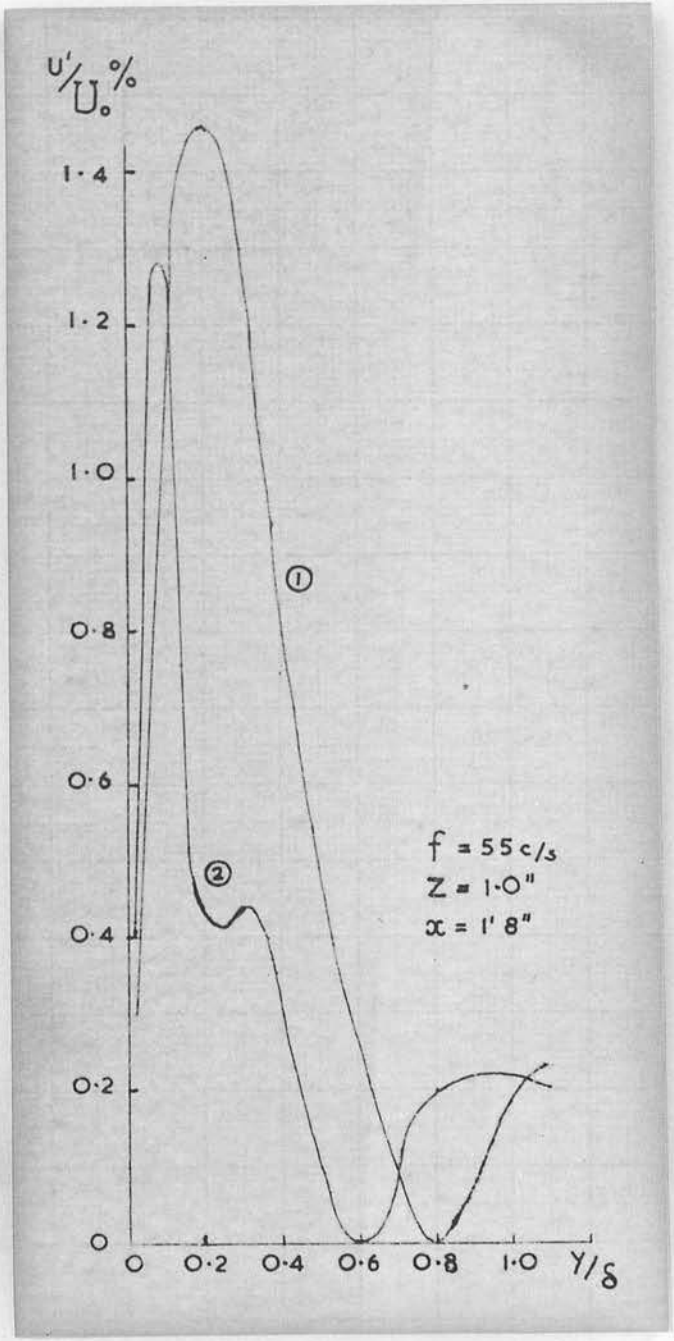

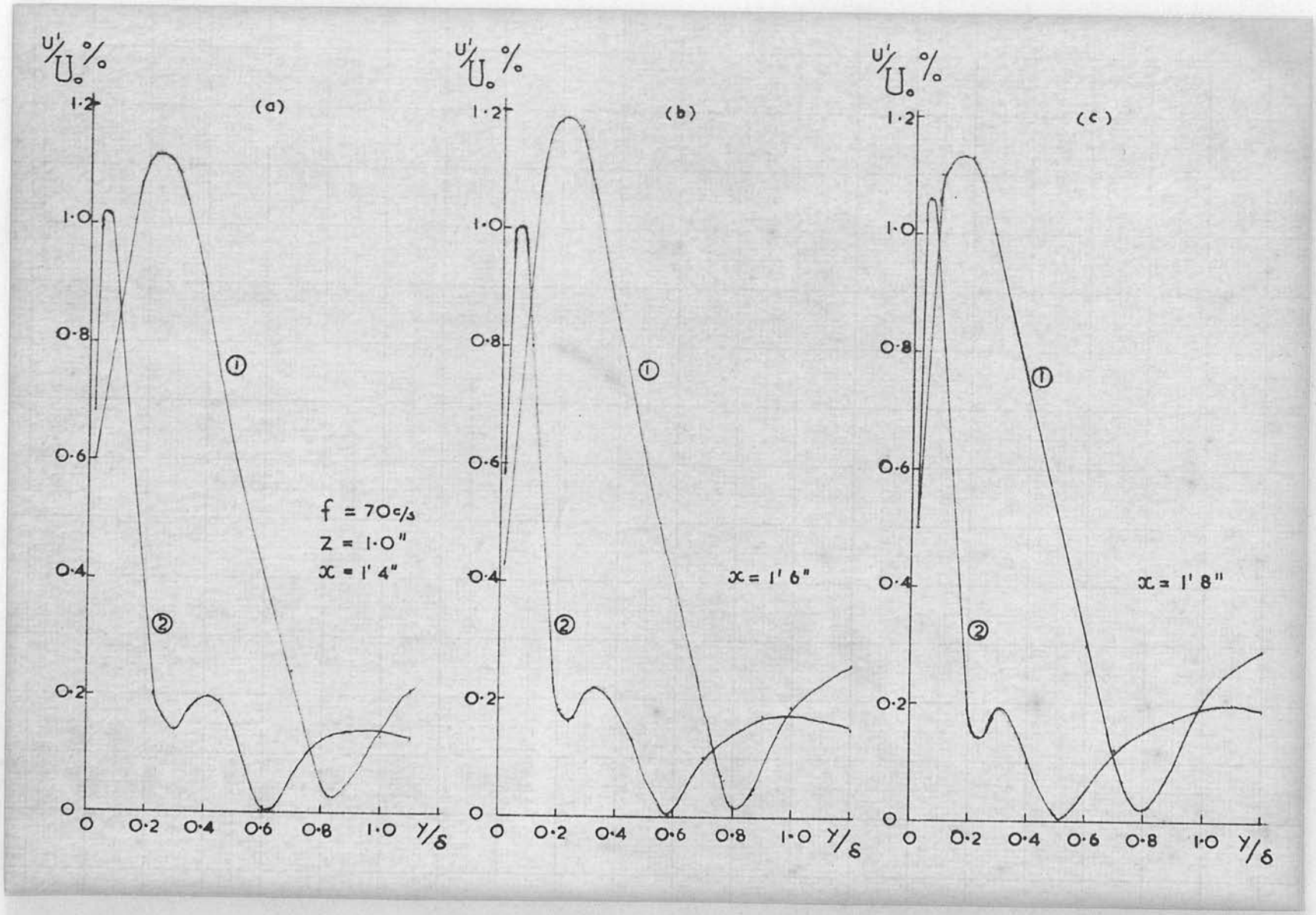

Figure VI.7.a-c. Distribution of Fundamental and Second Harmonic Intensities through the Boundary Layer.

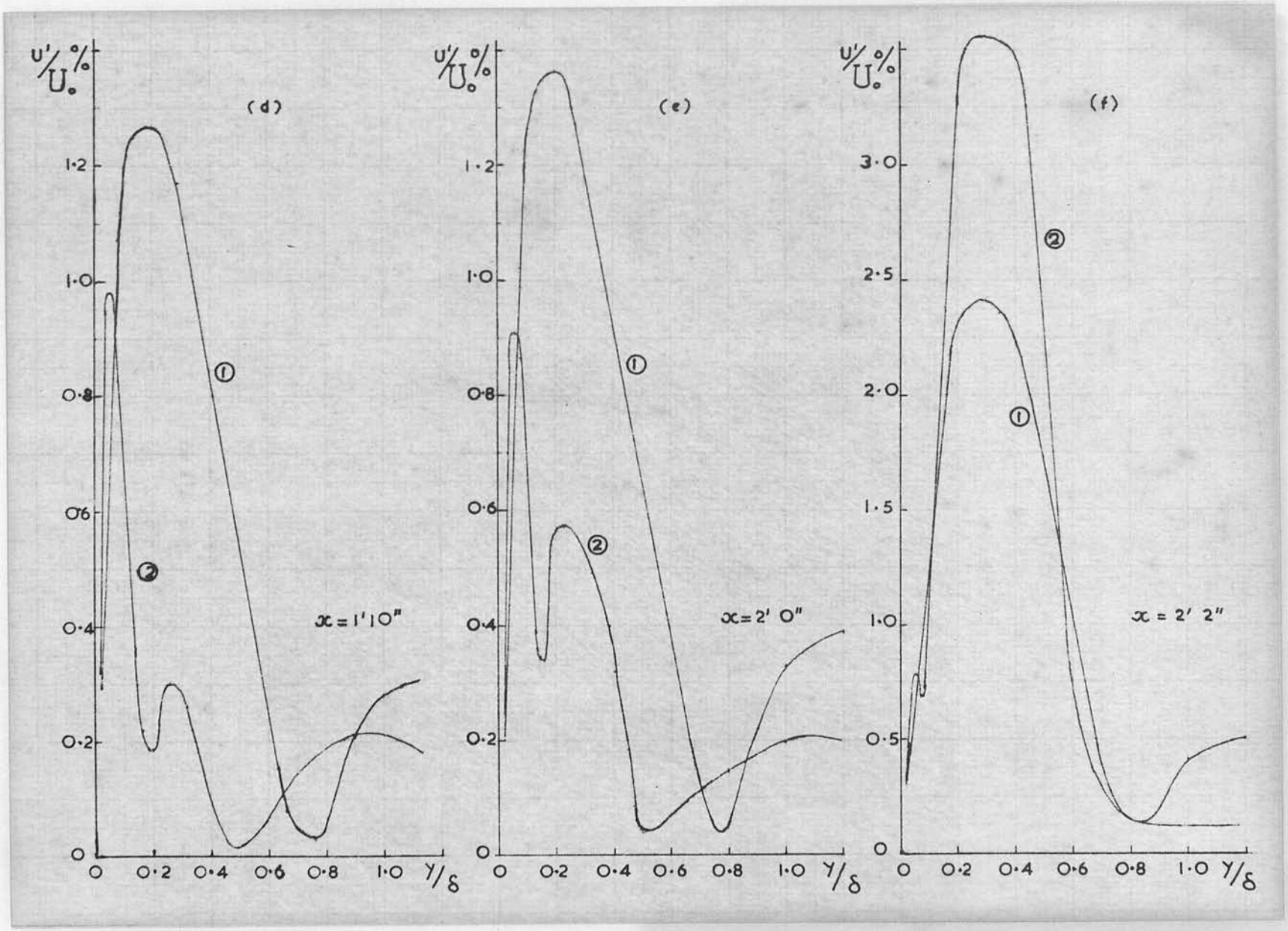

Figure VI.7.d-f. Distribution of Fundamental and Second Harmonic Intensities through the Boundary Layer.

Figure VI.8. Distribution of Fundamental, Second and Third Harmonic Intensities through the Boundary Layer.

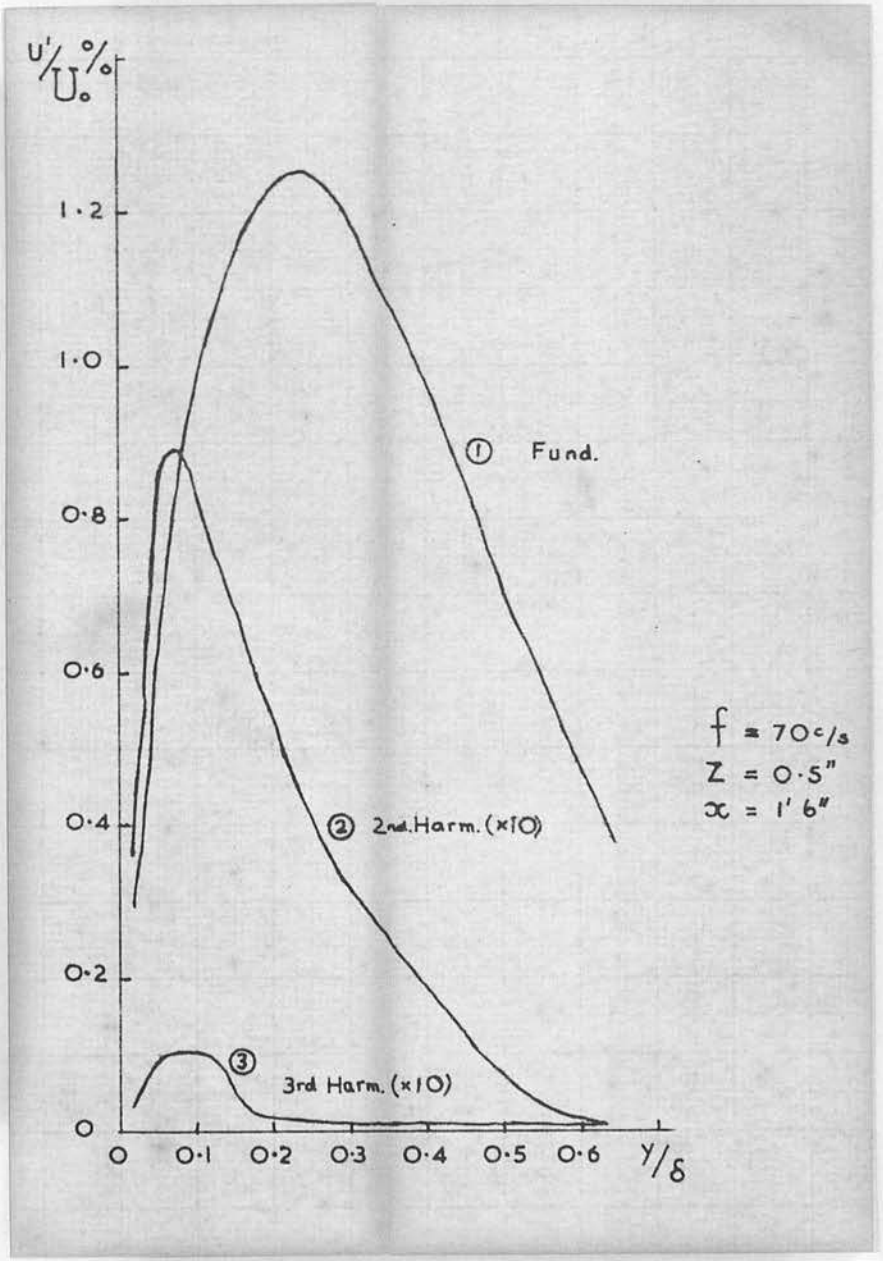

Figure VI.9. Distribution of Fundamental Intensity through the Boundary Layer for a Frequency of 110 c/s.

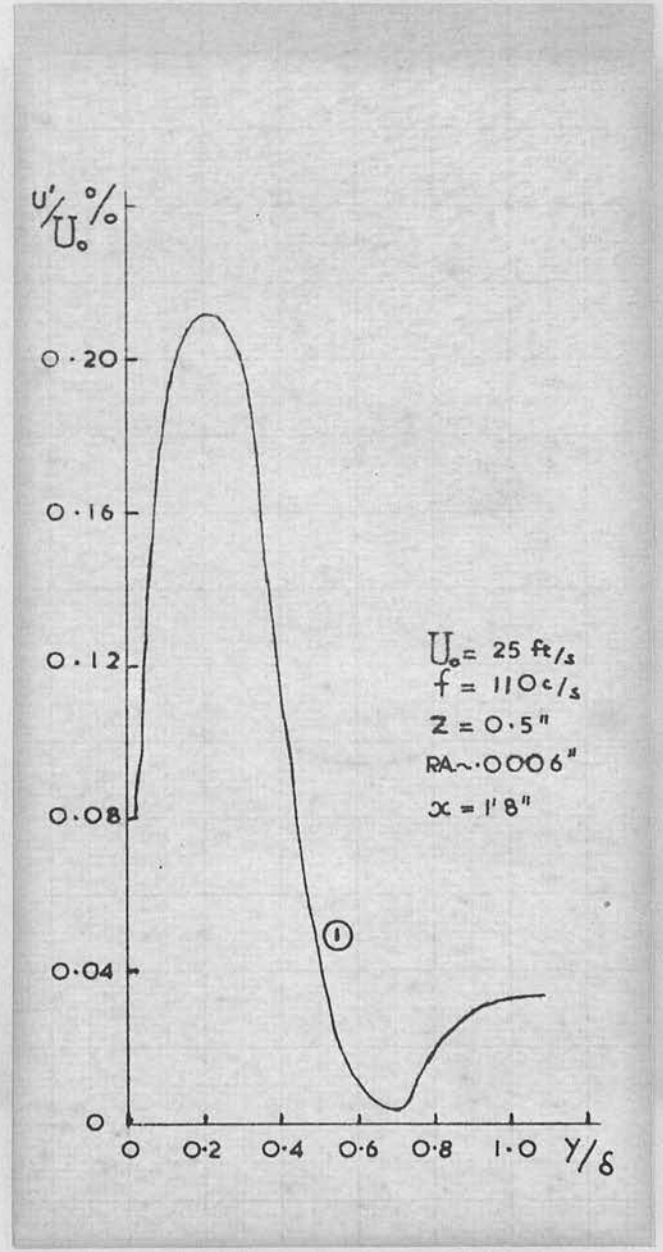

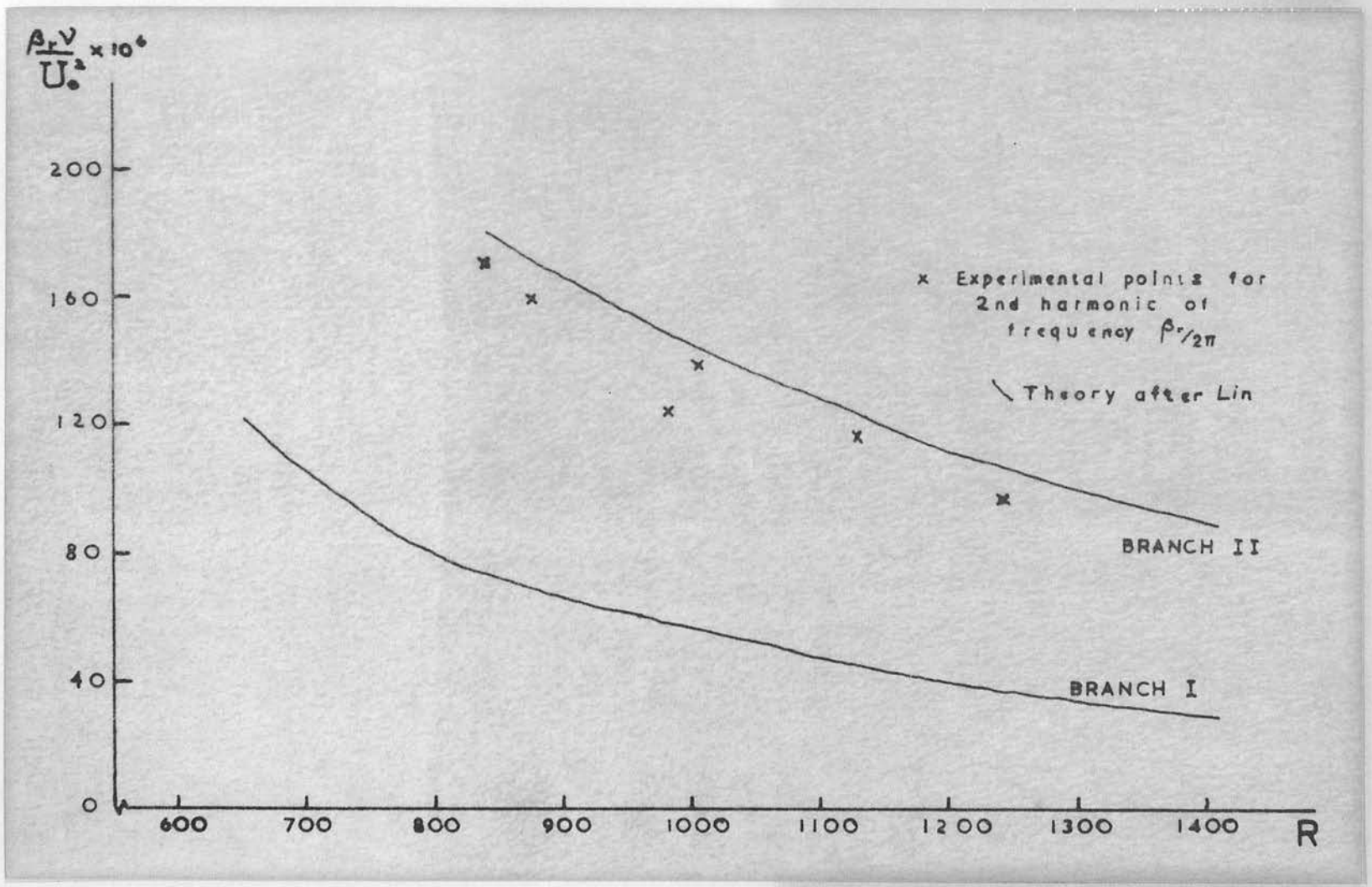

Figure VI.10. Points of Maximum Second Harmonic Intensity Plotted in Relation to the Neutral Curve.

Figure VI.11. Distribution of Fundamental and Second Harmonic Intensities through the Boundary Layer for Increased Ribbon Amplitude.

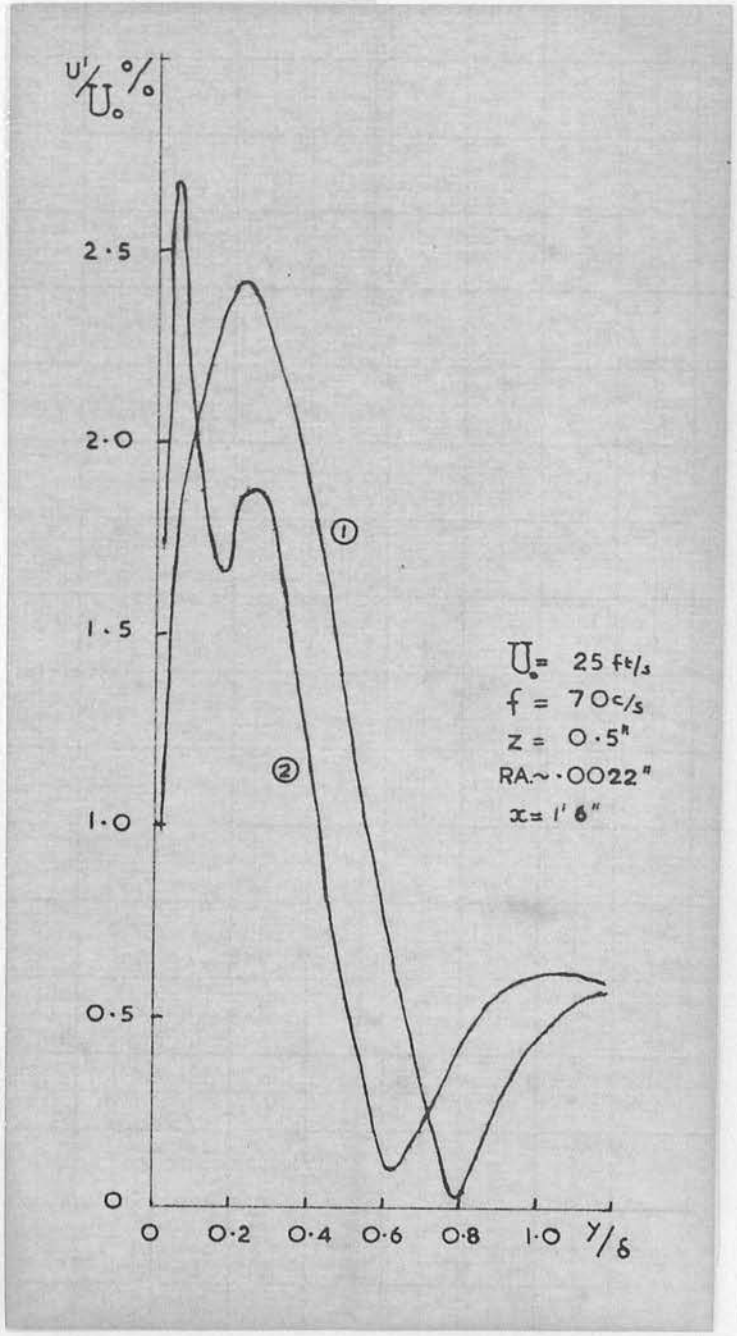

CHAPTER VII

CONCLUSIONS ON THE NATURE OF THE SECOND HARMONIC CONTENT

VII.1. Conclusions

The main feature of interest in the work reported in Chapter VI was the distribution of the second harmonic intensity through the boundary layer. The results show that in general the maximum second harmonic intensity occurs for $y/\delta < 0.1$ whilst the minimum intensity occurs at a y-position closer to the plate than that of the minimum fundamental intensity.

The second harmonic intensity distribution through the boundary layer has been considered neither theoretically nor experimentally. It is interesting to compare the limited experimental observations on downstream growth of the second harmonic made by Klebanoff, Tidstrom and Sargent (1962) with the results of the present work. From a hot-wire traverse downstream at constant y in the vicinity of the critical layer these workers noted that, at departure from 'linear' growth of the fundamental, the second harmonic intensity was some 5 per cent. of the fundamental, and, as breakdown was approached, this value increased to some 20 per cent.. These results are in broad agreement with those of the present work.

Measurements by Klebanoff et. al. in the region of $Y/\delta = 0.6$ demonstrated that the second harmonic content at this position was of the same order as the harmonic content in the vicinity of the critical layer, and at breakdown was even larger. It is interesting to note that these observations are in broad agreement with certain of the present results (c.f. Figure VI.5a. and Figure VI.5c.). However, from the observations reported in Chapter VI it would appear somewhat fortuitious that the two y-positions chosen by Klebanoff et. al. should give comparable values for harmonic content at the two y-positions. The present results are in agreement with the conclusion reached by Klebanoff et. al. from their studies that the order of magnitude analysis of Lin (1958) on the importance of higher harmonic in the instability process does not fit the experimental facts. Having reached this conclusion Klebanoff et. al. made no further studies on the second harmonic intensity distribution through the boundary layer.

A further link can be made between the present experimental results and the orders of magnitude predicted for the harmonic terms by Stuart and reported by Bradshaw, Stuart and Watson (1960). It has already been mentioned that these workers suggest that if the fundamental is of small order A, then the second harmonic will be of order A^2 and higher harmonics of order A^n ($n \geq 3$).

In the present work, for the second harmonic peak close to the plate, the fundamental intensity is of order 1/10 of the local mean velocity and the second and third harmonics are each successive orders smaller than this.

While the detailed features of the second harmonic intensity distributions through the boundary layer found experimentally cannot be fully explained by the present knowledge of the subject, certain suggestions can be offered in explanation of the more general features.

The similarities between the fundamental and second harmonic intensity distributions, namely the peaks close to the plate and the minima in the outer region of the boundary layer with a phase change of 180 degrees at each minimum, are striking. It is also interesting to note that second harmonic content was present even before significant departure of the fundamental oscillation from the predictions of linear theory. It would thus seem that a theoretical approach might be made by extending the two-dimensional linear theory to include the small order non-linear second harmonic terms. It seems possible that such an approach would show that the basic distribution through the boundary layer of second harmonic intensity had a maximum for $y/\delta < 0.1$ and a minimum with a phase change near $y/\delta = 0.6$. The present experimental results should prove to be a useful guide to a theoretician in such a study.

The results of this work indicate that this kind of theoretical approach could show that the second harmonic intensity had another minimum in the region of $Y/\delta = 0.2$ with a secondary maximum near $Y/\delta = 0.3$, the higher order eigenfunction having two maxima and two minima. This suggestion, however, seems to be unlikely, as the experimental results show that this type of second harmonic intensity distribution with twin maxima and minima was not common to all spanwise positions.

The results shown in Figure VI.10. suggest that second harmonic disturbances of neutral stability were present in a region where the fundamental was of a small order of magnitude and had not significantly departed from linear theory. A two-dimensional theory for the second harmonic of the kind mentioned above would, it is hoped, give confirmation of the existence of a curve of neutral stability for the second harmonic.

If a theory of this kind for the second harmonic yielded results similar in form to those of the small disturbance linearized theory for the fundamental as has been suggested then it seems reasonable to expect a mathematical singularity in the region of the maximum second harmonic intensity, just as the linear theory has a singularity at the critical layer where the wave velocity of the disturbance equals the local velocity and the fundamental disturbance has a maximum intensity.

Experimentally, for the second harmonic, the intensity peak was found in general to occur at a y-position closer to the plate than that of the fundamental and consequently in a region of lower local velocity. This would imply that the second harmonic wave velocity was less than that of the fundamental. However, the experimental measurements of second harmonic wave velocity showed that this was greater than that of the fundamental.

A two-dimensional theoretical approach of the kind suggested could not fully explain the results of the present work where the distribution of second harmonic intensity was found to be dependent on the spanwise position of the observations.

A theoretical examination of the second harmonic terms in the three-dimensional theory formulated by Lin and Benney (1960) and extended by Benney (1961) and (1964), will give information on the three-dimensional aspects of the second harmonic intensity distribution. Up to the present, however, interest in this theory has been centred on the aperiodic terms associated with longitudinal vortices.

Certain tentative suggestions can be offered to explain the nature of the three-dimensional second harmonic found experimentally. A possible explanation of the intensity distributions found for the second harmonic is that they were compiled from two separate components.

It is suggested that the general form of the basic two-dimensional component distribution was similar to that shown for the second harmonic in Figure VI.4c. with the maximum intensity close to the plate for $Y/\delta < 0.1$ and the minimum at about $Y/\delta = 0.6$. Superposed on this basic distribution there was a component which varied in the spanwise as well as the streamwise direction. This latter component has its greatest influence in the region of $Y/\delta = 0.3$.

A possible source of a three-dimensional component of second harmonic intensity is a longitudinal eddy system of the kind found experimentally by Klebanoff et. al. and confirmed theoretically by Lin and Benney. An eddy system of this type has associated with it a component of velocity in the y-direction at certain spanwise positions. Klebanoff et. al. have shown that an action of such an eddy system is to produce distortion of the fundamental wave and consequently to increase the second harmonic content. Thus in the present work it is suggested that the downstream growth of the second harmonic intensity in the region $0.2 < Y/\delta < 0.5$ was associated with the development of a longitudinal eddy system. With this explanation the outer peak of second harmonic intensity in Figure VI.5c. can be associated with the doubling of the eddy system when three dimensional effects dominate suggested by Lin and Benney and illustrated diagramatically by Klebanoff et. al. The different distributions

obtained at the two spanwise positions can be attributed to location of in these positions relative to an axis of the eddy system. Exact location of these relative positions is not possible for the results of the present work due to the limited information available on the three-dimensional nature of the boundary layer at the time of the experiments.

The observations of the phase of the second harmonic support this proposed two-component explanation of the intensity distributions. At $Y/\delta = 0.1$ the second harmonic oscillations were in phase at both z = positions for all x - stations where measurements were taken. However, a phase difference of approximately 120 degrees was detected between the second harmonic waves at the two z - positions for $Y/\delta \sim 0.3$ at an x - position where the peak in second harmonic intensity at this position was growing rapidly. This latter observation is consistent with the view that the second harmonic component at this x - station and position resulted from an eddy system.

Lack of knowledge of the exact three-dimensional nature of the mean boundary-layer flow and the exact positions of maximum and minimum boundary-layer thickness makes a more detailed explanation of the present results very difficult. However, the results obtained should provide a useful guide to future theoretical work on this aspect of local flow behaviour and they certainly suggest topics for further experimental study.

VII.2. Suggestions for further work

Since the completion of the work described in this thesis a new wind tunnel has been built in the Department of Natural Philosophy, Edinburgh University. Using this very low turbulence level tunnel together with the associated instrumentation and data handling facilities it should be possible to make detailed measurements of the second harmonic intensity distribution through the boundary layer. An exact knowledge of the three-dimensionality in the boundary layer will be of prime importance in any such studies. It thus may be necessary to control the three-dimensionality of the boundary layer by artificial means, or to introduce three-dimensional disturbances into the boundary layer. To finally establish the existance of an eddy system it will be necessary to use a V or X hot-wire probe system to measure the w - components associated with the disturbance. An instrument, which could possibly be developed using hot-film techniques, to study the $\bar{v}$ - components of fluctuating velocity would be a considerable asset in any future work.

APPENDIX I

AN OUTLINE OF THE THEORY OF LAMINAR OSCILLATIONS

The theory of laminar oscillations, as formulated by Tollmein and Schlichting and developed by others (see I.2d.), treats, in general only two-dimensional flow with two-dimensional disturbances.

The Navier -Stokes equations, for an incompressible, Newtonian fluid, can be simplified, for an undisturbed laminar boundary-layer flow with zero pressure gradient, to

$$U \frac{\partial U}{\partial x} + V \frac{\partial U}{\partial y} = \nu \frac{\partial^2 U}{\partial y^2} .$$

The equation of continuity gives

$$\frac{\partial U}{\partial x} + \frac{\partial V}{\partial y} = 0 ,$$

the boundary conditions being

$$y = 0 , \; U = 0 , \; V = 0 ; \qquad y = \infty , \; U = U_0 .$$

These are the equations which were solved by Blasuis, the results being tabulated by Howarth.

The basic flow can be assumed to be steady and a function of y only, while under most circumstances V is negligible in comparison with U . Thus the basic flow in the boundary layer can be assumed to have the form

$$U = U(y) \quad \text{and} \quad V = 0 .$$

The disturbances superposed on this flow are functions of x, y and time, and can be written

$$u = u\ (x, y, t)$$

$$v = v\ (x, y, t)$$

$$p = p\ (x, y, t)$$

where p represents the pressure due to the disturbances.

The components of the total velocity thus become $U + u$ and v. By introducing these components into the Navier Stokes equations and subtracting the corresponding equations for u = v = p = o, then neglecting terms of second order smallness, u and v being small, equations are obtained which are linear in the first order perturbation terms:

$$\frac{\partial u}{\partial t} + U\frac{\partial u}{\partial x} + v\frac{\partial U}{\partial y} = \nu\left(\frac{\partial^2 u}{\partial x^2} + \frac{\partial^2 u}{\partial y^2}\right) - \frac{1}{\rho}\frac{\partial p}{\partial x} \quad (1)$$

$$\frac{\partial v}{\partial t} + U\frac{\partial v}{\partial x} = \nu\left(\frac{\partial^2 v}{\partial x^2} + \frac{\partial^2 v}{\partial y^2}\right) - \frac{1}{\rho}\frac{\partial p}{\partial y} \quad (2)$$

The equation of continuity becomes:

$$\frac{\partial u}{\partial x} + \frac{\partial v}{\partial y} = 0 \quad (3)$$

The pressure terms may be eliminated from equations (1) and (2) to give:

$$\frac{\partial^2 u}{\partial y\,\partial t} + U\frac{\partial^2 u}{\partial x\,\partial y} + \frac{\partial U}{\partial y}\frac{\partial u}{\partial x} + v\frac{\partial^2 U}{\partial y^2} + \frac{\partial v}{\partial y}\frac{\partial U}{\partial y} - \frac{\partial^2 v}{\partial x\,\partial t}$$

$$- U\frac{\partial^2 v}{\partial x^2} = \nu\left(\frac{\partial^3 u}{\partial x^2\,\partial y} + \frac{\partial^3 u}{\partial y^3} - \frac{\partial^3 v}{\partial x^3} - \frac{\partial^3 v}{\partial x\,\partial y^2}\right) \quad (4)$$

A perturbation stream function (ψ) is now introduced such that the disturbance velocities satisfy equation (3)

$$u = \frac{\partial \psi}{\partial y} \quad ; \quad v = -\frac{\partial \psi}{\partial x}\ .$$

A solution is usually sought to the disturbance equations with a stream function of the form

$$\psi(x, y, t) = F(y)\, e^{i(\alpha x - \beta t)} = F(y)\, e^{i\alpha(x - ct)}$$

where F (y) represents the initial amplitude of the stream function and α is the wave number. The quantity β is taken to be complex with $\beta = \beta_r + i\beta_i$, where β_r is the angular frequency of the oscillation and β_i determines the degree of amplification or damping with time. In the same way, **c** is complex with **cr** representing the phase velocity of the wave and **ci** another form of the amplification factor.

By assuming α to be real and β complex, the wave is considered to be amplified with time but not distance. For the purposes of finding a neutral curve this assumption is immaterial. However, in an experimental verification it is convenient to measure amplification with distance when a steady state has been reached with respect to time.

Expressing lengths and velocities non-dimensionally in terms of δ^* and U_o and putting $F(y) = U_o \delta^* \phi(\eta)$ where $\eta = y/\delta^*$ the following equation is obtained,

$$(U - c)(\phi'' - \alpha^2\phi) - U''\phi = -\frac{i}{\alpha R}(\phi'''' - 2\alpha^2\phi'' + \alpha^4\phi) \quad (5)$$

where the prime denotes differentiation with respect to η. The boundary conditions require

$$\eta = 0 \,, \quad \phi = 0 \,, \quad \phi' = 0 \,;$$
$$\eta = \infty \,, \quad \phi = 0 \,, \quad \phi' = 0 \,.$$

This is the Orr-Sommerfeld equation for small disturbances.

With the mean flow $U(y)$ specified, for each pair of values for α and R the equation (5) defines one eigenfunction $\phi(y)$ and one complex eigenvalue c.

The methods of solution of equation (5) have been fully discussed by Lin (1955), suffice it to say here that two approximations to equation (5) can be considered in its solution. The first of these is that obtained by neglecting the viscous terms. This however, has singularities at the surface and at the point where the wave velocity is equal to the local stream velocity, the critical point. A second approximation to equation (5), neglecting all but the largest of the viscous terms, together with a change of variable, allows a solution to be made in the region of the critical point.

The solution of the Orr-Sommerfeld equation for real values of c (i.e. $c_i = 0$) enables the points of neutral stability to be plotted in the $(\alpha\delta^*, R)$ $(\beta_r\nu/U_o^2, R)$ or $(c_r/U_o, R)$ planes. The neutral stability curve in the $(\beta_r\nu/U_o^2, R)$ plane is shown in Figure A.I.1.

Using an indirect method, Shen (1954) has calculated points on curves of constant c_i, in the amplifying region,

in the ($\alpha\delta^*$, R), plane. From these results he was able to calculate the amplitude of disturbances with different values of $\beta_T \nu / U_0^2$ as they cross the region from Branch I to Branch II of the neutral stability curve. A graph of these results is shown in Figure AI.2.

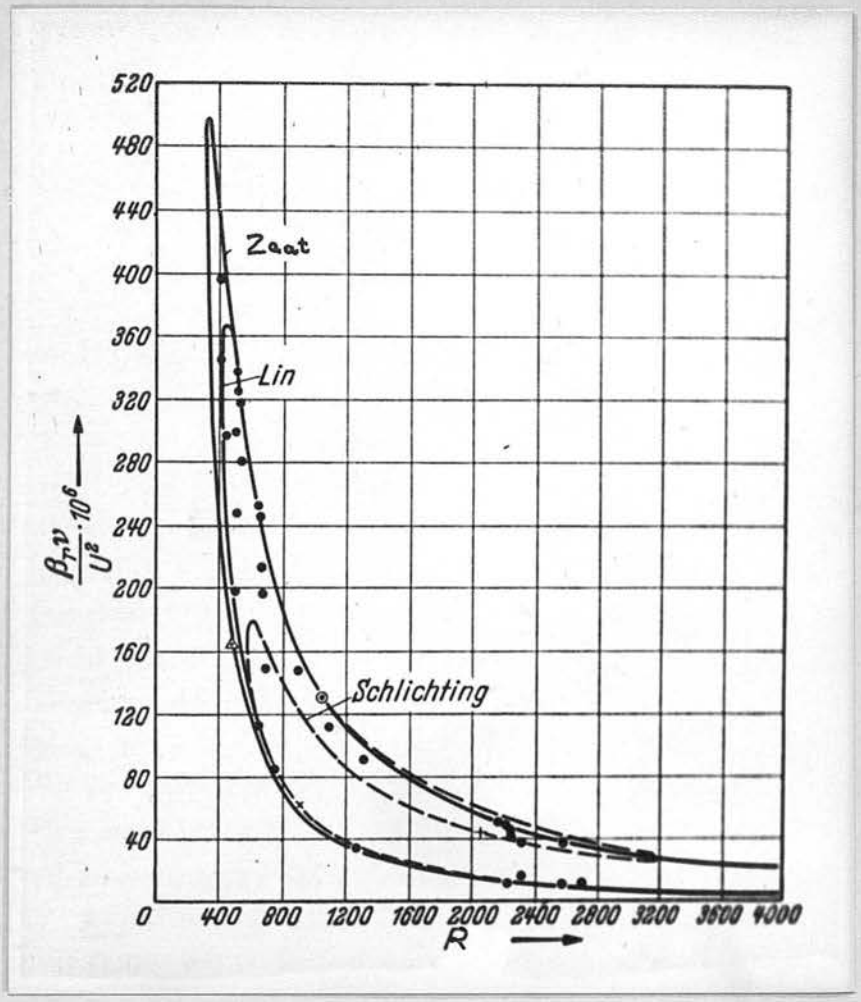

Figure A.I.1. Theoretical Curves of Neutral Stability.

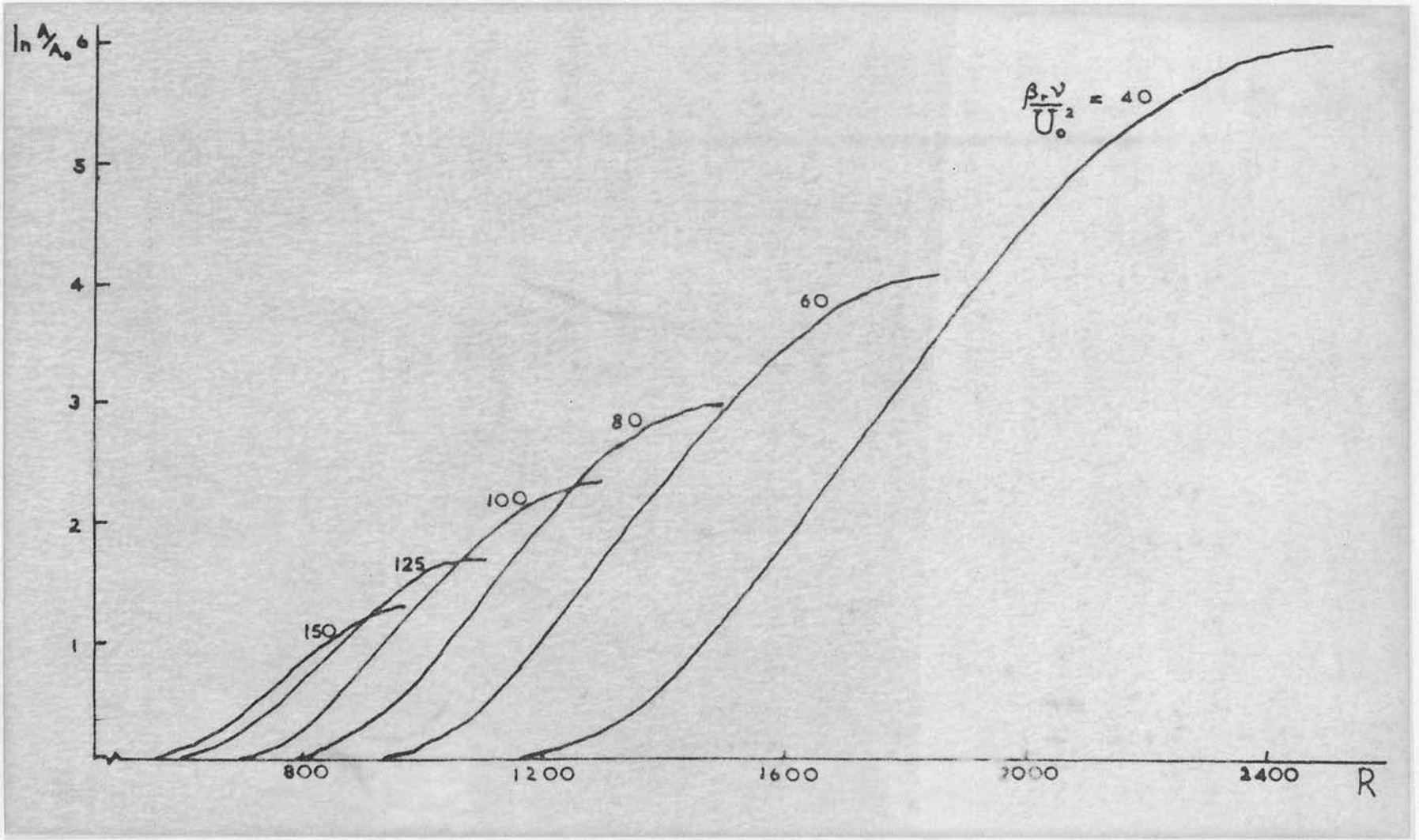

Figure A.I.2. Theoretical Growth Curves across the Amplifying Region of the Boundary Layer (after Shen).

APPENDIX II

OUTLINE OF THE THEORY OF HOT-WIRE MEASUREMENTS

a) Measurement of u'

The relation between the fluid velocity normal to a heated wire and the rate of heat loss from the wire was given by King (1914) as

$$H = (T_w - T_a)(D + F\sqrt{U}) \qquad (1)$$

where the terms D and F depend on the thermal conductivity, density and specific heat of the air and on the dimensions of the wire. However, due to the methods of using hot-wires in boundary-layer investigations these terms, D and F, may be regarded as constants.

From the conservation of energy, the difference between the heat generated in the wire and the heat lost to the air will be equal to the thermal energy accumulated in the wire. Thus

$$i^2 R_w - (T_w - T_a)(D + F\sqrt{U}) = ms\frac{dT_w}{dt} \qquad (2)$$

where m is the mass of the wire and s is the specific heat of the material of the wire.

If the mass of the hot-wire is small and the fluctuations are slow, then the right hand side of equation (2) can be neglected and a quasiequilibrium equation obtained.

$$i^2 R_w = (T_w - T_a)(D + F\sqrt{U}) \qquad (3)$$

The resistance of the wire at temperature T is given by

$$R = R_o (1 + \alpha_o (T - T_o)) \qquad (4)$$

where α_o is the temperature coefficient of resistance of the wire. The slope of the resistance-temperature curve, $\alpha_o R_o$, is nearly constant over a wide range of temperatures for most wire materials, so that

$$R_w - R_a = \alpha_o R_o (T_w - T_a) \qquad (5)$$

Substitution of equation (5) in equation (3) gives

$$\frac{R_w}{R_w - R_a} = \frac{1}{i^2 \alpha_o R_o} (D + F\sqrt{U}) \qquad (6)$$

With $\rho = R_w/(R_w - R_a)$,

$\rho_o = D/i^2 \alpha_o R_o$

$F_1 = F/i^2 \alpha_o R_o$

equation (6) becomes

$$\rho = \rho_o + F_1 \sqrt{U} \qquad (7)$$

For constant current operation of the hot-wire ρ_o and F_1 are constant for a given wire and given current, so that a linear relationship exists between ρ and $\sqrt{U}$ Using this relation the mean velocity of a fluid stream can be found. In the boundary-layer work where the range of velocities was large the modification of King's law due to Collis and Williams (1959) was found to give better agreement with the experimental results. Thus the relation

$$\rho = \rho_o + F_1 U^{0.45} \qquad (8)$$

has been used throughout the present work.

Fluctuations in the velocity of the fluid stream result in changes of the temperature of the wire. The resulting resistance changes produce fluctuations in the voltage across the wire. By differentiating equation (8) the resistance fluctuations can be related to the velocity fluctuations by the equation

$$\frac{d\rho}{\rho - \rho_o} = 0.45 \, dU/U \qquad (9)$$

But $$d\rho = R_a/(R_w - R_a)^2 \cdot dR_w \qquad (10)$$

Thus, substitution of equation (10) in equation (9) gives

$$\frac{dU}{U} = \frac{R_a}{0.45\,(R_w - R_a)^2(\rho - \rho_o)}\, dR_w \qquad (11)$$

If dU represents the turbulence intensity u' and the root mean square voltage fluctuation for constant current is $e' = i\, d\, Rw$, then equation (11) becomes

$$\frac{u'}{U} = \frac{(\rho - 1)^2}{0.45\, i\, R_a\, (\rho - \rho_o)}\, e' \qquad (12)$$

Thus the turbulence intensity can be determined from the voltage fluctuations.

b) Thermal lag

If the fluctuations are of high frequency then the right hand side of equation (2) cannot be neglected

Thus

$$i^2 R - (T - T_a)(D + F\sqrt{U}) = ms \frac{dT}{dt} \qquad (13)$$

Writing U in the form of a mean flow plus a component periodic in time, the resulting equating can be solved for the temperature fluctuations.

It is found that the ratio of the temperature fluctuation to that predicted by neglecting the right hand side of equation (13) is $1/(1+4\pi^2 f^2 M^2)^{1/2}$.

Thus the corresponding voltage variations are reduced in amplitude below that for zero frequency by this factor and lag in phase by the angle $\tan^{-1} 2\pi f M$.

For constant current operation the time constant (M) is given by the expression

$$M = \frac{J m s}{i^2 R_0 \alpha_0} \cdot \frac{R_w - R_a}{R_a}, \qquad (14)$$

which can be written in the form

$$M = \frac{J \pi^2 r^4 \rho_1 s}{\alpha_0 \sigma_0} \left(\frac{R_w - R_a}{i^2 R_a} \right), \qquad (15)$$

where J is the mechanical equivalent of heat, r the radius of wire, ρ_1 the density of the material of the wire and σ_0 the resistivity of the material of the wire at $0^\circ C$.

More detailed accounts of the theory of hot-wire measurements have been given by Dryden and Kuethe (1929), Schubauer and Klebanoff (1946) and Kovasznay (1947) and (1953).

APPENDIX III

SIRIUS AUTOCODE PROGRAM FOR THE REDUCTION OF BOUNDARY-LAYER TRAVERSE DATA

```
Jv1
10)Xv0=TAPE9
Xv0=v0
Xv1=v1
Xv2=v2
TEXT
BOUNDARY LAYER TRAVERSE

n0=0
1)v(9+n0)=v(1+n0)-v8
v(1+n0)=v(1+n0)-v0
v(1+n0)=v(1+n0)/v(9+n0)
n1=5Xn0
n1=n1+15
v(9+n0)=n1
v(9+n0)=LOGv(9+n0)
v(9+n0)=0.45Xv(9+n0)
v(9+n0)=EXPv(9+n0)
n0=n0+1
→1,n0≠7
v300=v8-v0
v300=v300/500
n0=0
Xv16=0
Xv17=0
Xv18=0
v19=0
2)v16=v16+v(9+n0)
v17=v17+v(1+n0)
v20=v(9+n0)Xv(9+n0)
v21=v(1+n0)Xv(9+n0)
v18=v18+v20
v19=v19+v21
n0=n0+1
→2,n0≠7
v20=7Xv18
v21=v16Xv16
v20=v20-v21
v21=v17Xv18
v22=v16Xv19
v21=v21-v22
v22=7Xv19
v23=v16Xv17
v22=v22-v23
v21=v21/v20
v22=v22/v20
TEXT
INTERCEPT

PRINTv21,4043
TEXT
GRADIENT

PRINTv22,4044
12)v1=TAPE3
n2=0
8)v25=TAPE*
Xn3=n0
Xn0=0
TEXT
   U        U/U0     CALIB
v4=v300Xv1
3)v24=v(25+n0)-v8
v(25+n0)=v(25+n0)-v0
v(25+n0)=v(25+n0)/v24
v5=v(25+n0)-v21
v5=LOGv5
v6=LOGv22
v5=v5-v6
v5=v5/0.45
v(125+n0)=EXPv5
v5=v(25+n0)-1
v5+v5Xv5
v5=v5/0.45
v6=v(25+n0)-v21
v5=v5/v6
v(25+n0)=v(125+n0)/v125
v5=v5Xv(25+n0)
v(225+n0)=v5/v4
PRINTv(125+n0),3042
Sv0=v0
Sv1=v1
PRINTv(25+n0),4022
Sv0=v0
Sv1=v1
PRINTv(225+n0),4042
v(25+n0)=1-v(25+n0)
n0=n0+1
→3,n0≠n3
v10=0
4)v(23+n0)=v(23+n0)Xv3
v10=v10+v(23+n0)
v11=v(24+n0)-v(23+n0)
v11=v11Xv3
v11=v11/2
v10=v10+v11
n0=n0-1
→4,n0≠1
v11=v25Xv3
v11=v11/2
v10=v10+v11
v11=1-v(24+n3)
v11=v11Xv2
v11=v11/2
```

```
PRINTv(25+no),4042
Sv0=v0
Sv1=v1
PRINTv(225+no),4042
v(25+no)=1-v(25+no)
no=no+1
→3,no≠n3
v10=0
4)v(23+no)=v(23+no)Xv3
v10=v10+v(23+no)
v11=v(24+no)-v(23+no)
v11=v11Xv3
v11=v11/2
v10=v10+v11
no=no-1
→4,no≠1
v11=v25Xv3
v11=v11/2
v10=v10+v11
v11=1-v(24+n3)
v11=v11Xv2
v11=v11/2
v10=v10+v11
v11=v(24+n3)Xv2
Xv10=v10+v11
Xv10=v10/0.341
TEXT
DELTA
PRINTv10,3023
Xv0=v0
Xv1=v1
TEXT
Y/DELTA

no=n3
5)v12=no-1
v13=v12Xv3
v14=v2+v13
v14=v14/v10
PRINTv14,3023
no=no-1
→5,no≠0
→9,n2=1
6)v24=TAPE
v25=TAPE*
Xn1=no
Xno=0
→11,n1≠n3
TEXT
UDASH/Uo PERCENT

v0=v0
7)v25=v(25+no)/v24
v25=v25Xv(225+no)
v25=v25X100
PRINTv25,3023
no=no+1
→.0≠n1
Xv0=v0
Xv1=v1
Xv2=v2
9)v23=TAPE
→6,v23=-1
n2=1
→8,v23=-2
→10,v23=-3
→12,v23=-4
11)TEXT
NUMBER OMITTED

STOP
→10
(→0)
```

APPENDIX IV

PROCEDURE FOR CALCULATION OF HARMONIC AMPLITUDES

u_0 to u_{11} are displacements of film trace at twelve equidistant points per cycle.

	$(u_0$ to $u_6)$	....	....	....	....	....	....	....
	$(u_{11}$ to $u_7)$		....	....	....	....	....	
Sums	$(v_0$ to $v_6)$	....	....	....	....	....	....	....
Diffs.	$(w_1$ to $w_5)$		....	....	....	....	....	

	$(v_0$ to $v_3)$	....	....	....	....	$(w_1$ to $w_3)$	....	....	....
	$(v_6$ to $v_4)$	....	....	....		$(w_5$ to $w_4)$	....	....	
Sums	$(p_0$ to $p_3)$	....	....	....	....	$(r_1$ to $r_3)$	....	....	....
Diffs.	$(q_0$ to $q_2)$	....	....	....		$(s_1$ to $s_2)$	....	....	

$\frac{1}{2}$ line above: $p_1=\ p_2=\ q_2=\ r_1=$ / $h_1=\ h_2=\ l_2=\ m_1=$

0.866 x line above: $q_1=\ r_2=\ s_1=\ s_2=$ / $l_1=\ m_2=\ n_1=\ n_2=$

	$p_0=$ .. $p_1=$ .. $p_2=$ .. $p_3=$ ..	$q_0=$ .. $l_1=$ .. $l_2=$ ..	$p_0=$ .. $h_1=$ .. $p_3=$ .. $h_2=$ ..	$p_0=$ .. $p_3=$ .. $h_1=$ .. $h_2=$ ..	$m_1=$ .. $m_2=$ .. $r_3=$ ..	$q_0=$ .. $q_2=$ ..	$n_1=$ .. $n_2=$ ...	$r_1=$ .. $r_3=$ ..
Sum of 1st Col.	....	....	....	....	....			
Sum of 2nd Col.								
Sum	.... $=12a_0$	.... $=6a_1$			.... $=6b_1$		..$=6b_2$	
Diff.	.... $=12a_6$	.... $=6a_5$	.... $=6a_4$	.... $=6a_2$	.... $=6b_5$	..$=6a_3$	..$=6b_4$	..$=6b_3$

Result: $u=a_0 + a_1\cos\theta + a_2\cos 2\theta + a_3\cos 3\theta + a_4\cos 4\theta + a_5\cos 5\theta + a_6\cos 6\theta$

$+ b_1\sin\theta + b_2\sin 2\theta + b_3\sin 3\theta + b_4\sin 4\theta + b_5\sin 5\theta$

APPENDIX V

SIRIUS AUTOCODE PROGRAM FOR NUMERICAL HARMONIC ANALYSIS

```
Jv1
TEXT
HARMONIC AMPLITUDES AND PHASES

Xv40=180/3.14159
Xv41=1.25
Xv42=SQRT11
2)v0=TAPE
Xv1=v1
Xv2=v2
TEXT
FUND  SEC  THIRD  FOURTH  FIFTH

AMPLITUDES

n3=0
1)n2=0
v0=TAPE12
v12=v0
v13=v1+v11
v14=v2+v10
v15=v3+v9
v16=v4+v8
v17=v5+v7
v18=v6
v19=v1-v11
v20=v2-v10
v21=v3-v9
v22=v4-v8
v23=v5-v7
v24=v12+v18
v25=v13+v17
v26=v14+v16
v27=v15
v28=v12-v18
v29=v13-v17
v30=v14-v16
v31=v19+v23
v32=v20+v22
v0=25/2
v1=v26/2
v2=v30/2
v3=v31/2
v4=v29Xo.866
v5=v32Xo.866
v6=v34Xo.866
v7=v35Xo.866
v12=v28+v2
v13=v12+v4
v13=v13/6
v14=v12-v4
v14=v14/6
v15=v24+v27
v16=v0+v1
v15=v15-v16
v15=v15/6
v17=v24+v0
v18=v27+v1
v17=v17-v18
v17=v17/6
v19=v3+v33
v20=v19+v5
v20=v20/6
v21=v19-v5
v21=v21/6
v22=v28-v30
v22=v22/6
v23=v6+v7
v23=v23/6
v24=v6-v7
V24=v24/6
v25=v31-v33
v25=v25/6
v36=v25
v32=v25
v25=v13
v30=v20
v26=v17
v31=v23
v27=v22
v28=v15
v33=v24
v29=v14
v34=v21
v5=90.0
->14,v20=0
v5=v13/v20
v5=ARCTANv5
v5=v5Xv40
14)v6=90.0
->15,v23=0
v6=v17/v23
v6=ARCTANv6
v6=v6Xv40
15)v7=90.0
->16,v2=0
v7=v22/v32
v7=ARCTANv7
v7=v7Xv40
16)v8=90.0
->17,v24=0
v8=v15/v24
v8=ARCTANv8
v8=v8Xv40
17)v9=90.0
->18,v21=0
v9=v14/v21
v9=ARCTANv9
v9=v9xv40
18)v13=v13xv13
```

```
14)v6=90.0
->15,v23=0
v6=v17/v23
v6=ARCTANv6
v6=v6Xv40
15)v7=90.0
->16,v2=0
v7=v22/v32
v7=ARCTANv7
v7=v7Xv40
16)v8=90.0
->17,v24=0
v8=v15/v24
v8=ARCTANv8
v8=v8Xv40
17)v9=90.0
->18,v21=0
v9=v14/v21
v9=ARCTANv9
v9=v9xv40
18)v13=v13xv13
v20=v20xv20
v0=v13+v20
v0=SQRTv0
PRINT v0,3042
Sv17=v17xv17
v23=v23*v23
v1=v17+v23
v1=SQRTv1
PRINT v1, 4042
Sv22=v22xv22
v36=v36
v2=v22+v36
v2=SQRTv2
PRINT v2,4042
Sv15=v15xv15
v24=v24xv24
v3=v15+v24
v3=v15+v25
v3=SQRTv3
Sv14=v14xv14
v21=v21x21
v4=v14+v21
v4=SQRTv4
PRINT v4,4042
5)n1=5xn3
n1=n1+n2
v(50+n1)=v(0+n2)
->19,v(25+n2)≠0
->20,v(30+n2)≠0
v(5+n2)=180+v(5+n2)
->21
20)v0=v0
->22,v(<'&n2)=0
v(5+n2)=360+v(5+n2)
->21
22)v(5+n2)=360-v(5+n2)
->21
19)v0=v0
->21,v(30+n2)≠0
v(5+n2)=180+v(5+n2)
21)v(150+n1)=v(5+n2)
n2=n2+1
->5,n2≠5
n3=n3+1
->1,n3≠12
Xv0=v0
TEXT
AVERAGE

n2=0
4)n3=0
v0=0
v1=0
3)n1=5xn3
n1=n1+n2
v0=v0+v(50+n1)
v1=v1+v(150+n1)
n3=n3+1
->3,n3≠12
v0=v0/12
v(210+n2)=v0
v1=v1/12
v(220+n2)=v1
PRINTv0,4042
Sn2=n2+1
->,n2≠5
Xn0=0
10)n2=0
9)n1=5xn2
n1=n1+n0
v(50+n1)=v(50+n1)-v(210+n0)
v(50+n1)=MODv(50+n1)
v(250+n1)=v(150+n1)-n(220+n0)
v(250+n1)=MODv(250+n1)
n2=n2+1
->9,n2≠12
n0=n0+1
->10,n0≠5
TEXT
STANDARD DEVIATION

n0=0
12)n1=0
v0=0
v240=0
11)n2=5xn1
n2=n2+n0
v0=v0+v(50+n2)
v240=v240+v(250+n2)
n1=n1+1
```

```
n1=n1+n0
v(50+n1)=v(50+n1)-v(210+n0)
v(50+n1)=MODv(50+n1)
v(250+n1)=v(150+n1)-n(220+n0)
v(250+n1)=MODv(250+n1)
n2=n2+1
->9,n2≠12
n0=n0+1
->10,n0≠5
TEXT
STANDARD DEVIATION

n0=0
12)n1=0
v0=0
v240=0
11)n2=5xn1
n2=n2+n0
v0=v0+v(50+n2)
v240=v240+v(250+n2)
n1=n1+1
->11,n1≠12
v0=v0/12
v0=v0/v42
v0=v0/v41
v240=v240/12
v240=v240/v42
v240=v240xv41
v(310+n09=v240
PRINTv0,4042
Sn0=n0+1
->12,n0≠5
Xv0=v0
Xv1=v1
Xv2=v2
Xv3=v3
TEXT
PHASES

n0=0
7)n1=5xn0
PRINTv(150+n1),3061
Sv0=v0
PRINTv(151+n1),4061
Sv1=v1
PRINTv(152+n1),4061
Sv2=v2
PRINTv(153+n1),4061
Sv3=v3
PRINTv(154+n1),4061
n0=n0+1
->7,n0≠12
Xv0=v0
TEXT
AVERAGE

n2=0
8)PRINTv(220+n2),4061
v(230+n2)=v(220+n2)-v220
Sn2=n2+1
->8,n2≠5
n2=0
Xn0=0
TEXT
STANDARD DEVIATION

23)PRINTv(310+n0),4061
Sn0=n0+1
->23,n0≠5
->2
(->0)
```

APPENDIX VI

ATLAS AUTOCODE PROGRAM FOR CALCULATION OF SECOND HARMONIC CONTENT RESULTING FROM NON-LINEARITY OF HOT-WIRE

```
begin
real a,b,c1,c2,c3,p,w,V1,V,A,U,B,t
integer i,j,k,l
array f(0:11) ,v(1:5)
V1=½ ; p=3 ; A=0.684 ; w=345
cycle  i=5,1,22
if i≤10 then U=i/10
if 11≤i≤19 then U=i-9
if i>19 then U=5i-85
newline
newline
print(U,2,1)
newline
cycle j=2,2,40
a=j/100
B=A*U*0.45
cyclek=0,1,11
t=0.5236k/w
b=(p+B*(1+a*cos(w*t))*0.45)
V=V1*b/(b-1)
f(k)=V
repeat
cycle l=1,1,5
v(l)=f(l)+f(12-l)
repeat
c1=1/6(f(0)-f(6)+0.866(v(1)-v(5))+½(v(2)-v(4)))
c2=1/6(f(0)+f(6)+½(v(1)+v(5)-v(2)-v(4))-v(3))
c3=1/6(f(0)-f(6)-v(2)-v(4))
newline
print(a,0,2);spaces(6)
print(100c2/c1,2,2);spaces(3)
print(100c3/c1,2,3)
repeat
repeat
end of program
***Z
```

REFERENCES

BENNETT, H. W. 1953 Kimberley-Clark Corporation Report, Neenah, Wisconsin.

BENNEY, D. J. 1961 J. Fluid Mech. 10, 209.

BENNEY, D. J. 1964 Phys. Fluids, 7, 319.

BETCHOV, R. and WELLING, W. 1949 N.A.C.A. T.M. 1223.

BLASIUS, H. 1908 Z. Math. u Physik, 56, 1.

BRADSHAW, P. 1961 N.P.L./Aero/427.

BRADSHAW, P. 1964 J. Roy. Aero. Soc. 68, 198

BRADSHAW, P. and JOHNSON, R. F. 1961 N.P.L./Aero/434

BRADSHAW, P., STUART, J. T. and WATSON, J. 1960. Paper prepared for A.G.A.R.D. Wind Tunnel Panel Meeting on Boundary-Layer Research, London, April 1960.

BURGERS, J. M. 1925 Proc. 1st. Internat. Cong. Appl. Mech., Delft, 113

BURNS, J. G. 1958 Ph.D. Thesis, University of Edinburgh.

COLLIS, D. C. and WILLIAMS, M. J. 1959 J.Fluid Mech. 6, 357.

COOPER, R. D. and TULIN, M. P. 1955 AGARD ograph, N.A.T.O., Paris.

DHAWAN, S. and NARASIMHA, R. 1958 J.Fluid Mech 3, 418.

DRYDEN, H. L. 1936 N.A.C.A. T.M. 562.

DRYDEN, H. L. 1955a Proc. Conf. High-Speed Aeronautics, Brooklyn, 41.

DRYDEN, H. L. 1955b Science, 121, 375.

DRYDEN, H. L. 1956 Z.Flugwiss. 4 , 89.

DRYDEN, H. L. and KUETHE, A. M. 1929 N.A.C.A. Rep.No.320.

EMMONS, H. W. 1951 J.Aero Sci. 18, 490.

FALES, E. N. 1955 J.Franklin Inst. 259, 491.

GOLDSTEIN, S. 1930 Proc. Camb. Phil. Soc. 26, 1.

GÖRTLER, H. and WITTING, H. 1958 Proc. Symp. Boundary Layer Res. (Ed. Görtler) I.U.T.A.M. Freiburg (1957), 110.

GOULD, R. W. F. 1945 A.R.C. R. amd M. No.2240.

HAMA, F. R. 1960 Proc. 1960 Heat Transfer and Fluid Mech. Inst. (Eds. Mason, Reynolds and Vincenti), 92.

HAMA, F. R., LONG, J. D. and HEGARTY, J. C. 1957 J. Appl. Phys. 28, 388.

HARRIS, H. E. 1951 Electronics, May 1951, 130.

van der HEGGE ZIJNEN, B. G. 1951 Appl. Sci. Res. A. 2.

HEISENBERG, W. 1924 Ann. Phys. Lpz. (4), 74, 577. see N.A.C.A. T.M. 1291.

HOWARTH, L. 1938 Proc. Roy. Soc. A 164, 547.

KING, L. V. 1914 Phil. Trans. Roy. Soc. A 214, 373.

KLEBANOFF, P. S. and TIDSTROM, K. D. 1959 N.A.S.A. T.N. D-195.

KLEBANOFF, P. S., TIDSTROM, K. D. and SARGENT, L. M. 1962 J. Fluid Mech. 12, 1.

KOVASZNAY, L. S. G. 1947 N.A.C.A. T.M. 1130.

KOVASZNAY, L. S. G. 1953 N.A.C.A. T.N. 2839.

KOVASZNAY, L. S. G. 1959 Appl. Mech. Rev. 12, 6, 1.

KOVASZNAY, L. S. G. 1960 Proc. Durand Cent. Conf., Stanford. Aeronautics and Astronautics (Eds. Hoff and Vincenti), Pergamon, London, 1960.

KOVASZNAY, L. S. G., KOMODA, H. and VASUDEVA, B. R. 1962 Proc. 1962 Heat Trans. and Fluid Mech. Inst. (Ed. Ehlers), 1.

KUETHE, A. M. 1956 J. Aero. Scl. 23, 444.

LANDAU, L. D. 1944 C.R. (Doklady) Acad. Sci. U.R.S.S. 44, 311.

LAUFER, J. and VREBALOVICH, T. 1960. J. Fluid Mech. 9 257.

LIN, C. C. 1945 Quart. Appl. Math. 3, 117, 218, 277.

LIN, C. C. 1955 'Theory of Hydrodynamic Stability', Cambridge University Press.

LIN, C. C. 1958 Proc. Sym. Boundary Layer Res. (Ed. Görtler) I.U.T.A.M. Freiburg (1957) 144.

LIN, C. C. and BENNEY, D. J. 1960 Phys. Fluids. 4, 656.

LORENTZ, H. A. 1896 Collected Papers, 4, 15. Martinus Nijhoff, The Hague (1937).

van MEEL, D. A. and VERMIJ, H. 1963 J. Sci. Instrum. 40, 607.

MEKSYN, D. 1964 Z. für Phys. 178, 159.

MEKSYN, D. and STUART, J. T. 1951 Proc. Roy. Soc. A 208 517.

MILLER, J. A. 1963 Rev. Sci. Instrum. 34, 1143.

MOCK, W. C. Jr. and DRYDEN, H. L. 1932 N.A.C.A. Rep. No.448.

MORGAN, J. 1964 Ph.D. Thesis, University of Edinburgh.

MORKOVIN, M. V. 1958 Trans. Amer. Soc. Mech. Eng. 80, 1121.

NARASIMHA, R. 1957 J. Aero. Sci. 24, 711.

NICOL, A. A. 1958 Ph.D. Thesis, University of Edinburgh

NIKURADSE, J. 1933 Z. a. Math. Mech. 13, 174.

NIKURADSE, J. 1942 Monograph, Zentrale f. wiss. Berichtaresen, Berlin.

NOETHER, F. 1921 Z. a. Math. Mech. 1, 125.

ORR, W. M. F. 1907 Proc. R. Irish Acad. A, 27, 9 and 69.

OWER, E. 1933 'Measurement of Air Flow', Chapman and Hall, London.

PRANDTL, L. 1904 Proc. 3rd. Internat. Math. Cong., Heidelberg. sec N.A.C.A. T.M. 452.

PRANDTL, L. 1914 Nachr. Ges. Wiss., Göttingen, Math. - phys. Kl. 177.

PRANDTL, L. 1935 'Aerodynamic Theory', III, (Ed. Durand), Berlin, 34.

RAYLEIGH, Lord. 1887 Scientific Papers, 3, 2.

REYNOLDS, O. 1883 Phil. Trans. 174, 935.

ROSENHEAD, L. (Ed.) 1963 'Laminar Boundary Layers', Oxford University Press.

de SANTO, D. F. and KELLER, H. B. 1962 J. Soc. Ind. App. Math. 10, (4), 569.

SCHLICHTING, H. 1933a Z. a. Math. Mech. 13, 260.

SCHLICHTING, H. 1933b Nachr. Ges. Wiss., Göttingen, Math.-phys. Kl. 181.

SCHLICHTING, H. 1935 Nachr. Ges. Wiss., Göttingen, Math-phys. Kl. Fachgruppe, 1, 47. see N.A.C.A. T.M. 1265, (1950)

SCHLICHTING, H. 1955 'Boundary-Layer Theory' Pergamon, London.

SCHLICHTING, H. 1959 'Handbuch der Physik', VIII /1, (Ed. Flügge), Berlin

SCHLICHTING, H. 1960a Paper prepared for A.G.A.R.D. Wind Tunnel Panel Meeting on Boundary-Layer Research, London, April, 1960.

SCHLICHTING, H. 1960b J. Roy. Aero. Soc. 64, 590, 63

SCHUBAUER, G. B. 1958 Proc. Symp. Boundary-Layer Res. (Ed. Görtler) I.U.T.A.M. Freiburg (1957), 85.

SCHUBAUER, G. B. and KLEBANOFF, P. S. 1946 N.A.C.A. A.C.R. 5K27.

SCHUBAUER, G. B. and KLEBANOFF, P. S. 1955 Proc. Symp. Boundary-Layer Effects Aerodyn., N.P.L..

SCHUBAUER, G.B. and SKRAMSTAD, H. K. 1947 J. Res. Nat. Bur. Stand. 38, 251.

SHEN. S. F. 1954 J. Aero. Sci. 21, 62.

SIMMONS, L. F. G. and BAILEY, A. 1927 Phil. Mag. 3, 13, 81.

SQUIRE, H. B. 1933 Proc. Roy. Soc. A142, 321

STUART, J. T. 1960a Proc. Xth Internat. Cong. Appl. Mech., Stresa, 63.

STUART, J. T. 1960b J. Fluid Mech. 9, 353.

STUART, J. T. 1960c Proc. 2nd. Internat. Cong. Aeronaut. Sci., Zurich, 1960. see Advances in the Aeronautical Sciences, Vol 3, 121.

TANI, I. 1960 Proc. 2nd Internat. Cong. Aeronaut. Sci., Zurich, 1960. see Advances in the Aeronautical Sciences, Vol 3, 143.

TANI, I. and KOMODA, H. 1962 J.Aerosp. Sci. Apr.62, 440.

TAYLOR, G. I. 1936 Proc. Roy. Soc. A 156, 307.

TAYLOR, G. I. 1938 Proc. Vth Internat. Cong. Appl. Mech., Cambridge, Mass., 294.

THEODORSEN, T. 1955 50 Jahre Grenzschicht - forschung (Eds. Görtler and Tollmein), 55.

TIETJENS, O. G. 1925 Z. a. Math. Mech. 5, 200.

TOLLMEIN, W. 1929 Nachr. Ges. Wiss, Göttingen. 21. see N.A.C.A. T.M. 603, (1931).

TOWNSEND, A. A. 1947 Proc. Camb. Phil. Soc. 43, 4, 560

WATSON, J. 1960a J.Fluid Mech. 9, 371.

WATSON, J. 1960b Proc. Roy. Soc. A254, 562.

WESKE, J. R. 1957 Inst. Fluid Dyn. and Appl. Mech., University of Maryland. T.N. B.N.-91.

WHITELEGG, MISS S. M. 1961, Ph.D. Thesis, University of Edinburgh.

WHITTAKER, Sir E. and ROBINSON, G.
1946 'The Calculus of Observations', Blackie, London.

WISE, B. and SCHULTZ, D. L. 1955 A.R.C. 18373, F.M.2390.

ZAAT, J. A. 1958 Proc. Symp. Boundary-Layer Res. (Ed. Görtler) I.U.T.A.M. Freiburg, (1957), 127.

ACKNOWLEDGMENTS

I should like to thank Dr. M. A. S. Ross for suggesting the topic of this thesis and for her continued help and encouragement during the work, Dr. J. G. Burns for his active interest and many helpful suggestions, and Professor W. H. J. Childs for providing laboratory accomodation, workshop and computing facilities. I am indebted to Professor N. Feather, F.R.S. for the use of facilities in the Department of Natural Philosophy, University of Edinburgh.

My thanks go also to the Ministry of Aviation for a maintainance grant during part of this work.